MISR overview and observational principles
Data products
Example data applications

David J. Diner
Jet Propulsion Laboratory, California Institute of Technology

Exploring and Using MISR Data
New Orleans, LA
May 2005

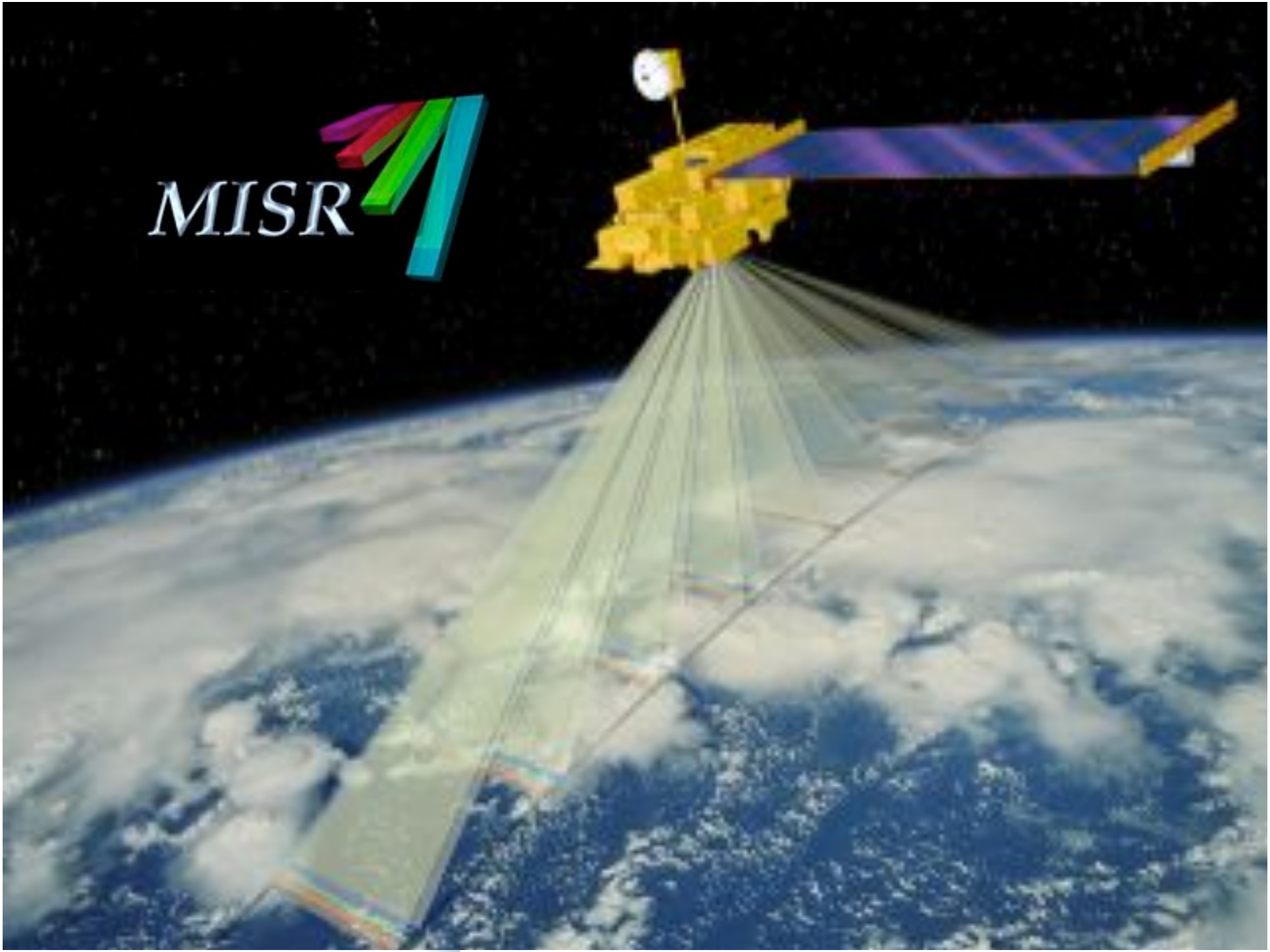

Distributed by the Atmospheric Science Data Center
http://eosweb.larc.nasa.gov

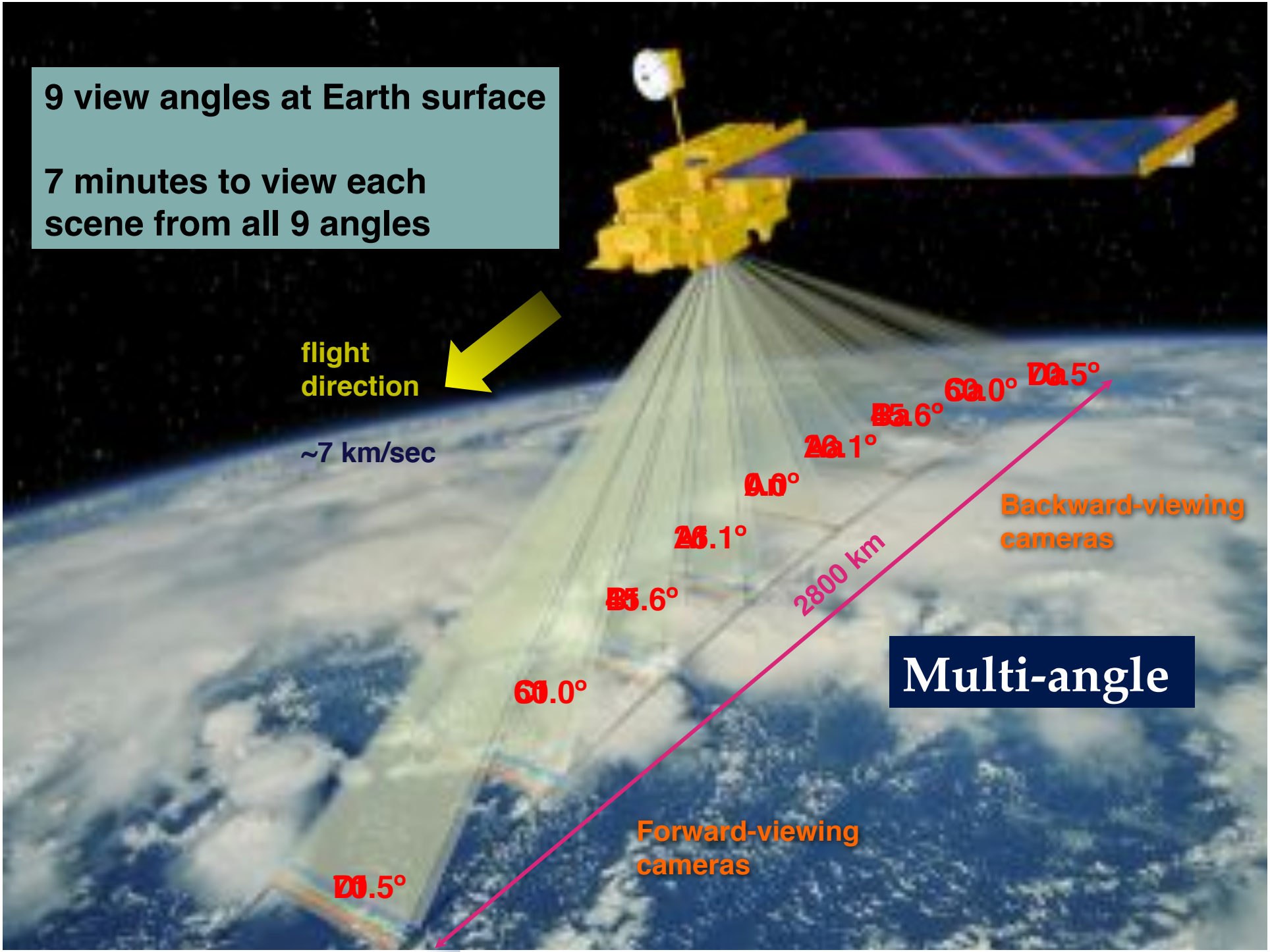
9 view angles at Earth surface
7 minutes to view each scene from all 9 angles
flight direction
~7 km/sec
Backward-viewing cameras
2800 km
Multi-angle
Forward-viewing cameras

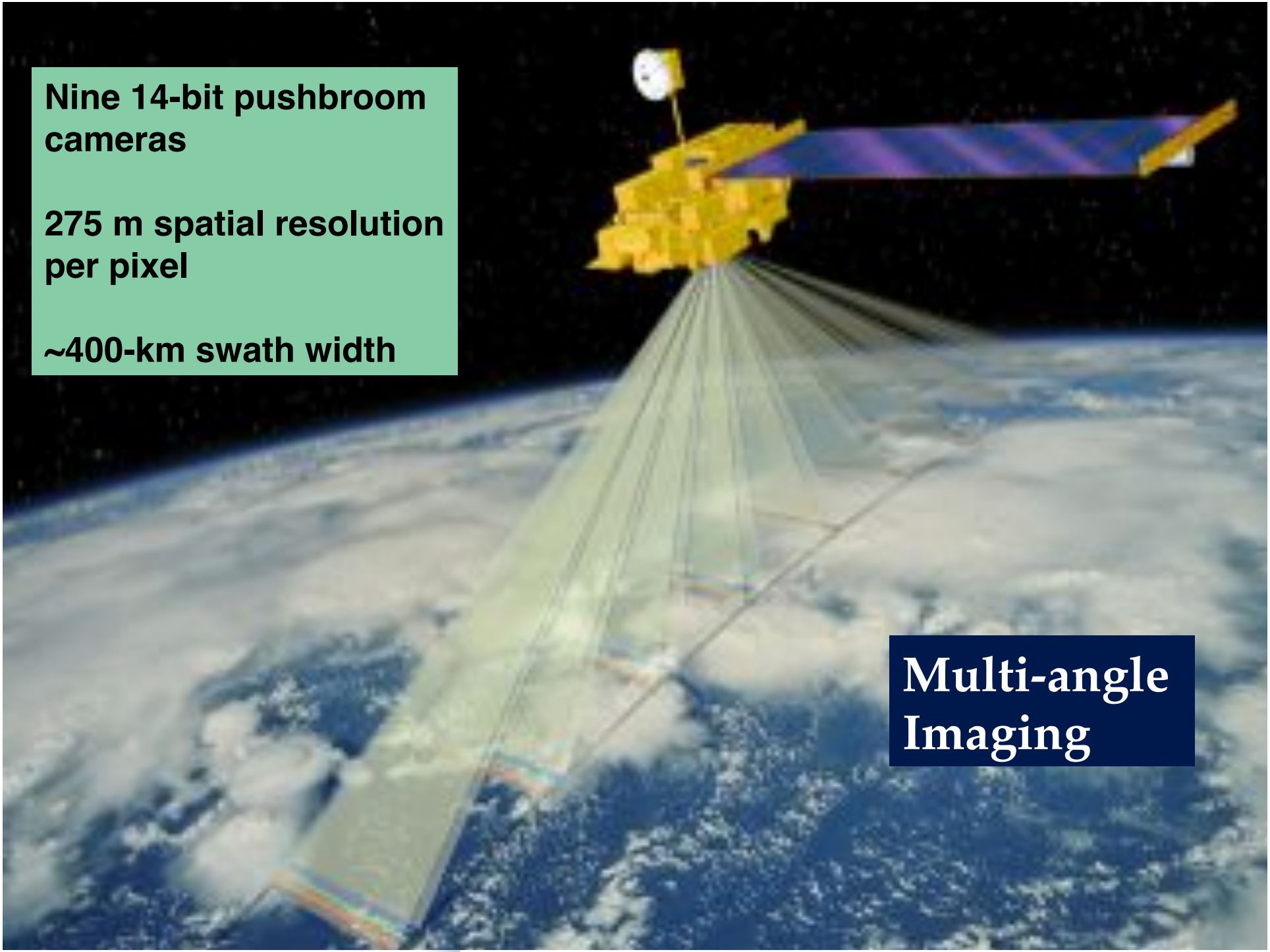
Nine 14-bit pushbroom cameras
275 m spatial resolution per pixel
~400-km swath width
Multi-angle Imaging

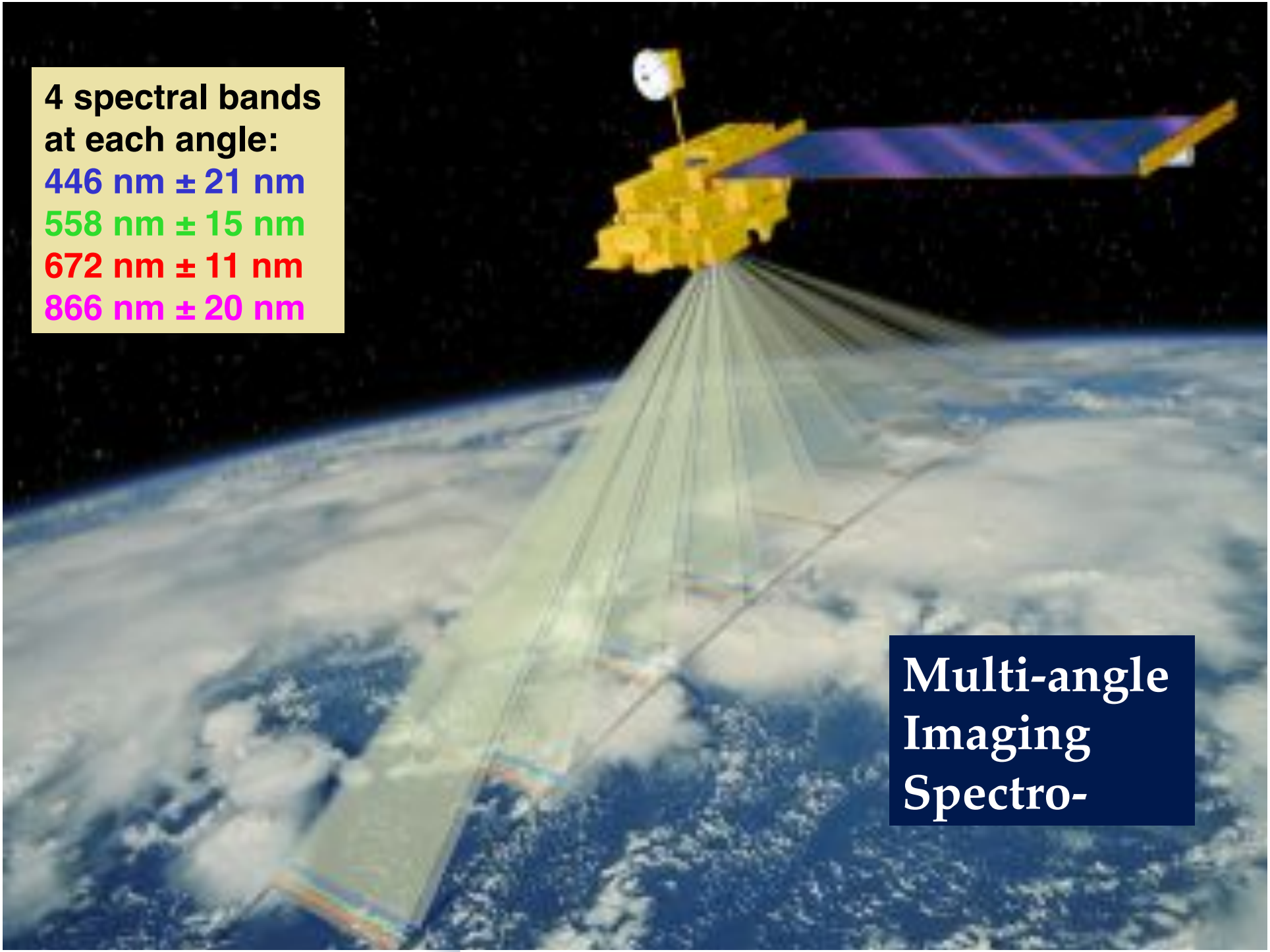

Distributed by the Atmospheric Science Data Center
http://eosweb.larc.nasa.gov

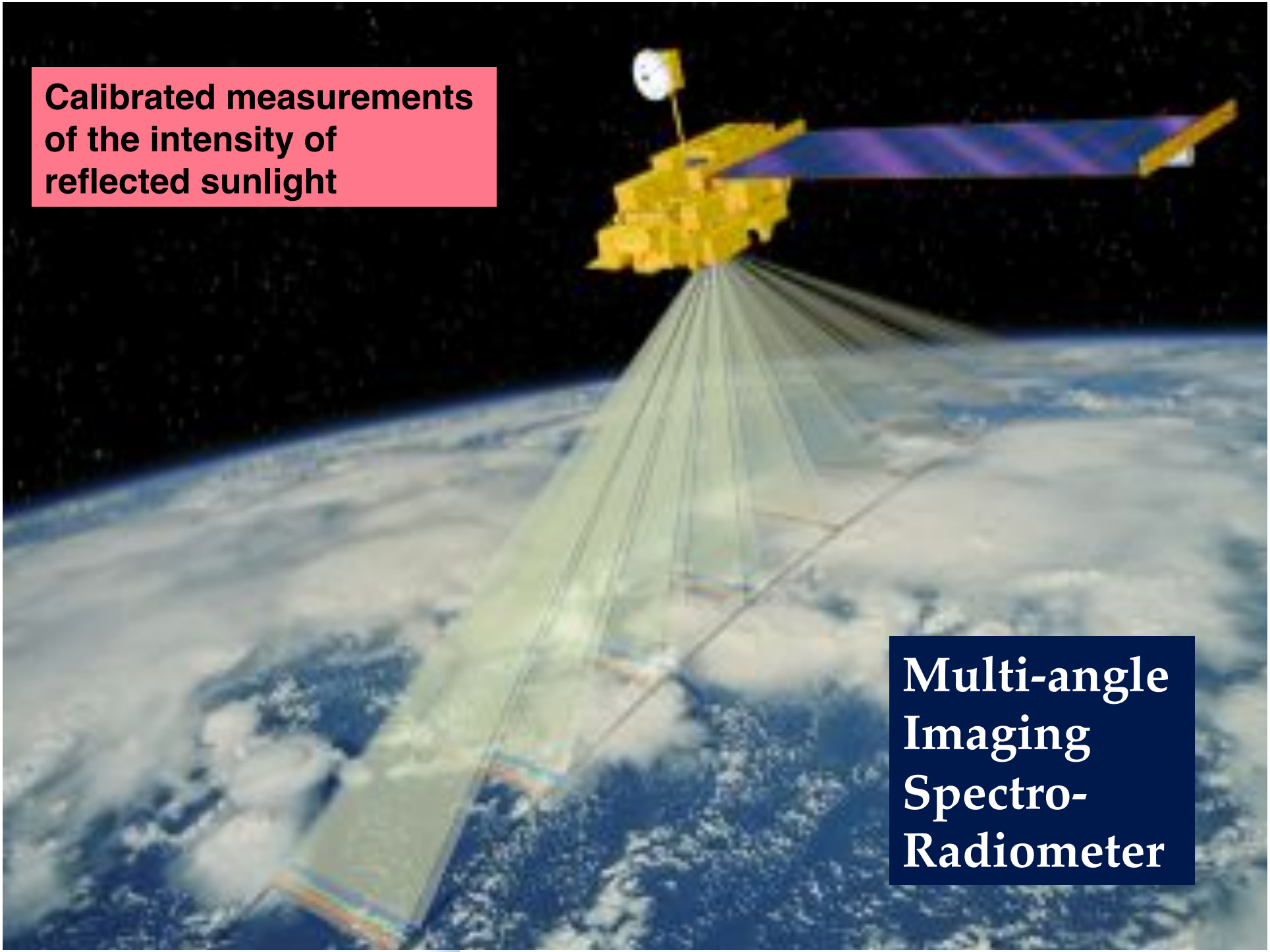
Calibrated measurements of the intensity of reflected sunlight
Multi-angle Imaging Spectro-Radiometer

MISR's partners on Terra

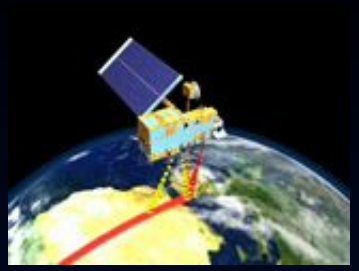

ASTER—The "zoom lens"

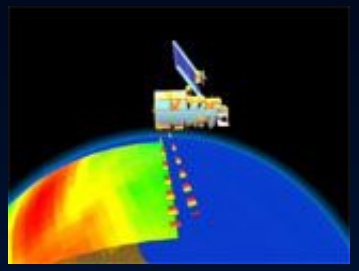

CERES—Global shortwave and longwave radiant energy budgets

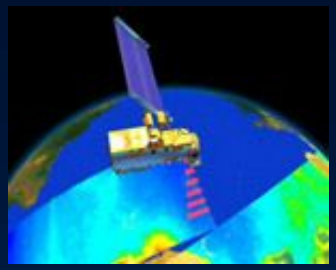

MODIS—Global, synoptic views of the atmosphere, land, and oceans

MOPITT—Global measurements of carbon monoxide (CO)

Why multi-angle?

1. Change in brightness, color, and contrast with angle helps distinguish different types of surfaces, clouds, and airborne particles (aerosols)

2. Oblique slant paths through the atmosphere enhance sensitivity to aerosols and thin cirrus

3. Changing geometric perspective provides 3-D views of clouds

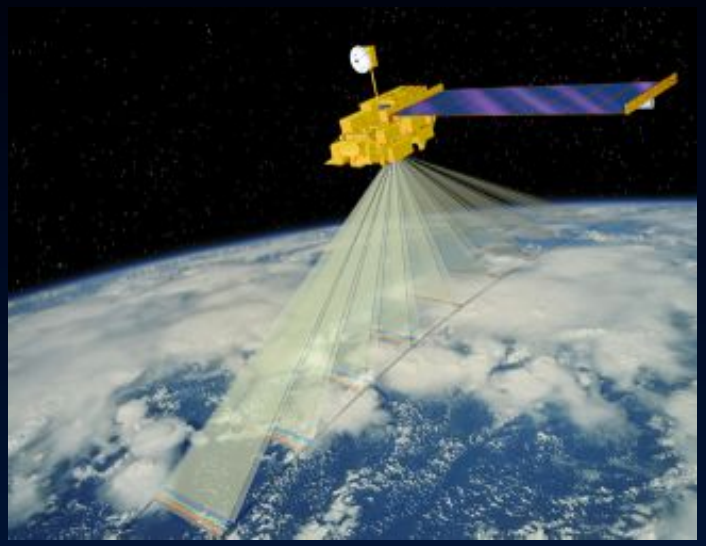

4. Time lapse from forward to backward views makes it possible to use clouds as tracers of winds aloft

5. Different angles of view enable sunglint avoidance or accentuation

6. Integration over angle is required to estimate hemispherical reflectance (albedo) accurately

Distributed by the Atmospheric Science Data Center
http://eosweb.larc.nasa.gov

Example areas of research

What is the abundance and distribution of different aerosol types, and how are these related to source locations and characteristics?

How does the surface respond to climate change or other disturbances? How does vegetation canopy structure affect photosynthetic and shortwave radiation fluxes?

How does 3-dimensional cloud structure affect our ability to relate cloud hydrological and radiative properties?

New ways of using MISR data are still likely to be discovered.

MISR instrument

Family portrait

The “V-9” optical bench

Undergoing test

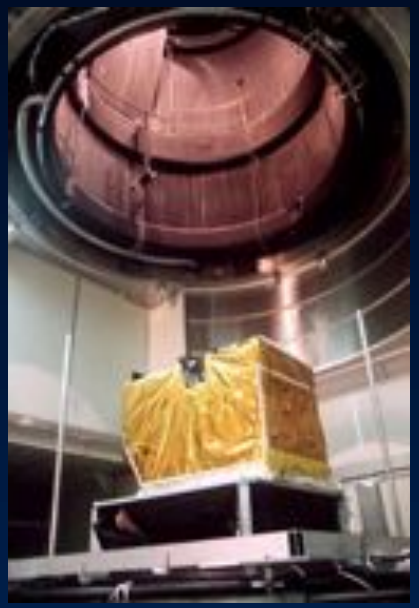

JPL’s Space Simulator Facility

MISR on Terra spacecraft

Terra launch 18 December 1999

Distributed by the Atmospheric Science Data Center
http://eosweb.larc.nasa.gov

MISR calibration

Absolute radiometric uncertainty 4%
Relative radiometric uncertainty 2%
Temporal stability 1%
Geolocation uncertainty 50 m
Camera-to-camera registration < 275 m

MISR On-Board Calibrator

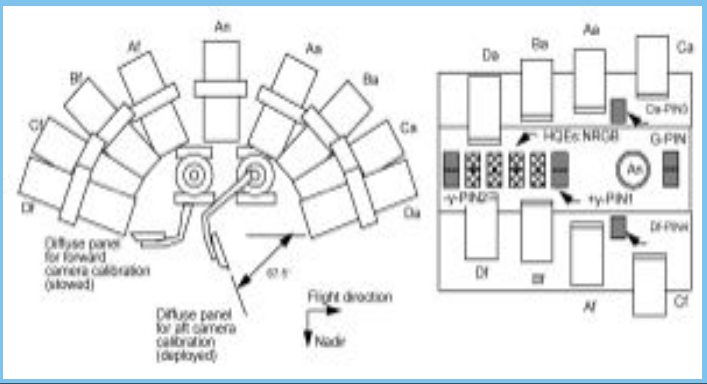

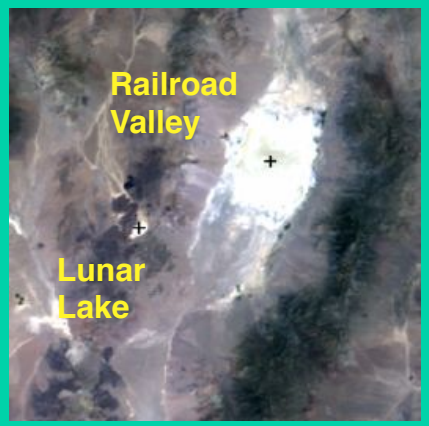

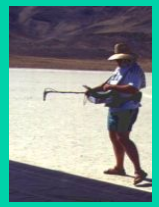

Vicarious calibrations and validations over desert playas and dark water sites

AirMISR

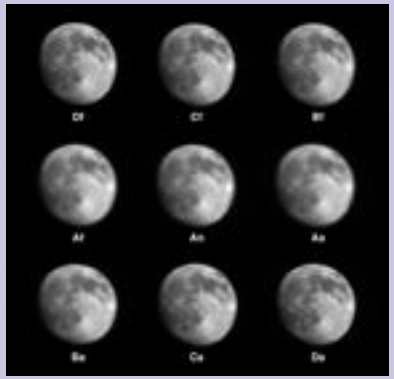

MISR lunar images

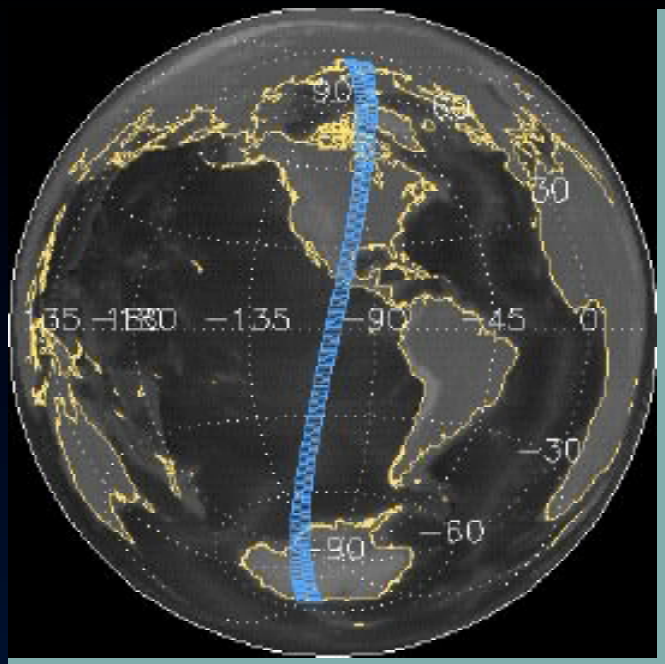

Calibration, geolocation, resampling, and co-registration occurs during Level 1 processing

Space Oblique Mercator projection

233 unique paths in 16-day repeat-cycle of Terra orbit

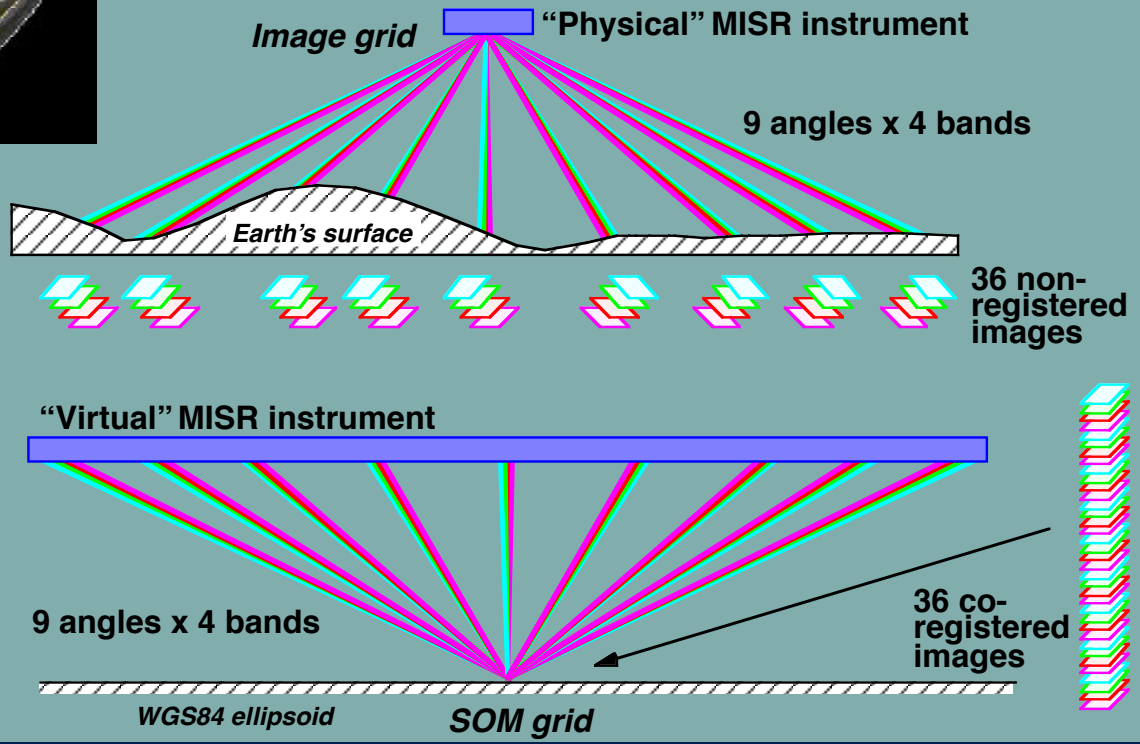

Instrument science modes

Global

- Pole-to-pole coverage on orbit dayside
- Full resolution in all 4 nadir bands, and red band of off-nadir cameras (275-m sampling)
- 4x4 pixel averaging in all other channels (1.1-km sampling)

Local

- Implemented for pre-established targets (1-2 per day)
- Provides full resolution in all 36 channels (275-m sampling)
- Pixel averaging is inhibited sequentially from camera Df to camera Da over targets approximately 300 km in length

Calibration

- Implemented bi-monthly
- Spectralon solar diffuser panels are deployed near poles and observed by cameras and a set of stable photodiodes

Distributed by the Atmospheric Science Data Center
http://eosweb.larc.nasa.gov

Objects along a camera line-of-sight have multiple “locations” on the Space Oblique Mercator grid

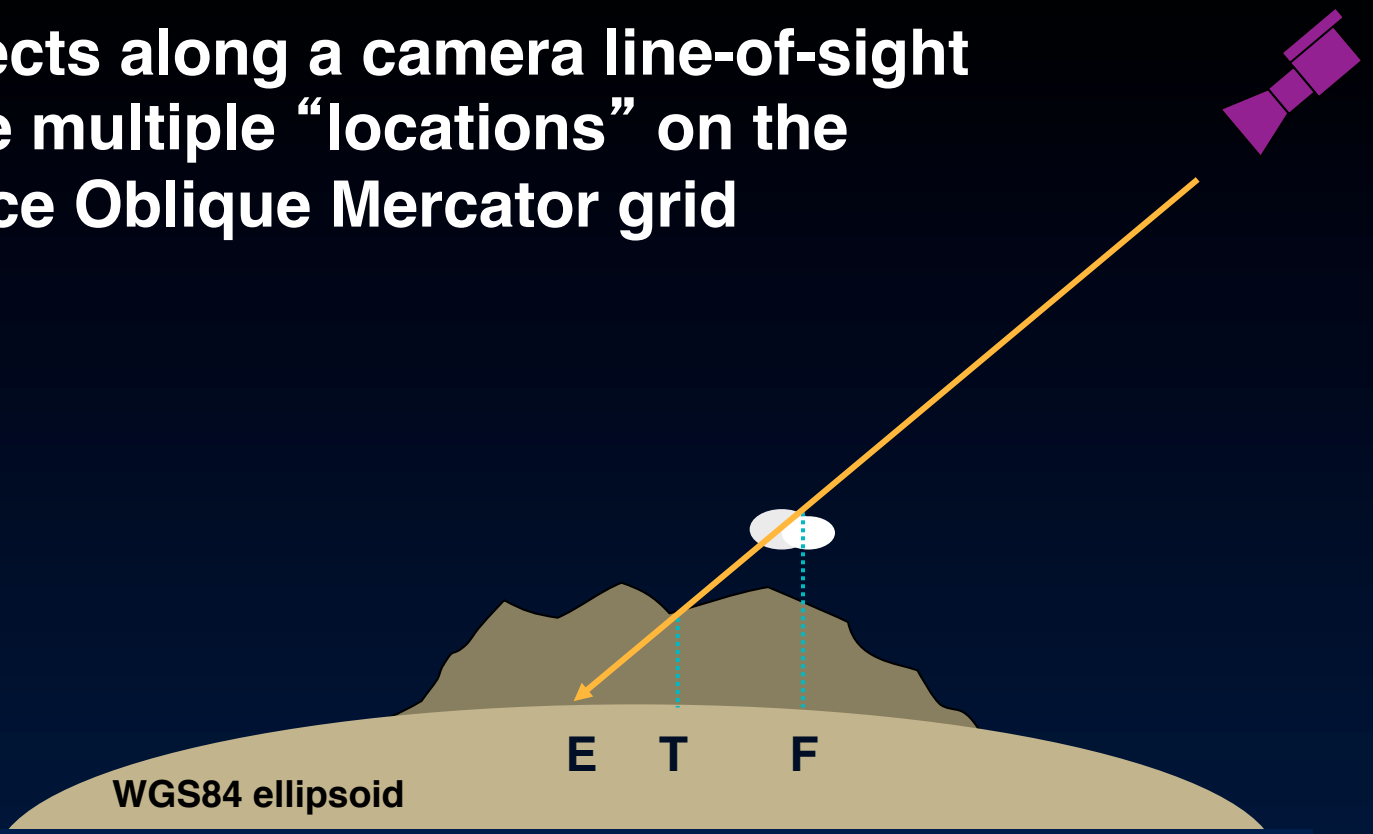

E = ellipsoid-projected location
T = terrain-projected location
F = feature-projected location

Camera-to-camera co-registration requires establishing a reference altitude

"Ellipsoid projection" is to the WGS84 ellipsoid
- performed during Level 1 processing
- used as input to stereoscopic processing

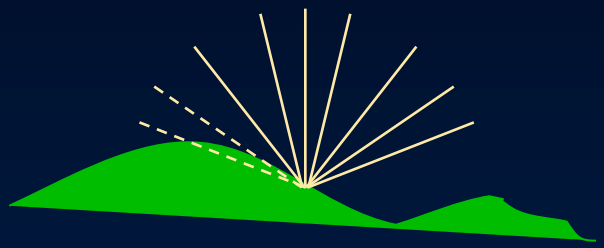

"Terrain projection " is to a digital elevation model
- performed during Level 1 processing
- used as input to aerosol/surface processing
- some views may be obscured

"Feature projection" uses stereoscopically derived cloud heights
- performed during Level 2 processing
- used as input to albedo and cloud classifiers processing

MISR data product generation

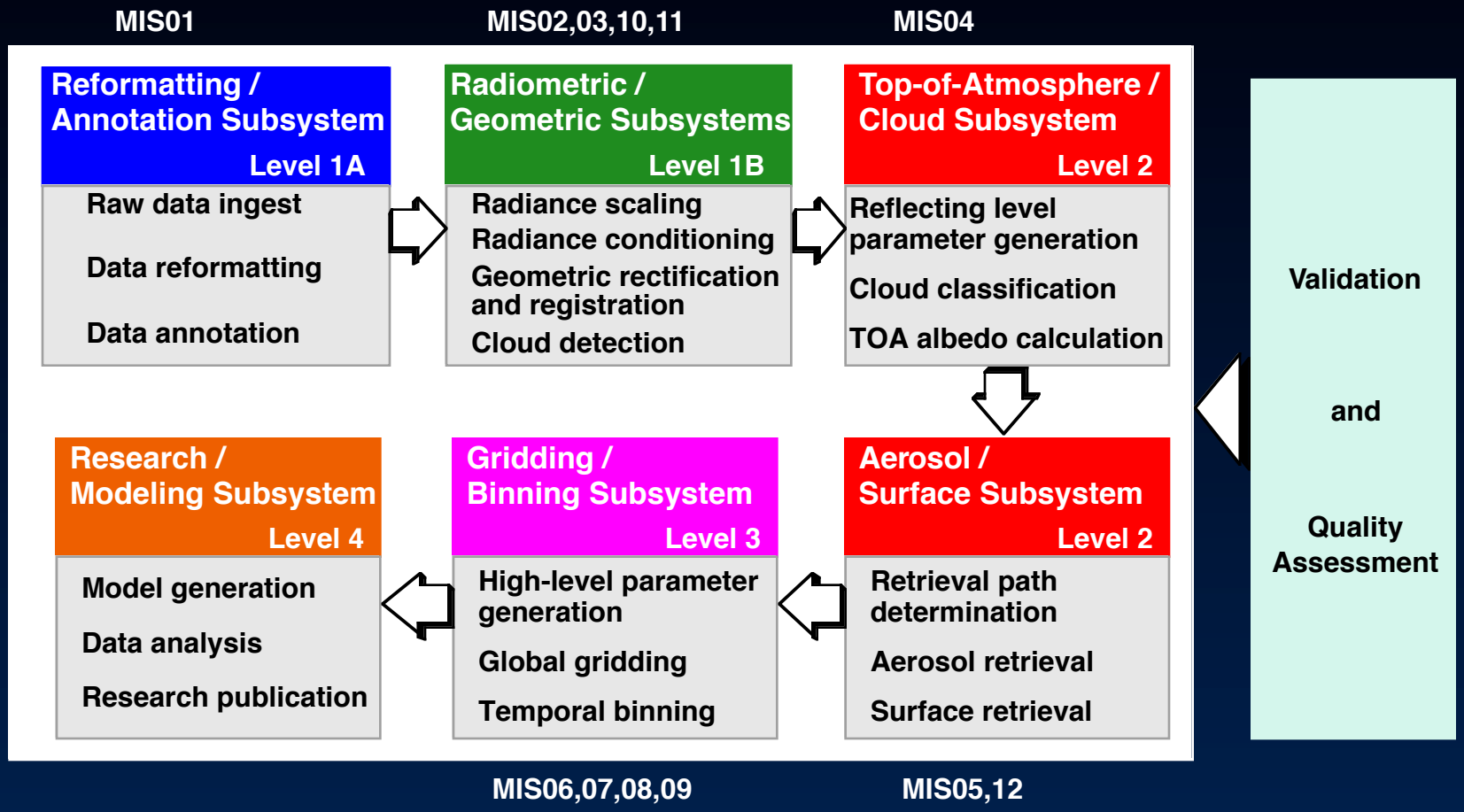

Level 1 Standard Products

Level 1 standard products

- Level 1A reformatted, annotated product
- Level 1B1 radiometric product
- Level 1B2 georectified radiance product, in two flavors:
  - ellipsoid
  - terrain (blocks containing land only)
- Level 1B2 browse (JPEG)
- Level 1B2 geometric parameters
- Level 1B2 radiometric camera-by-camera cloud mask

Space Oblique Mercator is used as the projection to minimize resampling distortions

Level 1 processing operates on each camera individually

A data "granule" is an entire pole-to-pole swath

L1B2 Georectified Radiance Product (MIS03)

Georectified (Earth-projected) radiance data

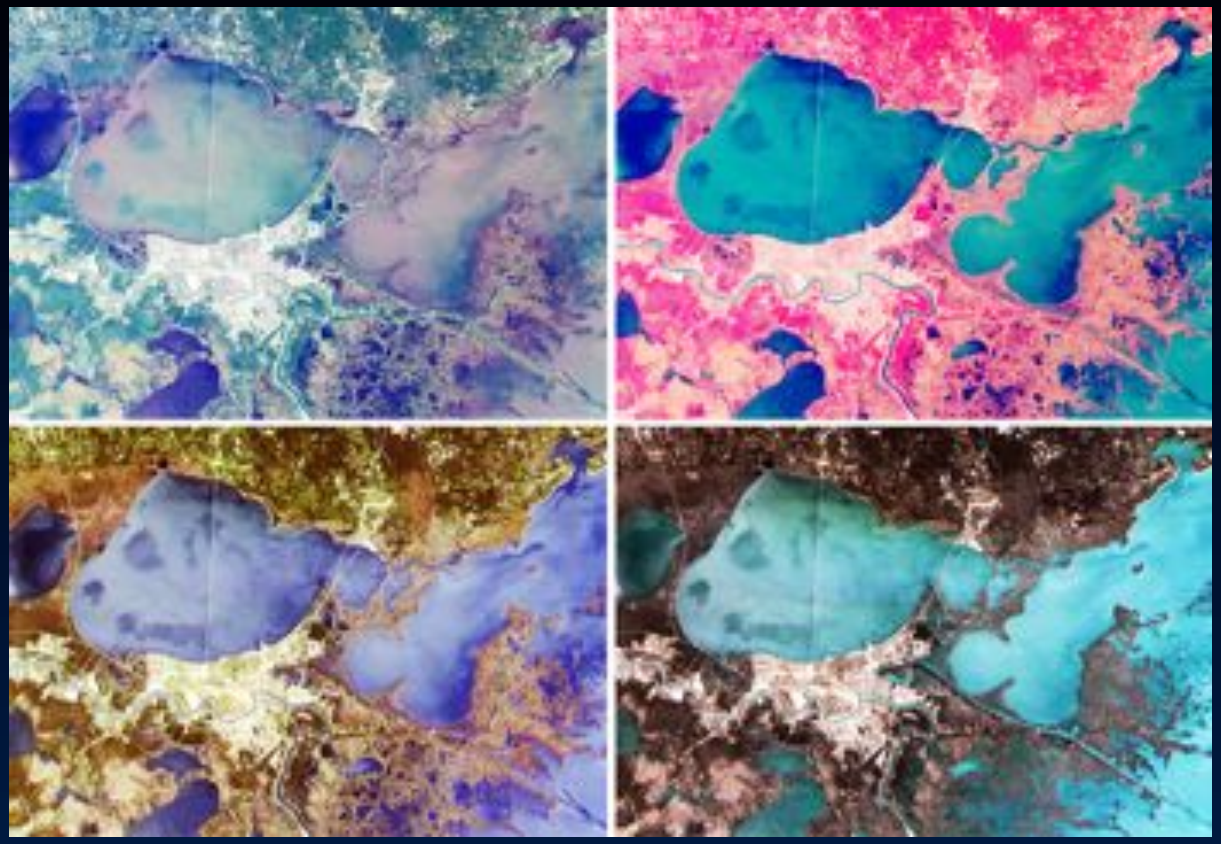

Multi-spectral, multi-angle composites of New Orleans and the Gulf Coast,
15 October 2001

CONTENTS

- Space-Oblique Mercator map-projected calibrated radiances and radiometric data quality indicators (RDQI)
- Scale factors to convert radiances to top-of-atmosphere BRF's

Changes in scene brightness with angle

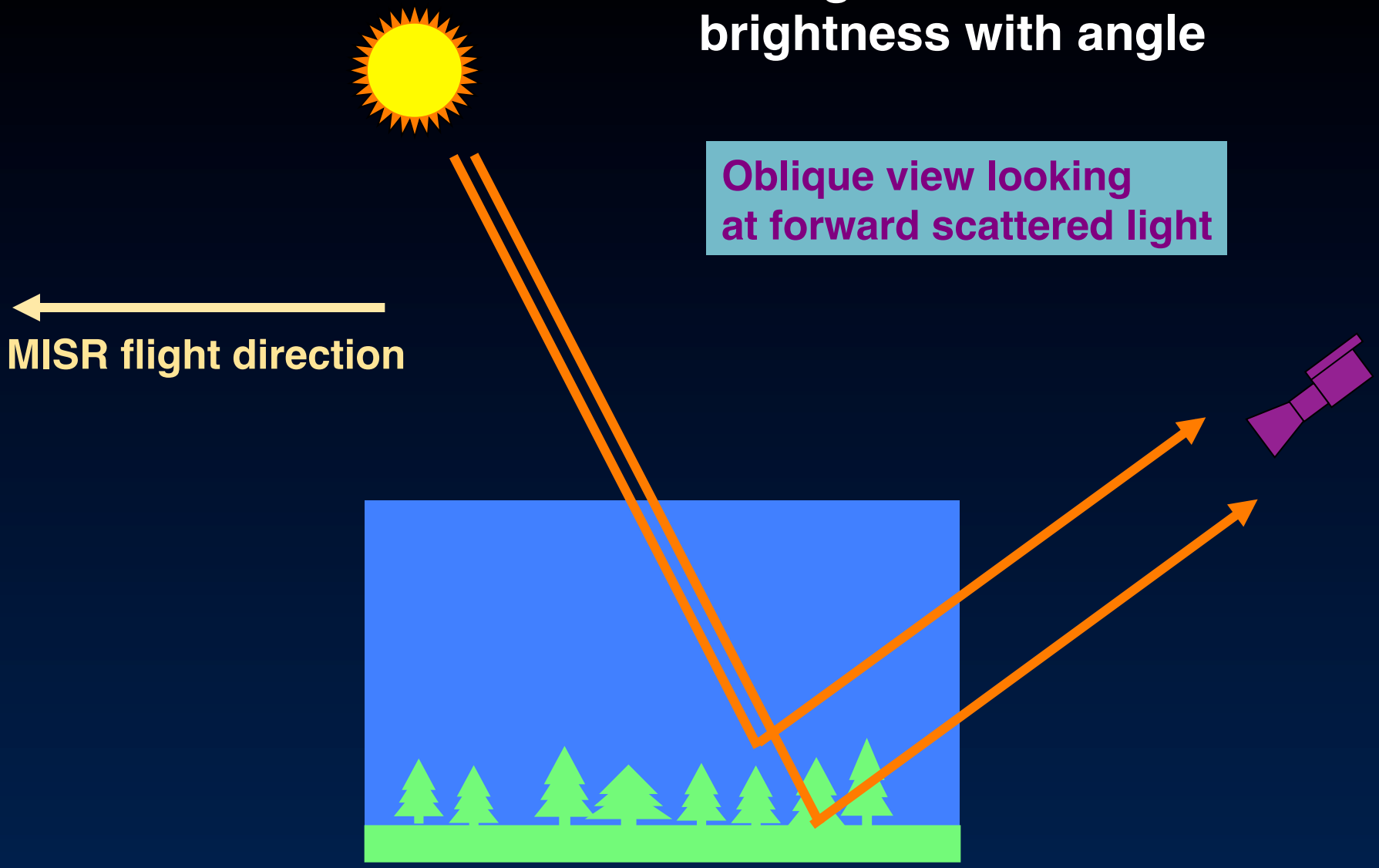

Changes in scene brightness with angle

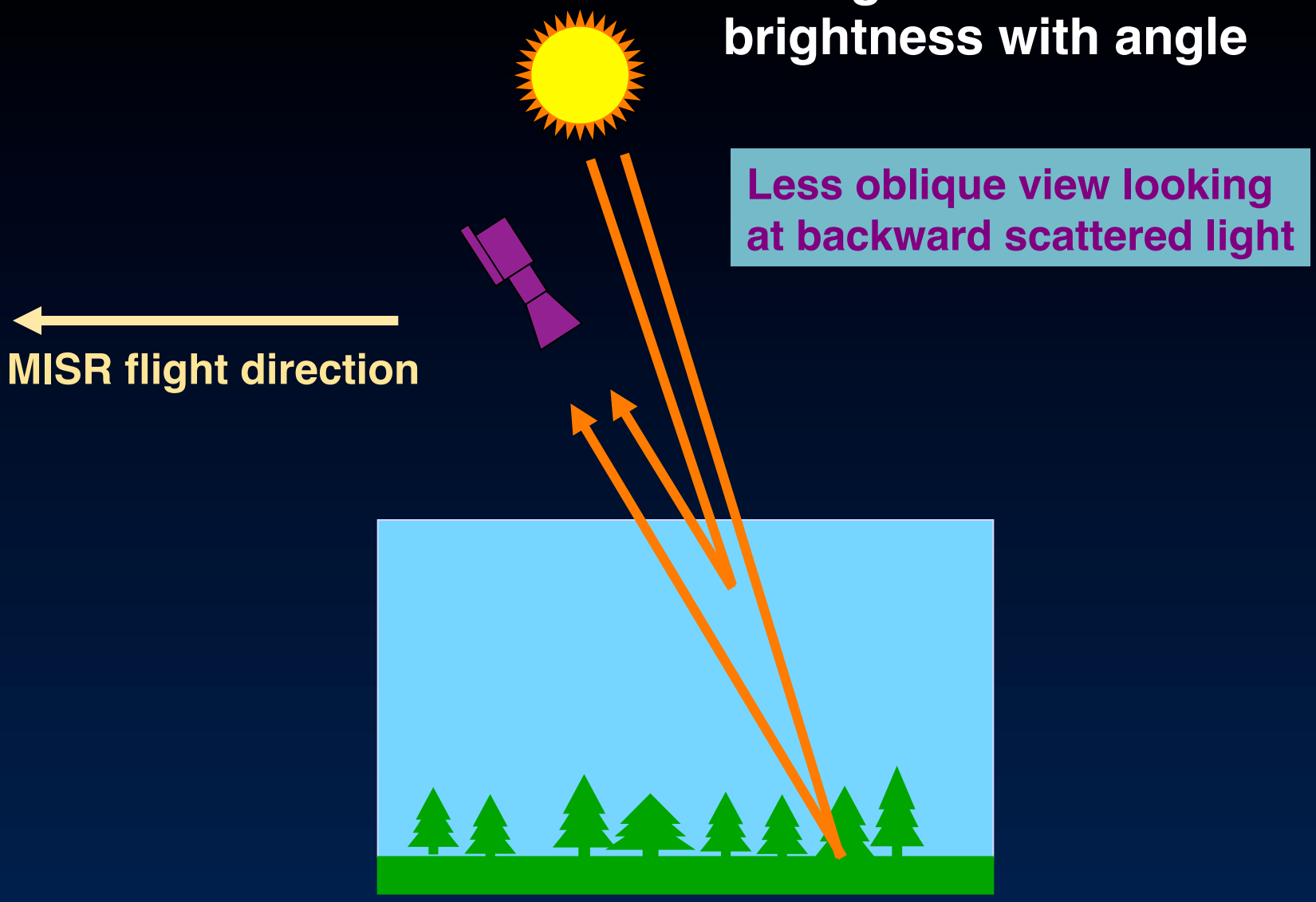

Visualizing surface texture

multi-spectral compositing

Hudson and James Bays
24 February 2000

nadir blue band

nadir green band

nadir red band

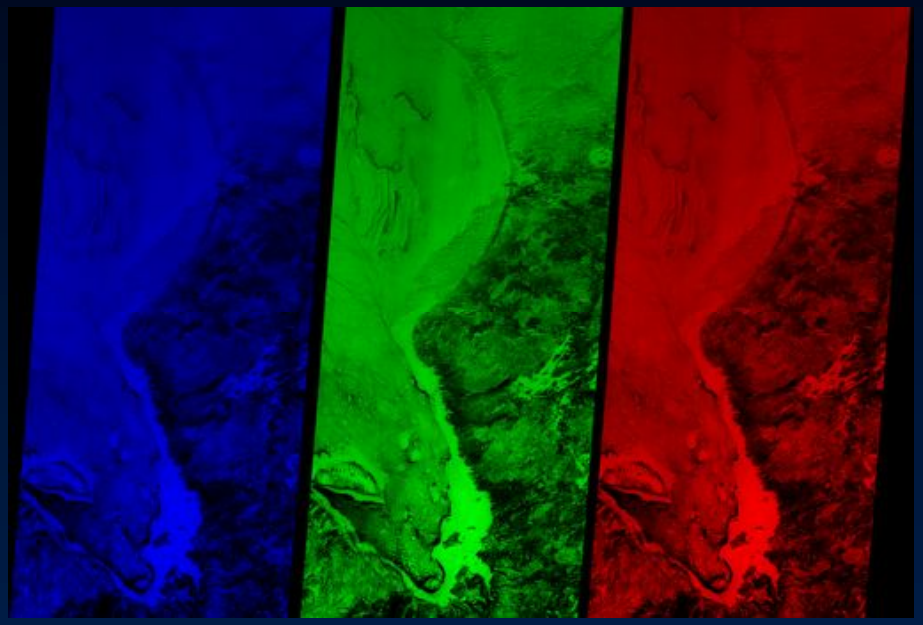

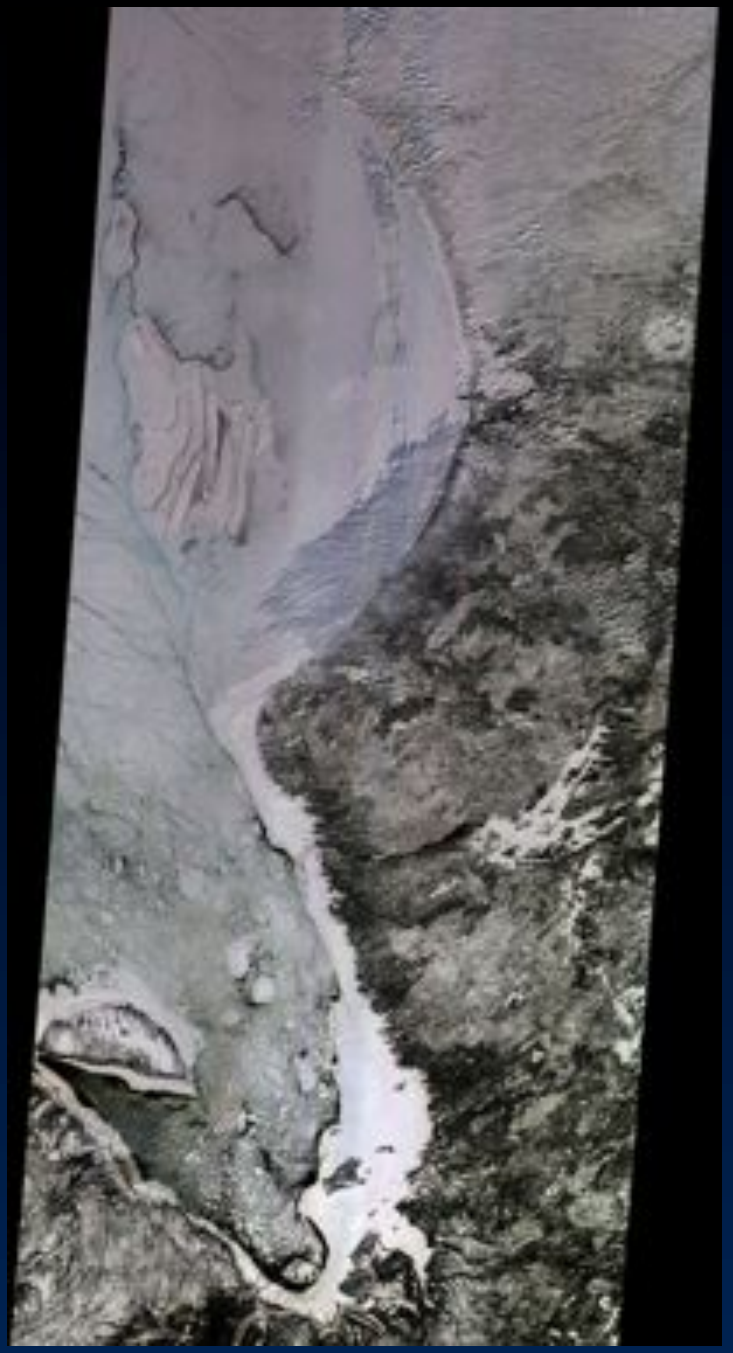

Visualizing surface texture

multi-angle compositing

Hudson and James Bays
24 February 2000

70° forward red band | nadir red band | 70° backward red band

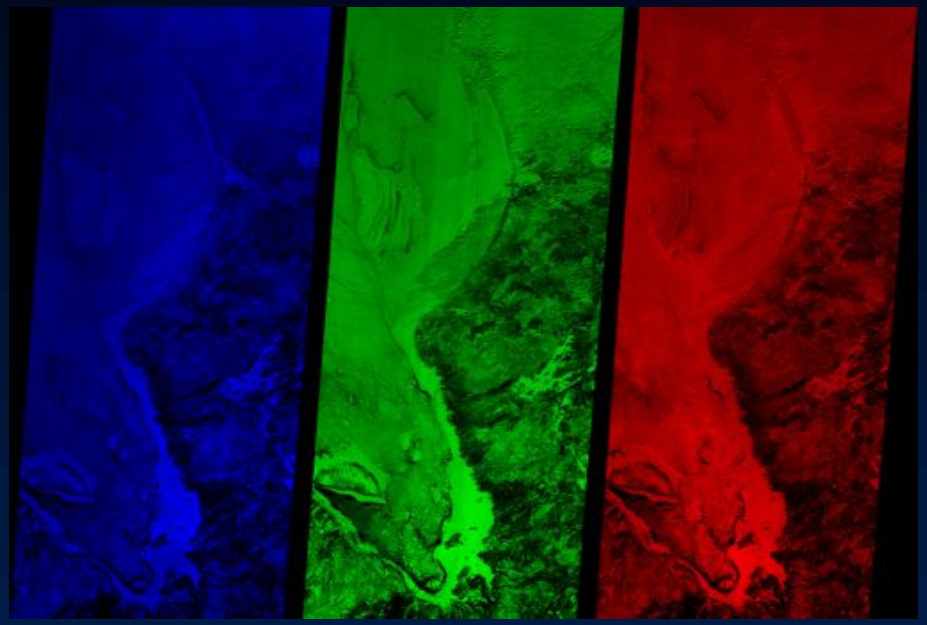

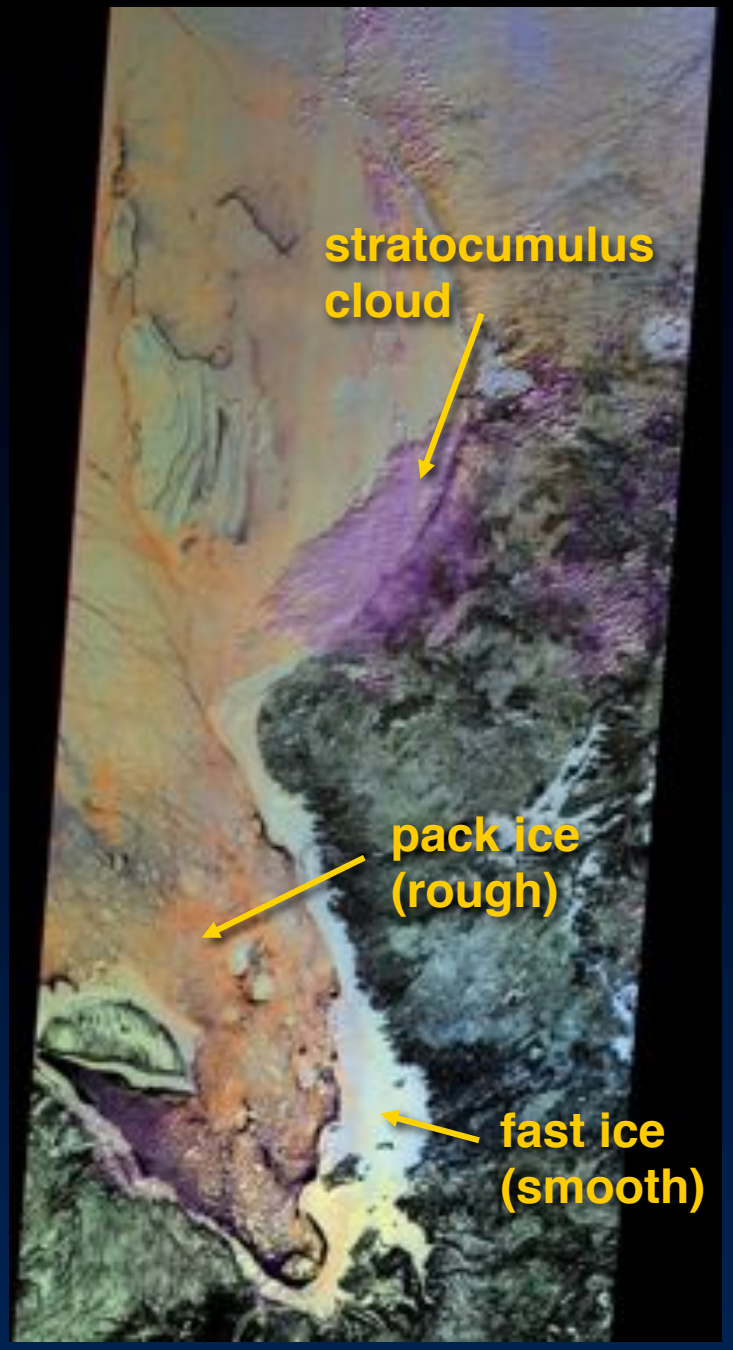

Cloud and ice bidirectional reflectances

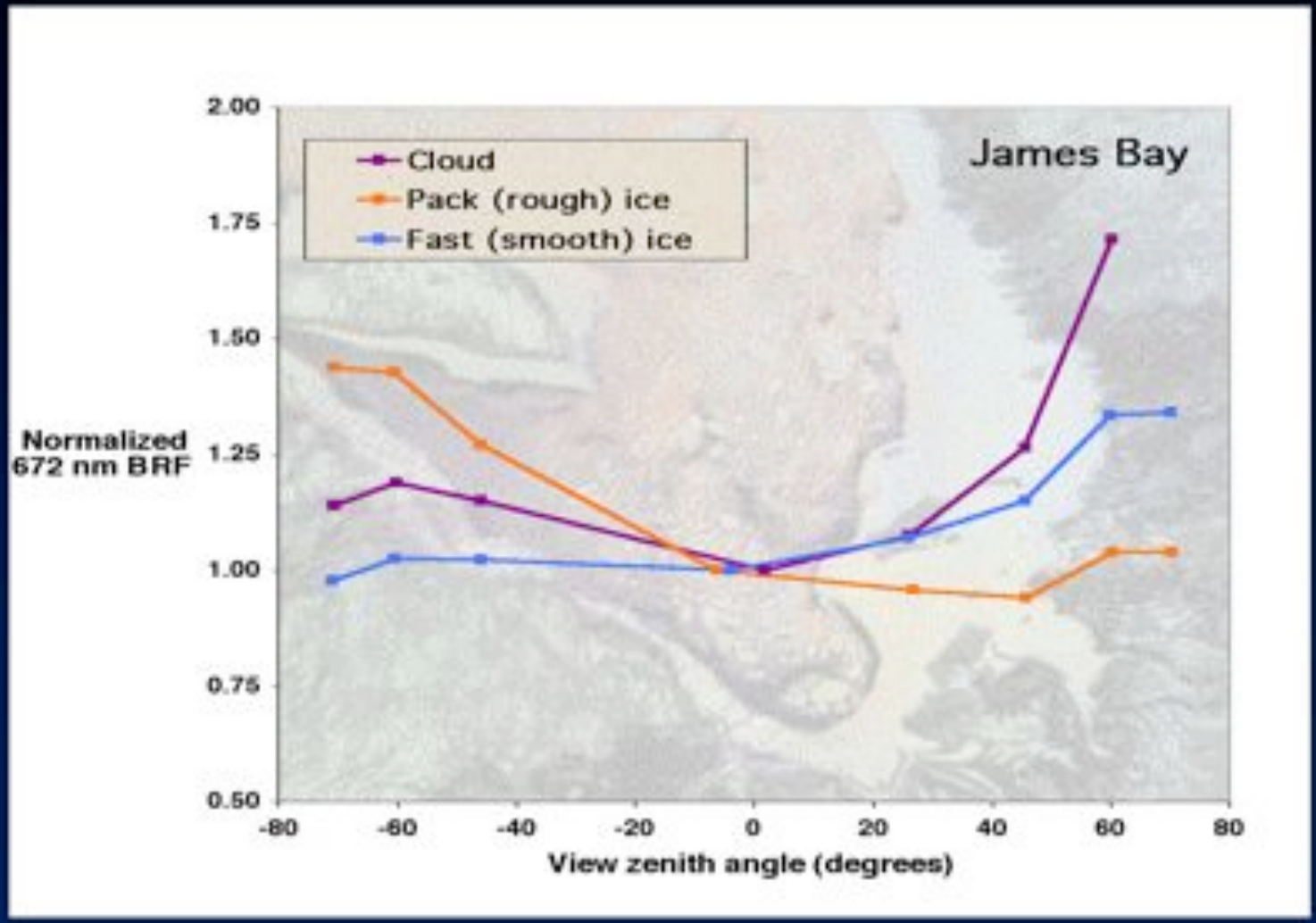

Changes in ice sheet surface roughness

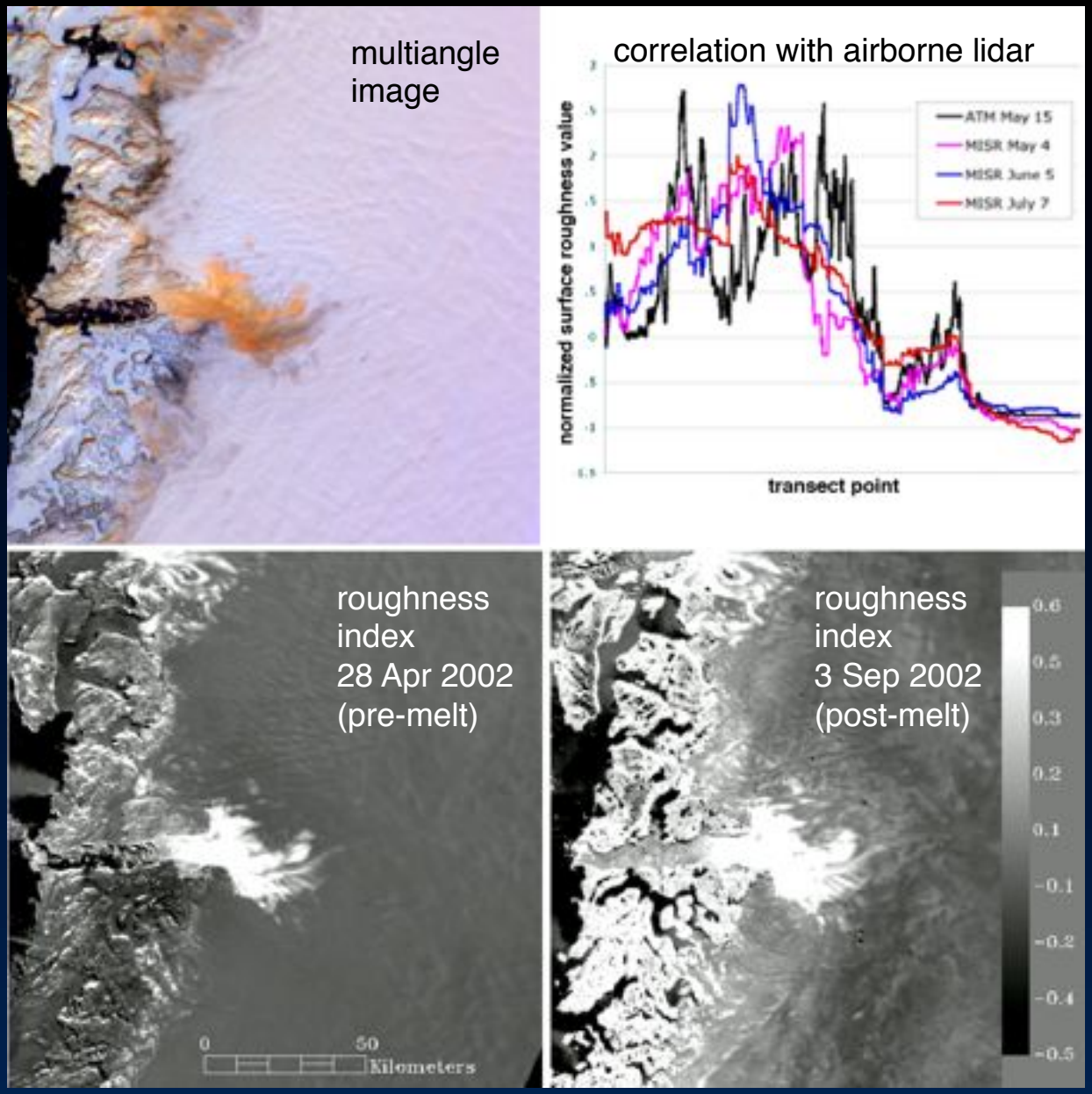

Surface morphology is influenced by ice accumulation, ablation, and melt.

Spatial and temporal changes in ice sheet roughness are revealed in MISR data.

Jakobshavn glacier, Greenland

A. Nolin et al. (2002), TGARS

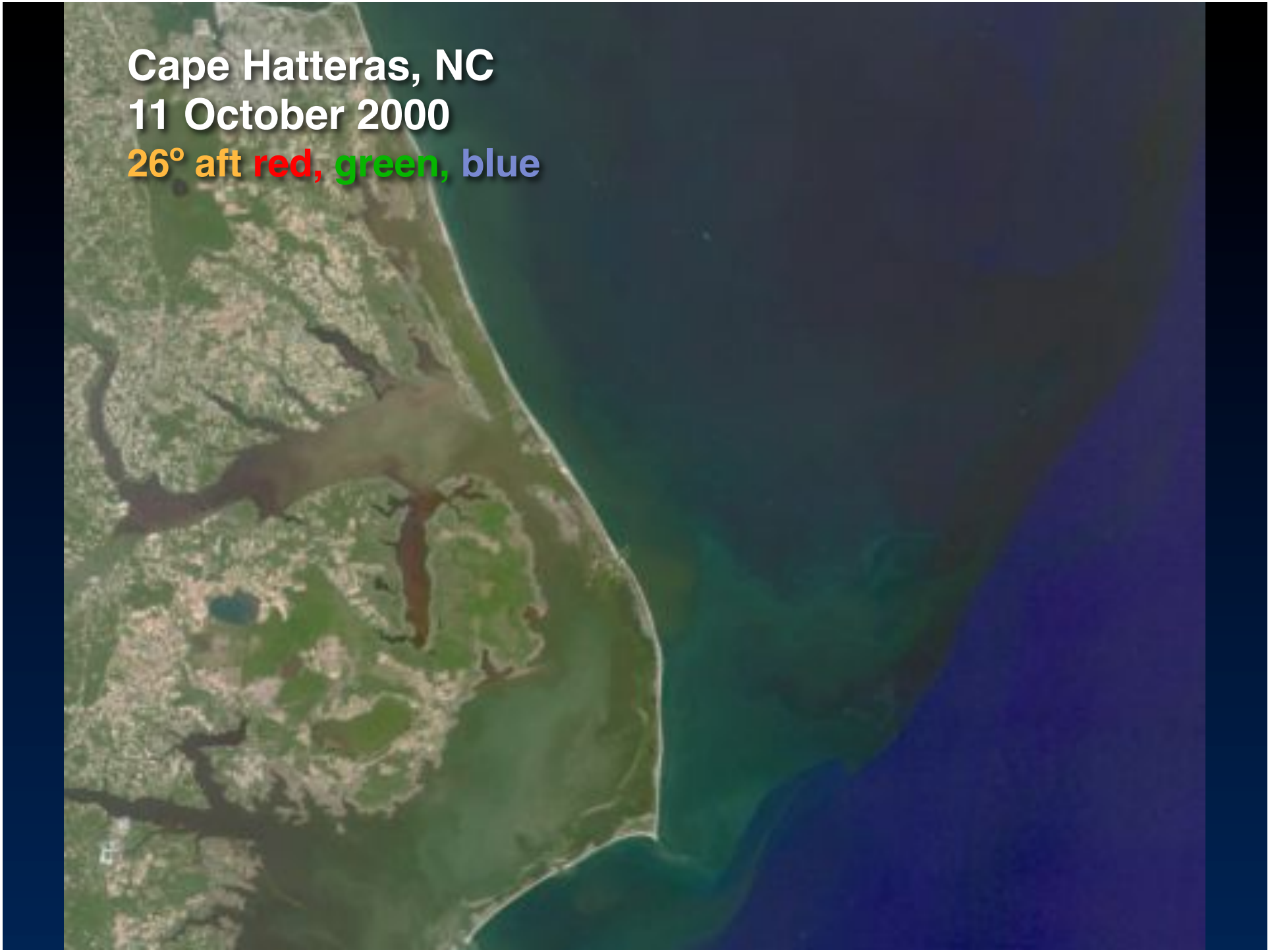
Cape Hatteras, NC
11 October 2000
26° aft red, green, blue

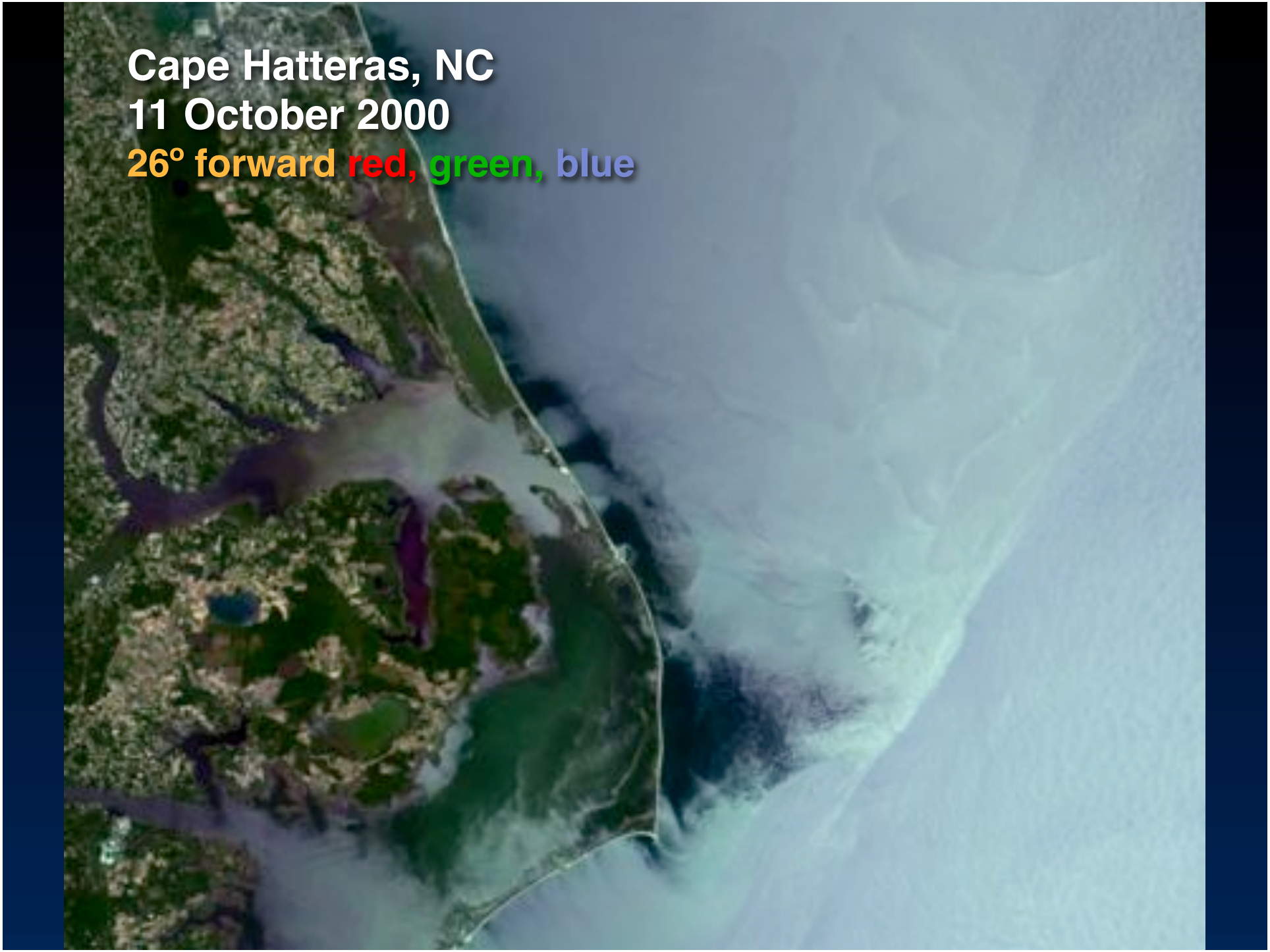
Cape Hatteras, NC
11 October 2000
26° forward red, green, blue

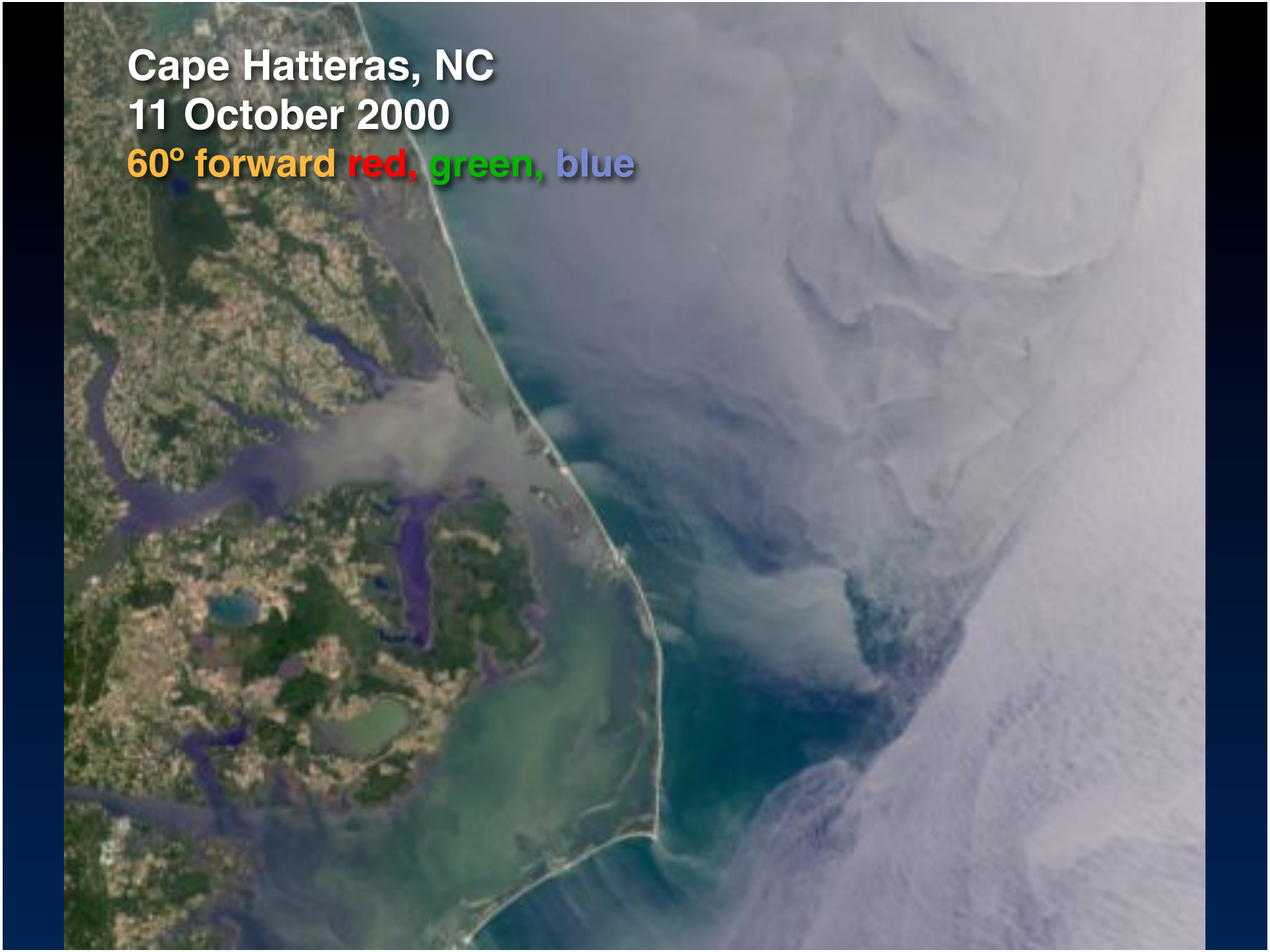
Cape Hatteras, NC
11 October 2000
60° forward red, green, blue

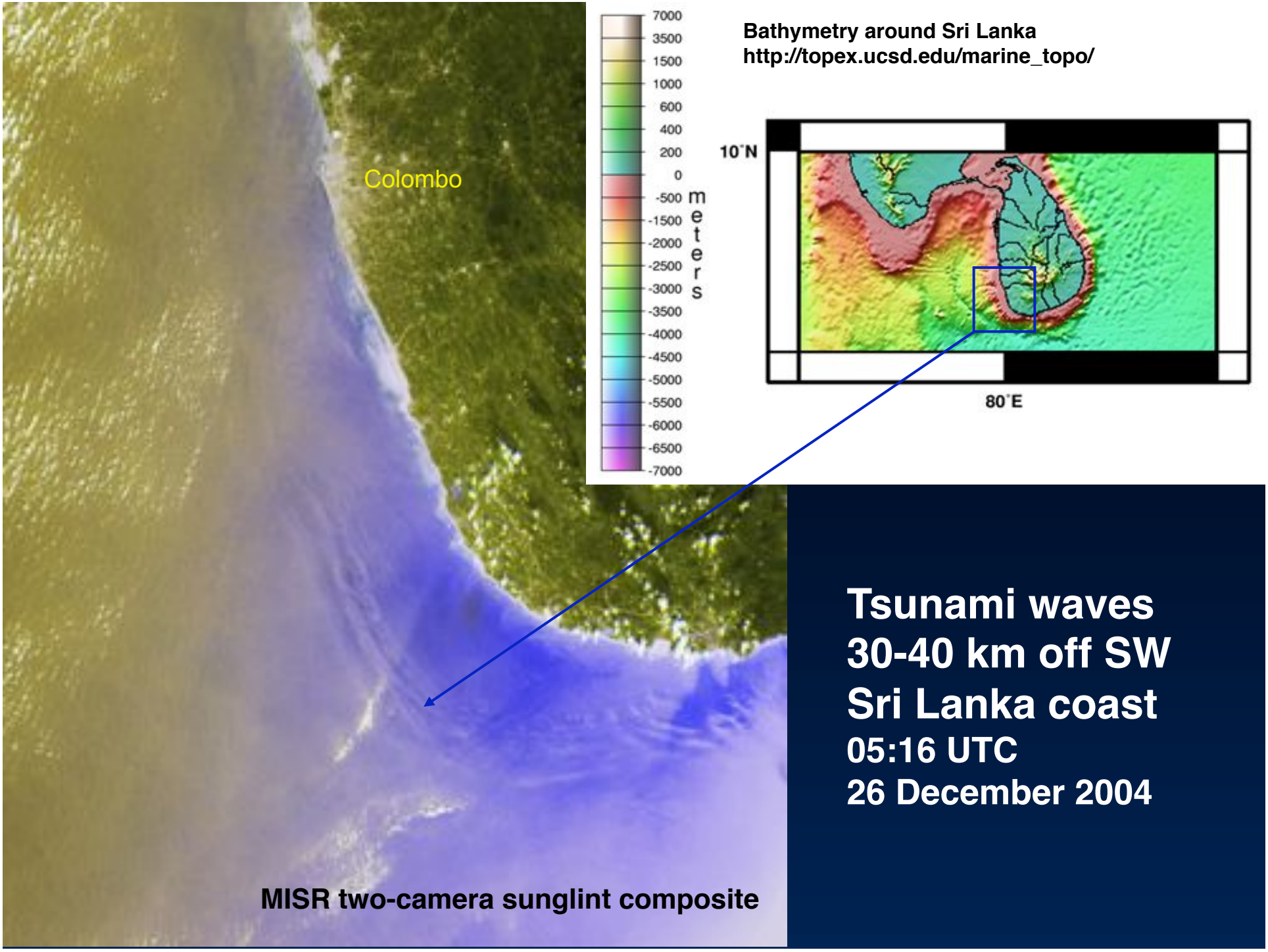
Colombo
7000
3500
1500
1000
600
400
200
0
-500
-1500
-2000
-2500
-3000
-3500
-4000
-4500
-5000
-5500
-6000
-6500
-7000
meters
Bathymetry around Sri Lanka
http://topex.ucsd.edu/marine_topo/
10˚N
80˚E
MISR two-camera sunglint composite
Tsunami waves
30-40 km off SW
Sri Lanka coast
05:16 UTC
26 December 2004

San Joaquin Valley
3 January 2001

Nadir (An)

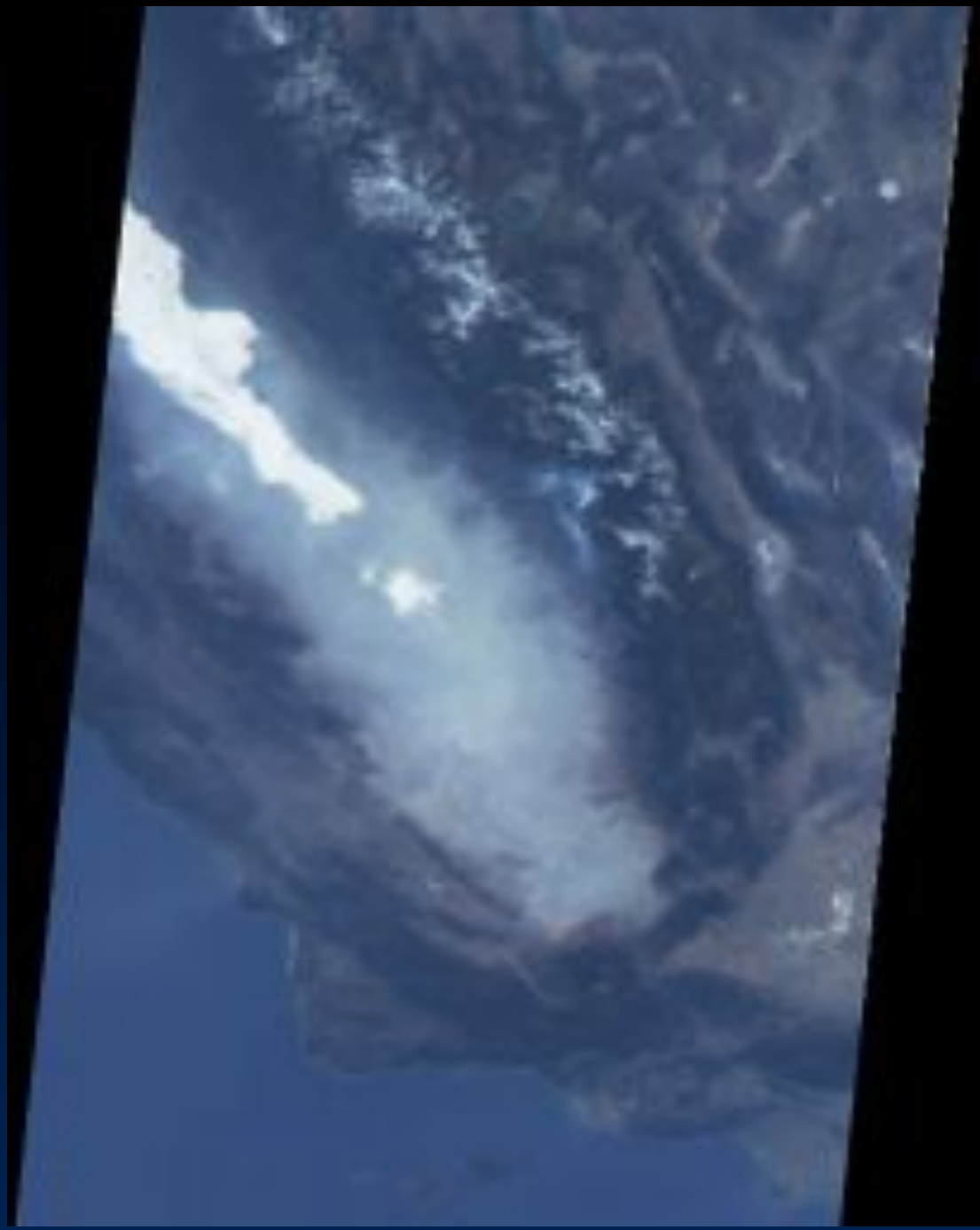

San Joaquin Valley
3 January 2001

70° forward (Df)

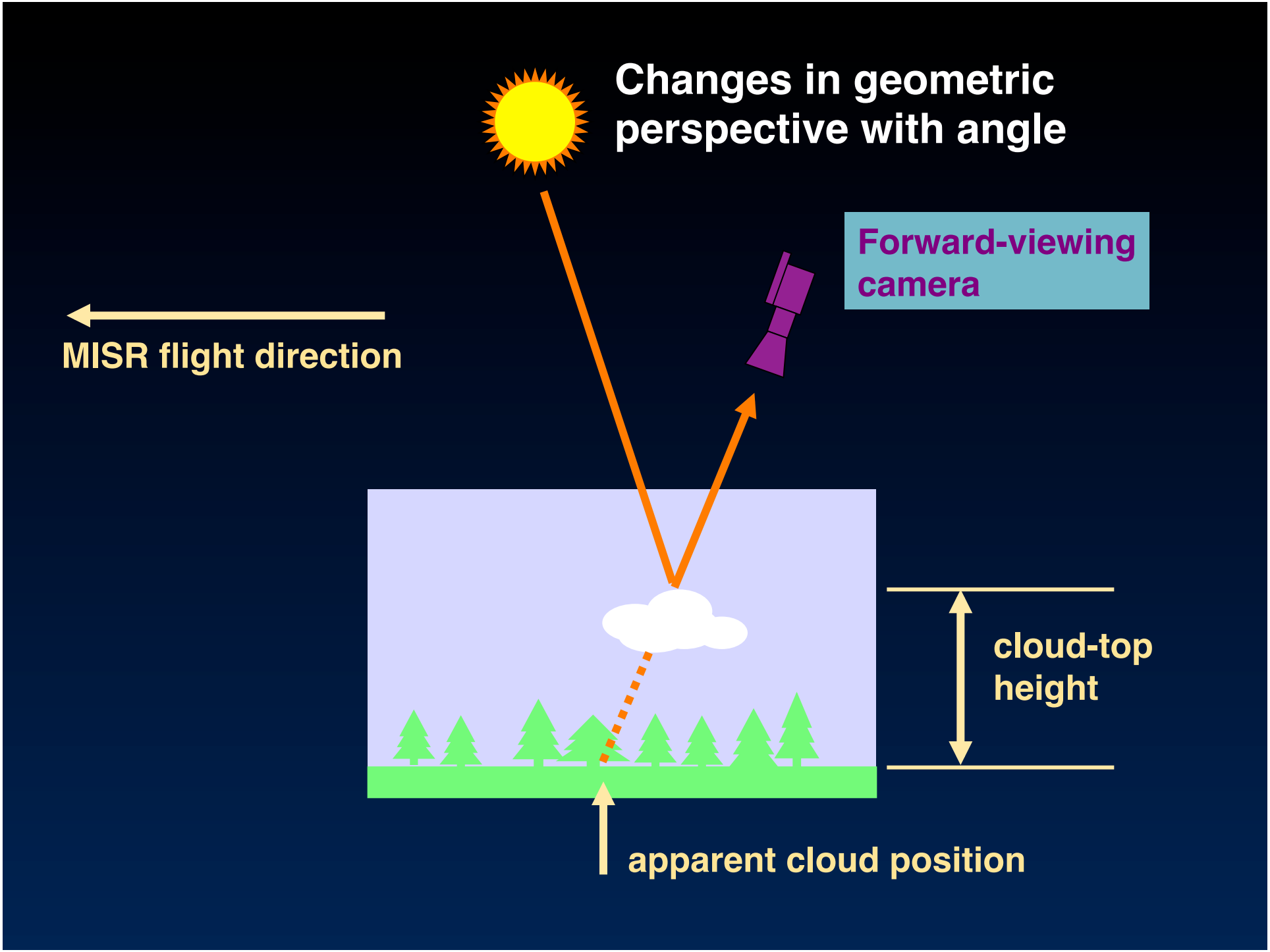
Changes in geometric perspective with angle
Forward-viewing camera
MISR flight direction
cloud-top height
apparent cloud position

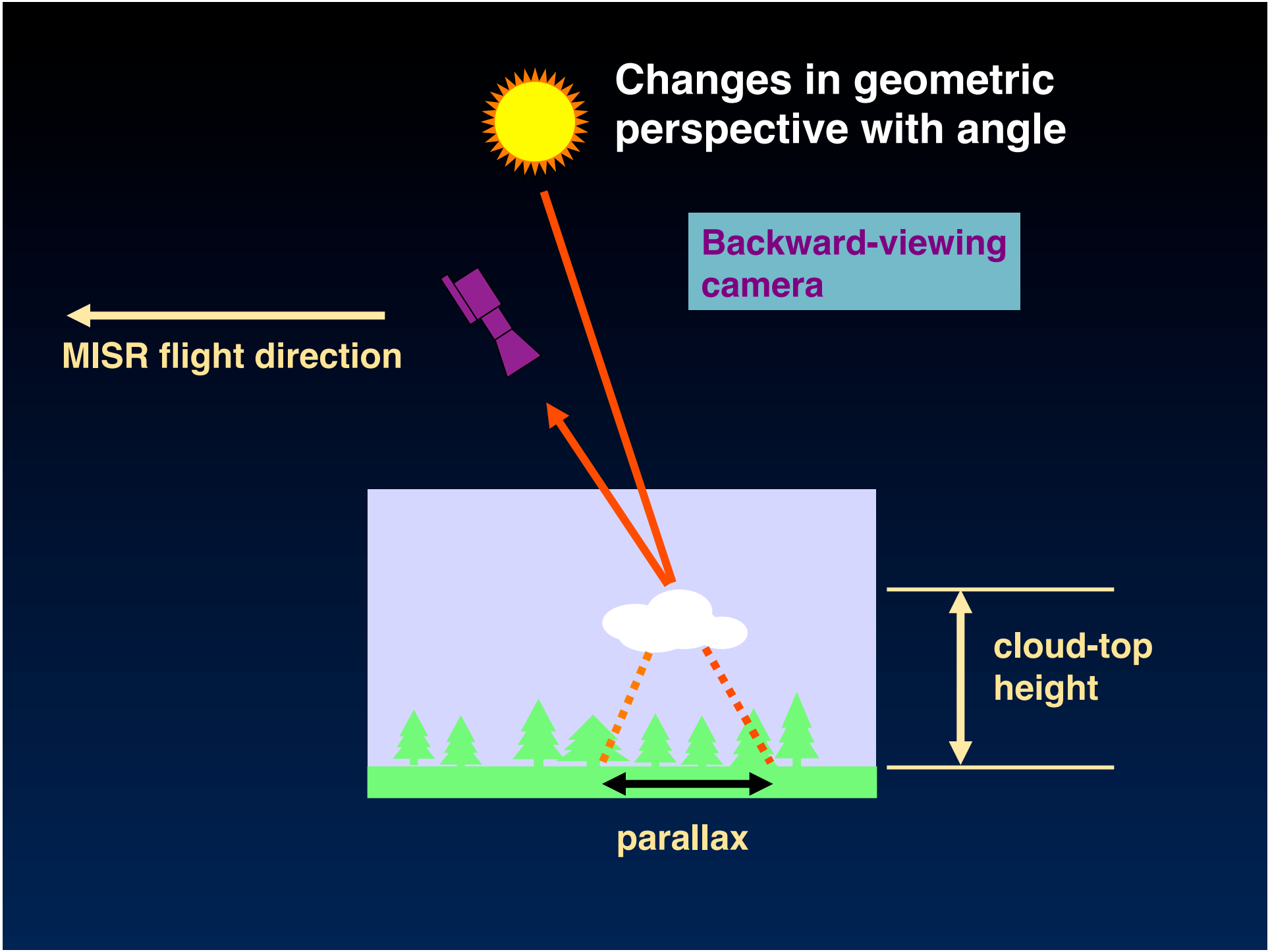
Changes in geometric perspective with angle
Backward-viewing camera
MISR flight direction
cloud-top height
parallax

Georgian Bay, Ontario, 6 March 2000

Nadir (An)

70° forward (Df)

Georgian Bay, Ontario, 6 March 2000

Nadir (An)

60° forward (Cf)

Georgian Bay, Ontario, 6 March 2000

Nadir (An)

46° forward (Bf)

Georgian Bay, Ontario, 6 March 2000

Nadir (An)

26° forward (Af)

Cloud reflection in water

Less oblique MISR camera

MISR flight direction

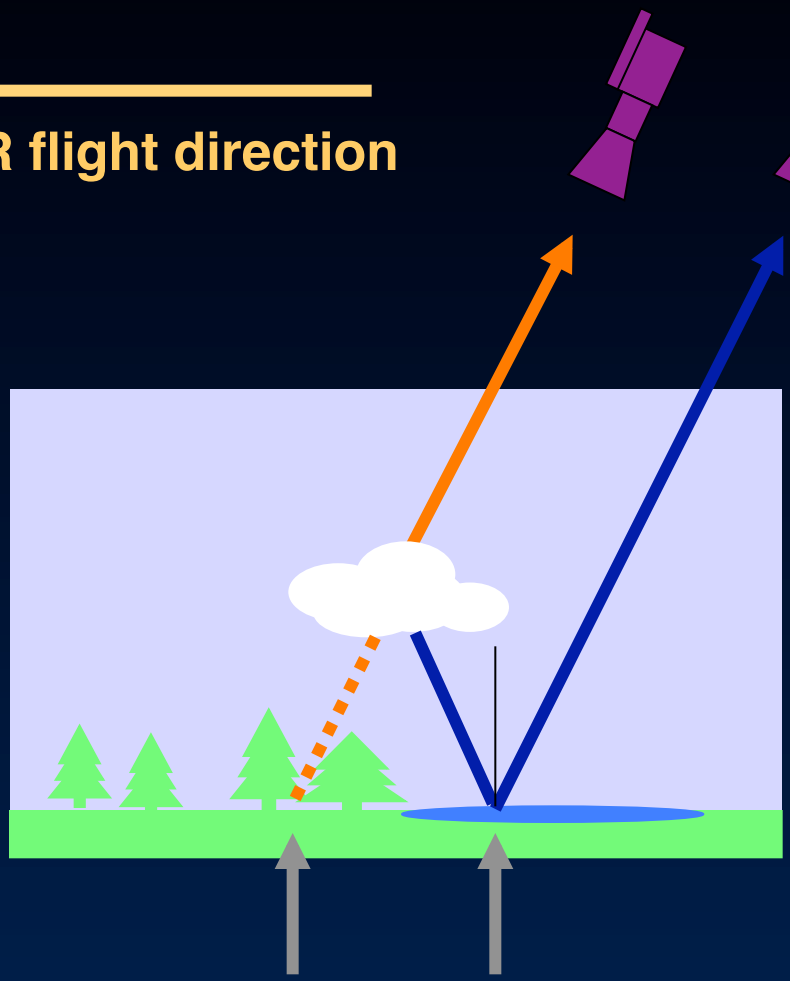

apparent cloud position

reflection position

Cloud reflection in water

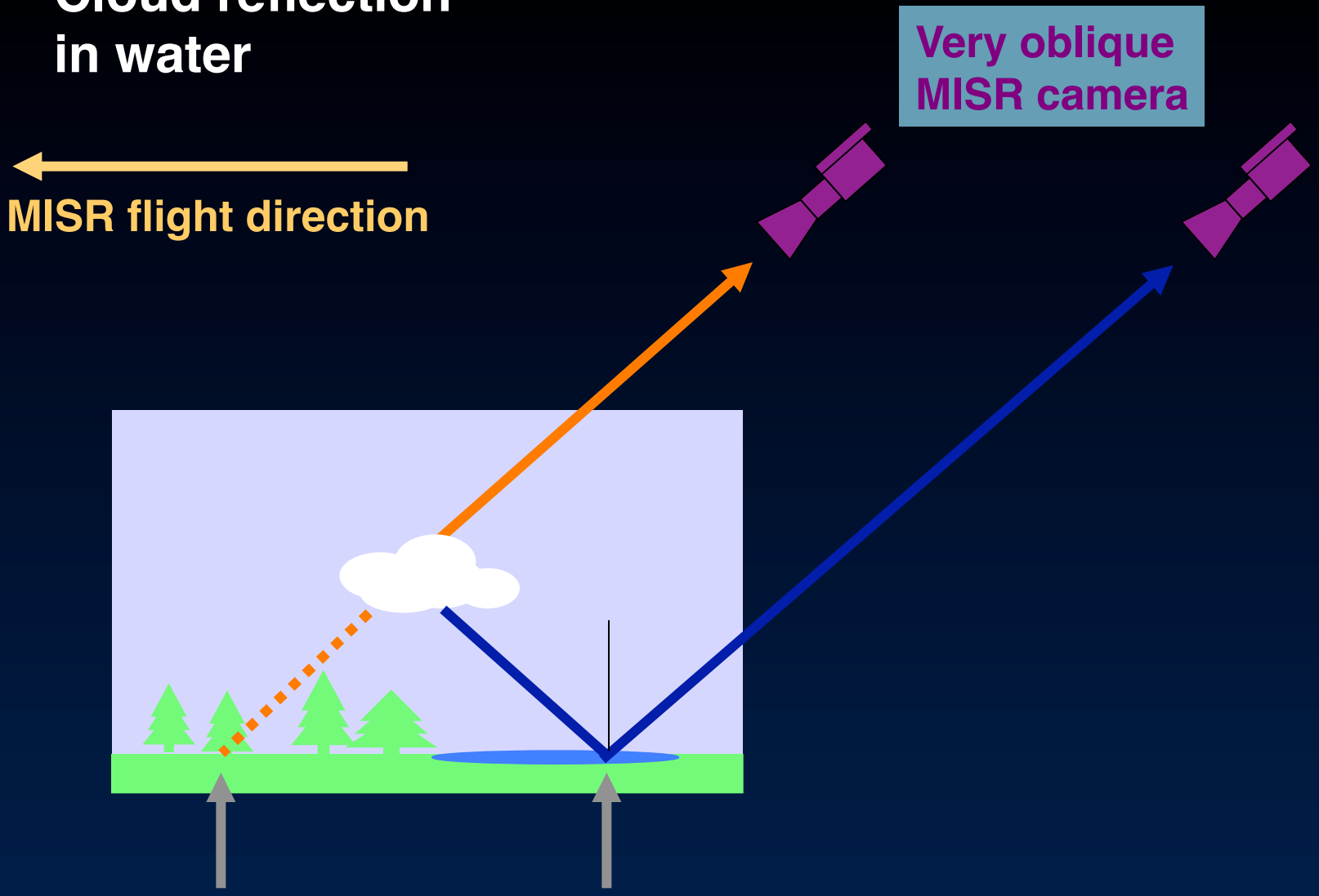

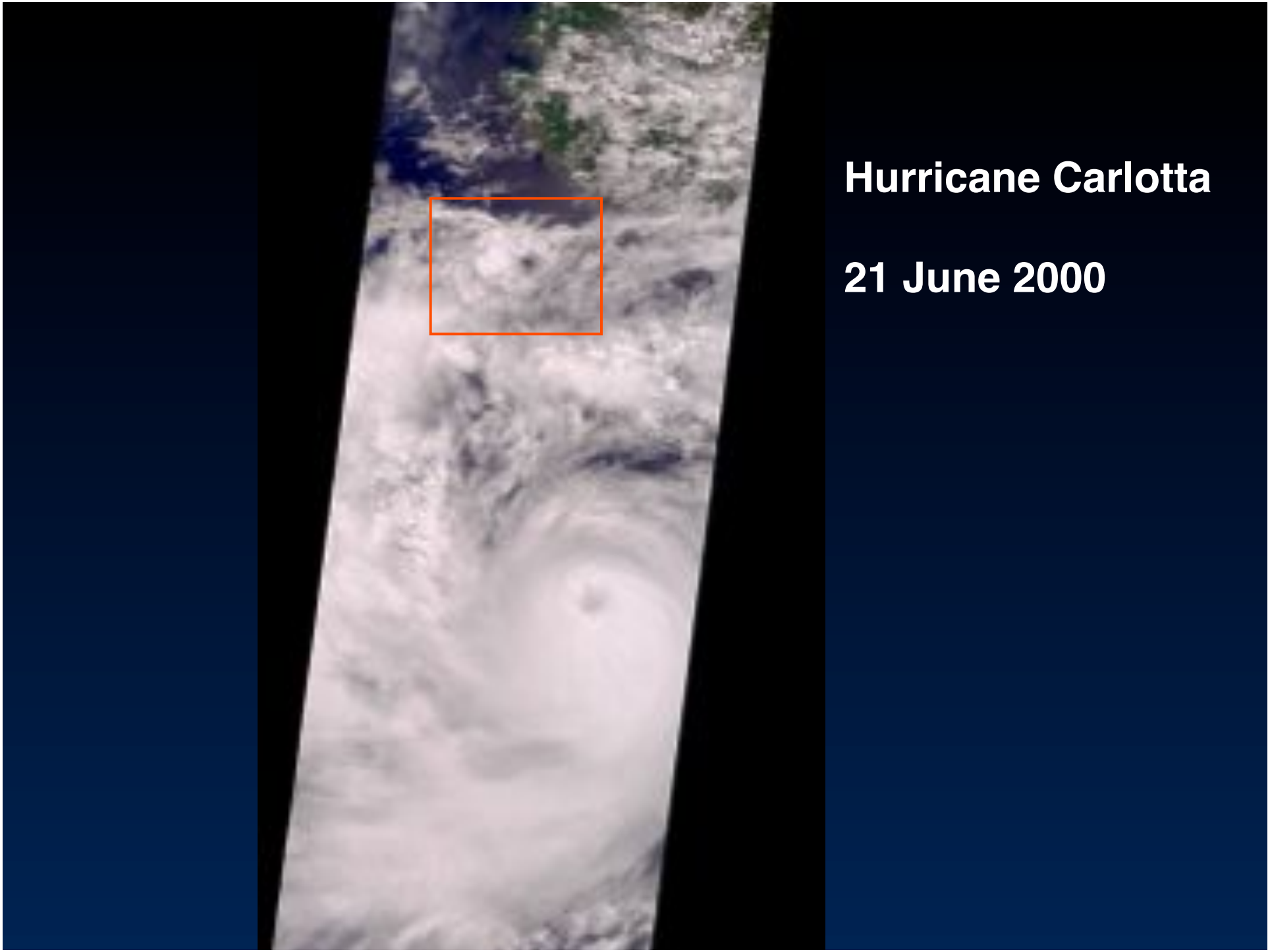
Hurricane Carlotta
21 June 2000

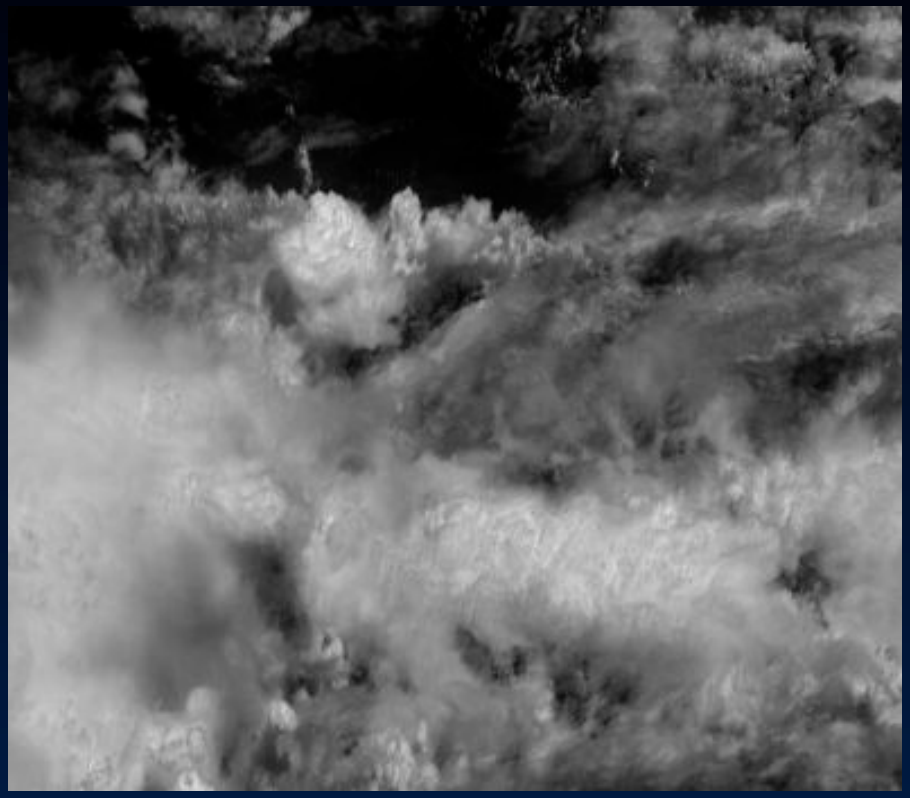

Multi-angle "fly-over" of Hurricane Carlotta thunderclouds

19 August 2000

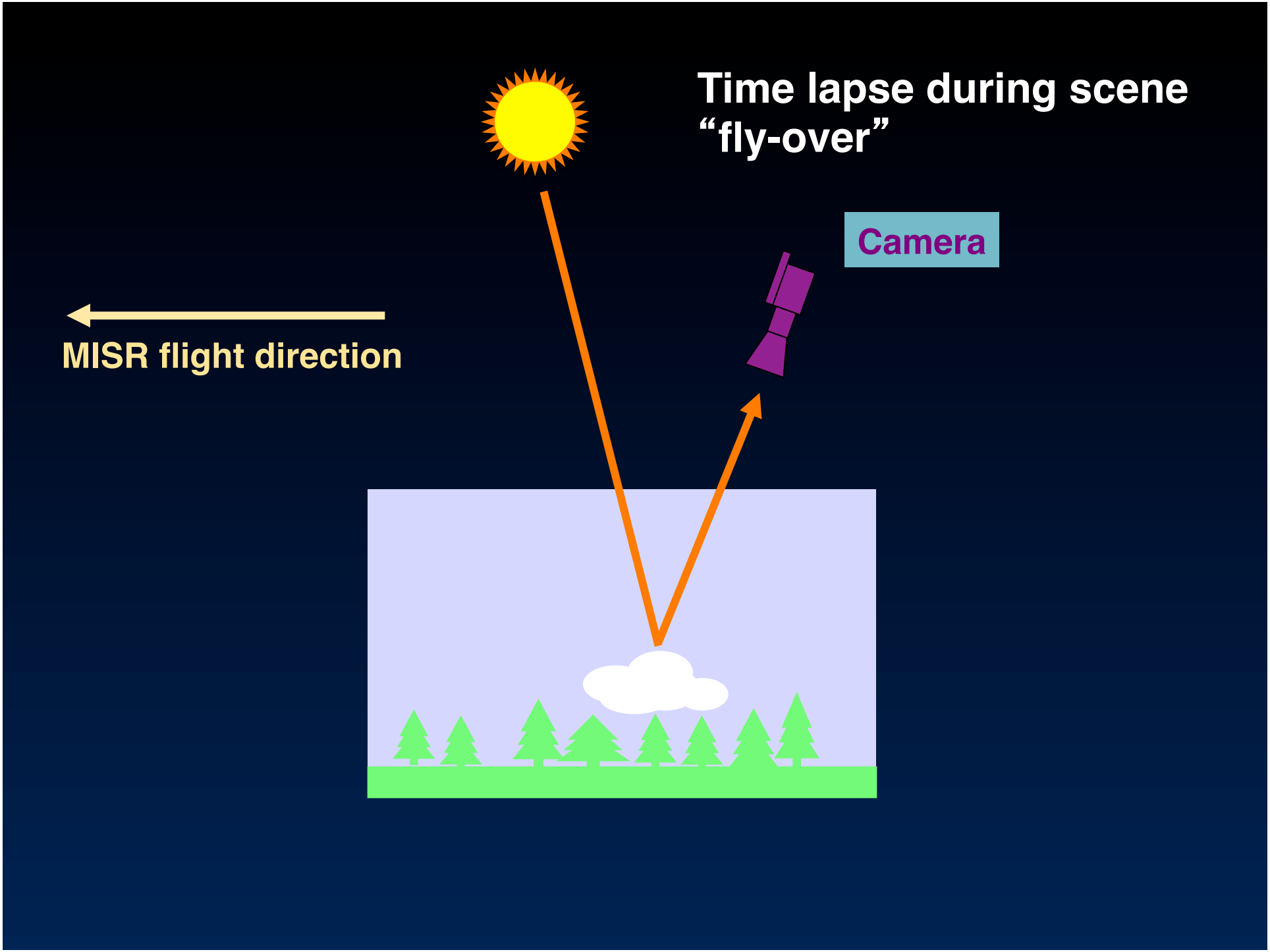
Time lapse during scene
“fly-over”
Camera
MISR flight direction

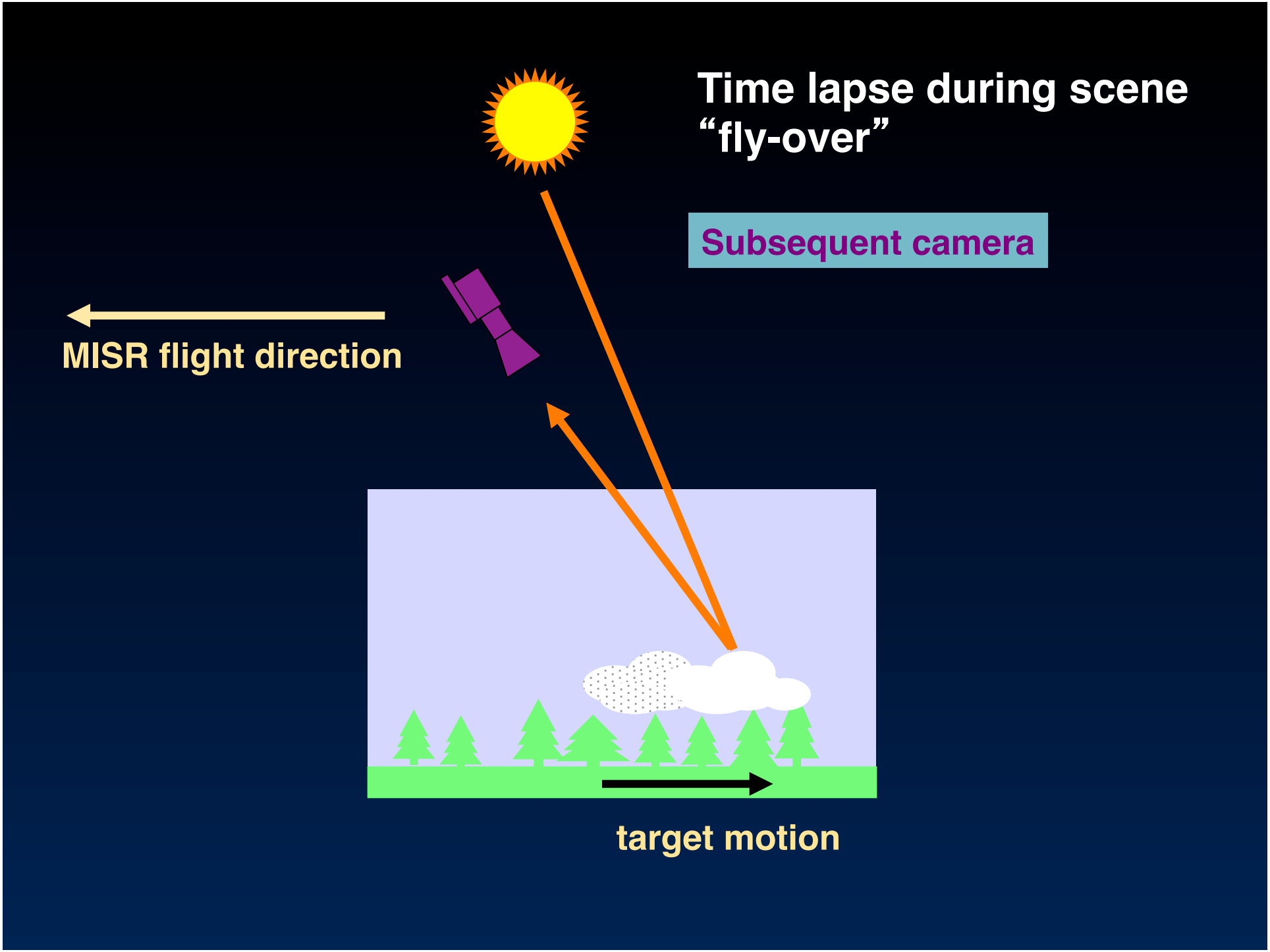
Time lapse during scene
“fly-over”
Subsequent camera
MISR flight direction
target motion

Von Karman vortex street near Jan Mayen Island
6 June 2001

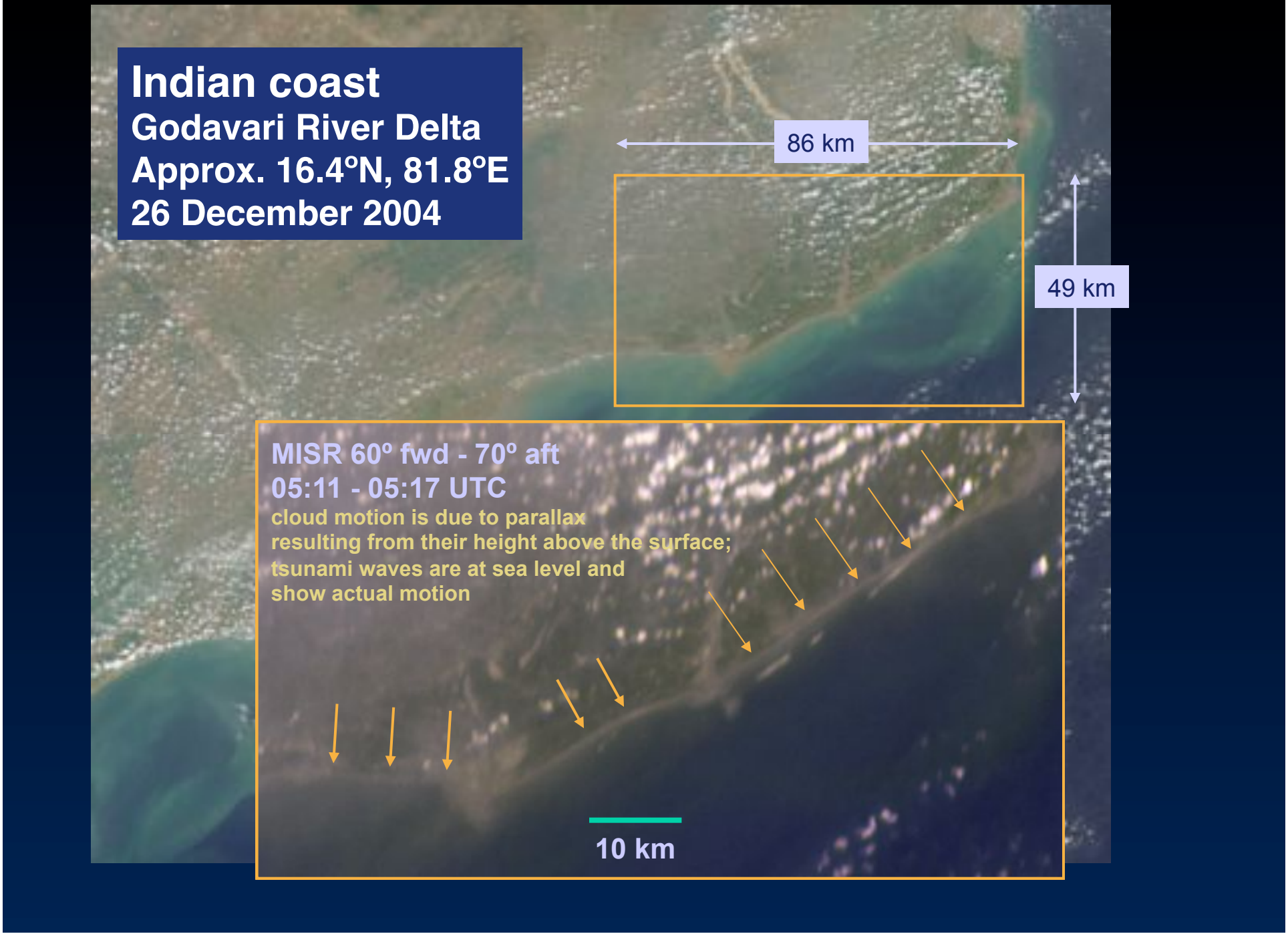
Indian coast
Godavari River Delta
Approx. 16.4°N, 81.8°E
26 December 2004
86 km
49 km
MISR 60° fwd - 70° aft
05:11 - 05:17 UTC
cloud motion is due to parallax
resulting from their height above the surface;
tsunami waves are at sea level and
show actual motion
10 km

L1B2 Geometric Parameters (MIS03)

Provided on 17.6-km centers

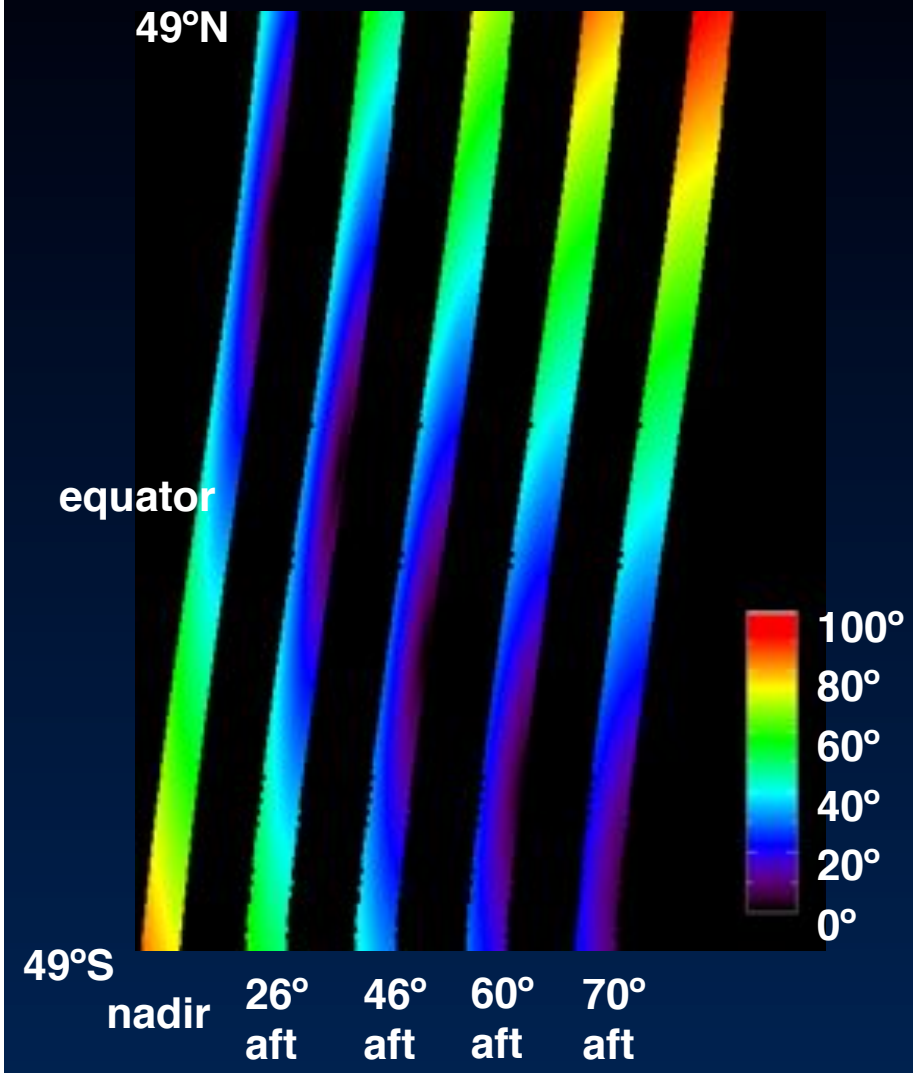

CONTENTS

- View zenith and azimuth angles per camera; azimuths measured relative to local north
- Solar zenith and azimuth angles correspond to midpoint viewing time of only those cameras which observed the point
- Scatter and glitter angles also included in product

Example of glitter angle July 3

L1B2 Radiometric Camera-by-camera Cloud Mask (MIS03)

Radiometric threshold-based cloud mask

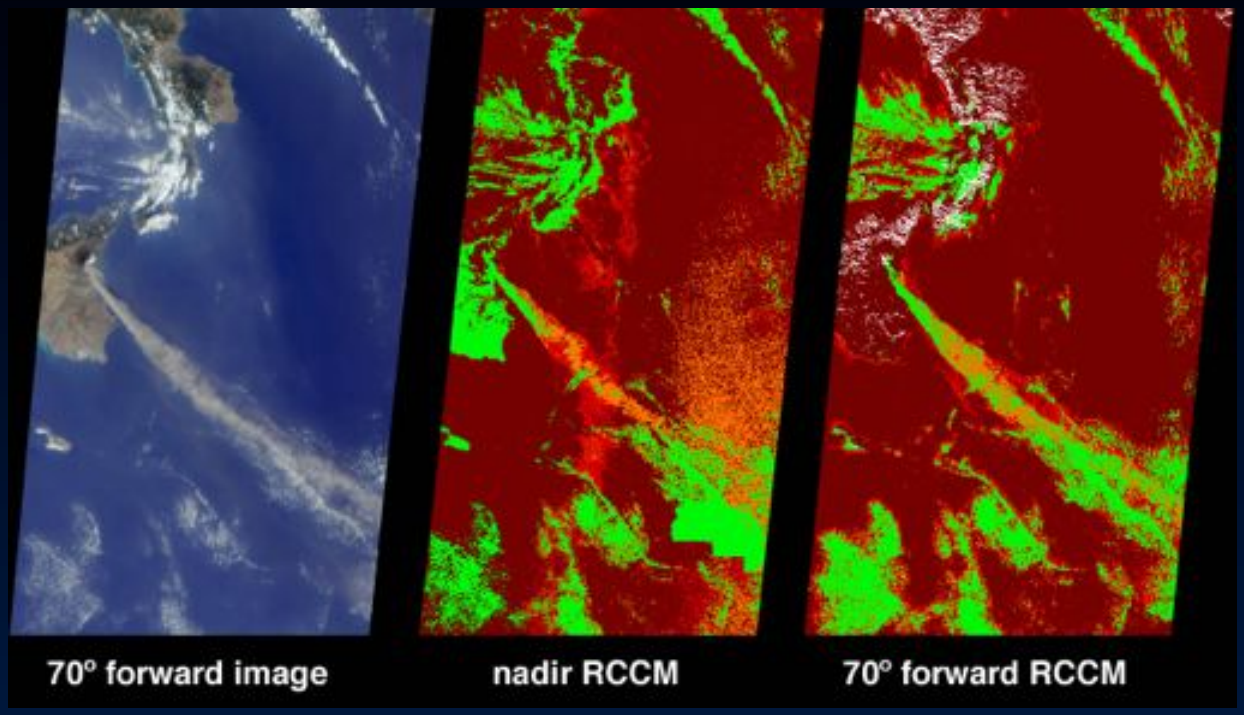

Mt. Etna eruption,
22 July 2001

- No retrieval
- High confidence clear
- Low confidence clear
- Low confidence cloud
- High confidence cloud

Level 2 Standard Products

Level 2 standard products

- Level 2TC stereo
- Level 2TC cloud classifiers
- Level 2TC top-of-atmosphere albedo
- Level 2AS aerosol
- Level 2AS land surface

Level 2 processing uses multiple cameras simultaneously

- Angular radiance signatures
- Geometric parallax
- Time lapse

L2 TOA/Cloud Stereo Product (MIS04)

Retrieved cloud heights and cloud-tracked winds

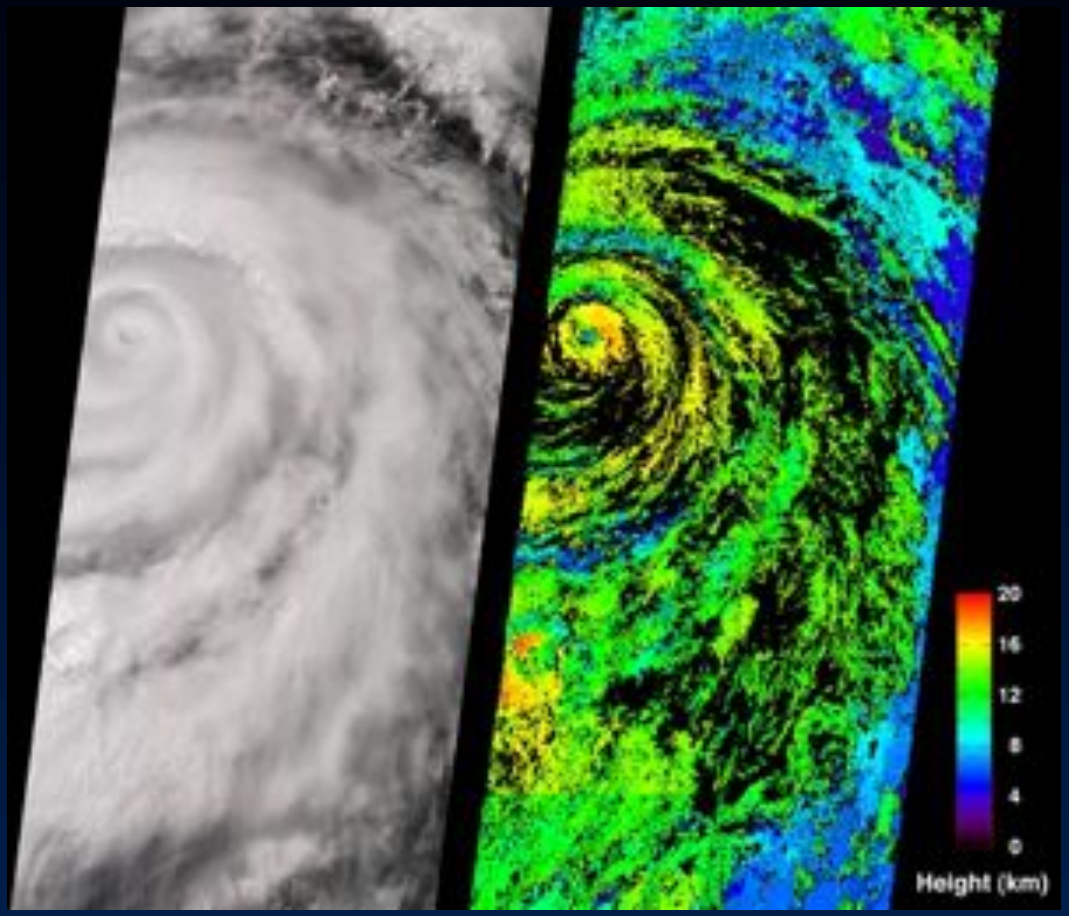

ATTRIBUTES

- Purely geometric retrievals of height
- Independent of temperature profiles and cloud emissivity
- Independent of radiometric calibration
- Accuracy 500 -1000 m

Hurricane Juliette
26 September 2001

Comparison of MISR and ASTER stereo cloud heights

Switzerland, 12 April 2002

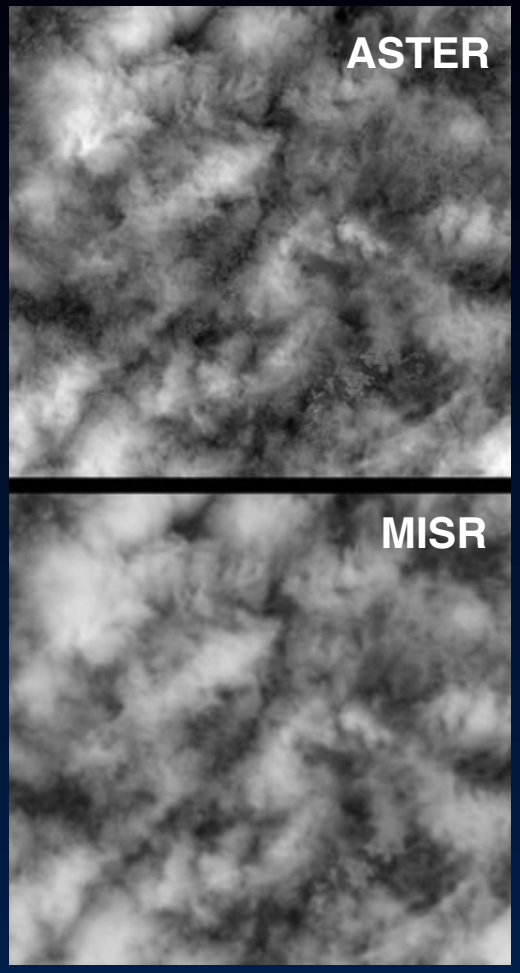

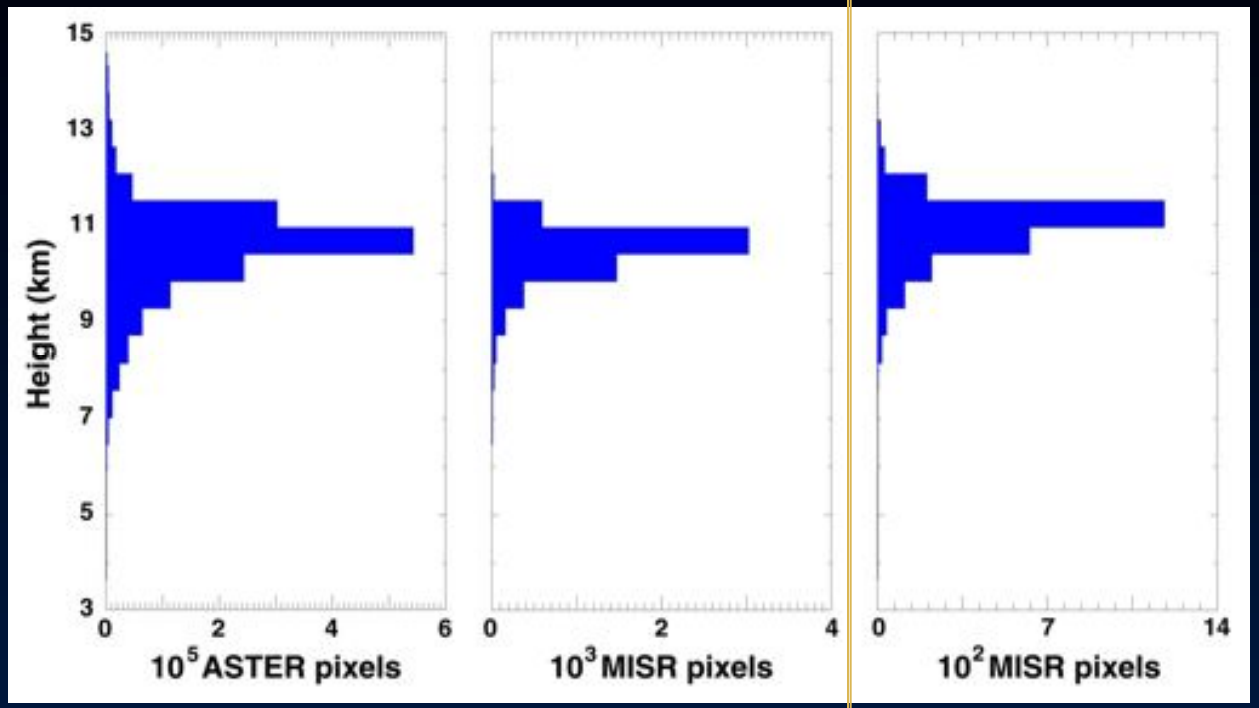

Using computationally intensive stereo image matcher

Using computationally fast operational MISR matcher

G. Seiz (ETH)

Measuring aerosol plume injection heights
California Cedar Fire, October 2003

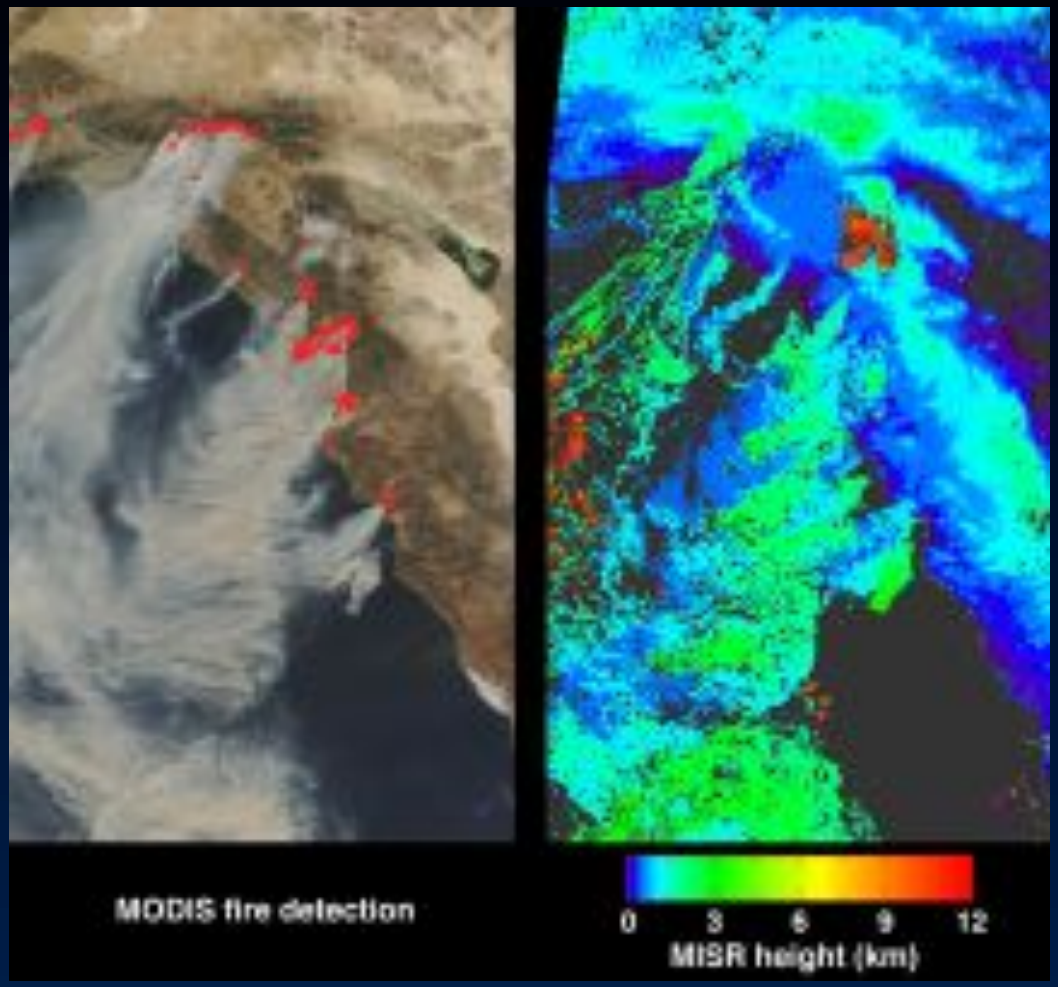

MISR: Stereo retrieves plume-top heights, oblique views enhance plume sensitivity
MODIS: Thermal channels pinpoints fire locations

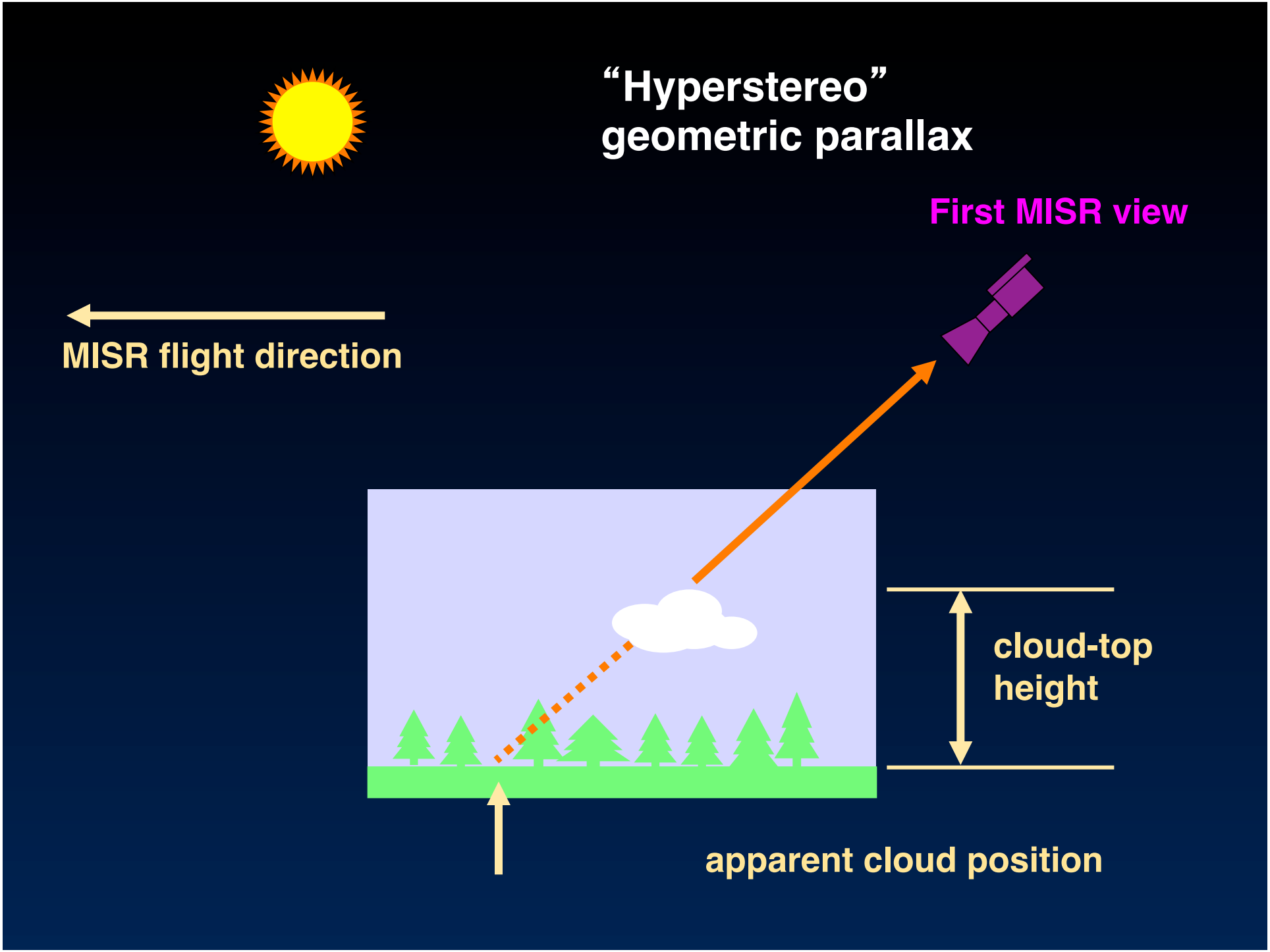
"Hyperstereo"
geometric parallax
First MISR view
MISR flight direction
cloud-top
height
apparent cloud position

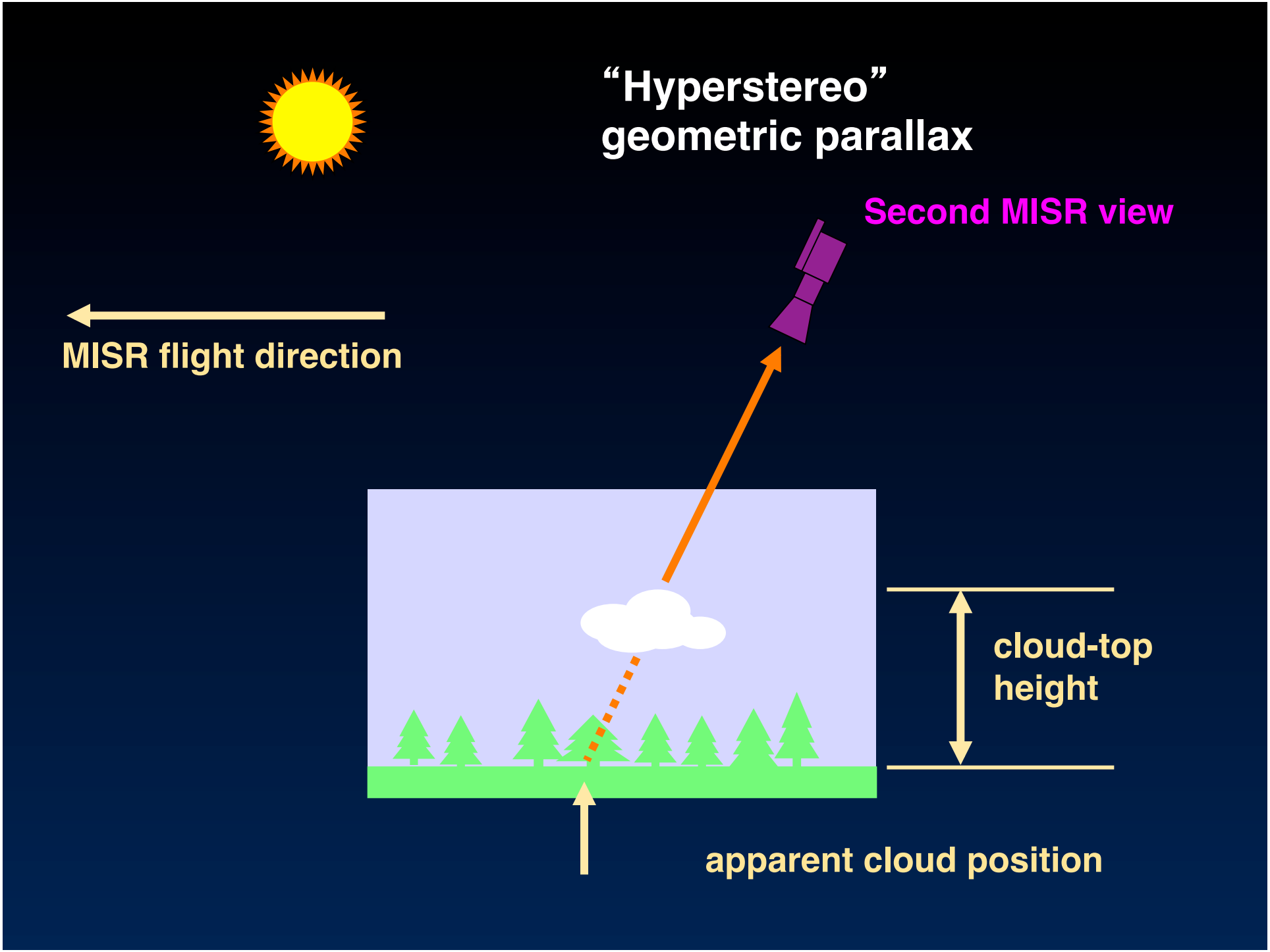
"Hyperstereo"
geometric parallax
Second MISR view
MISR flight direction
cloud-top
height
apparent cloud position

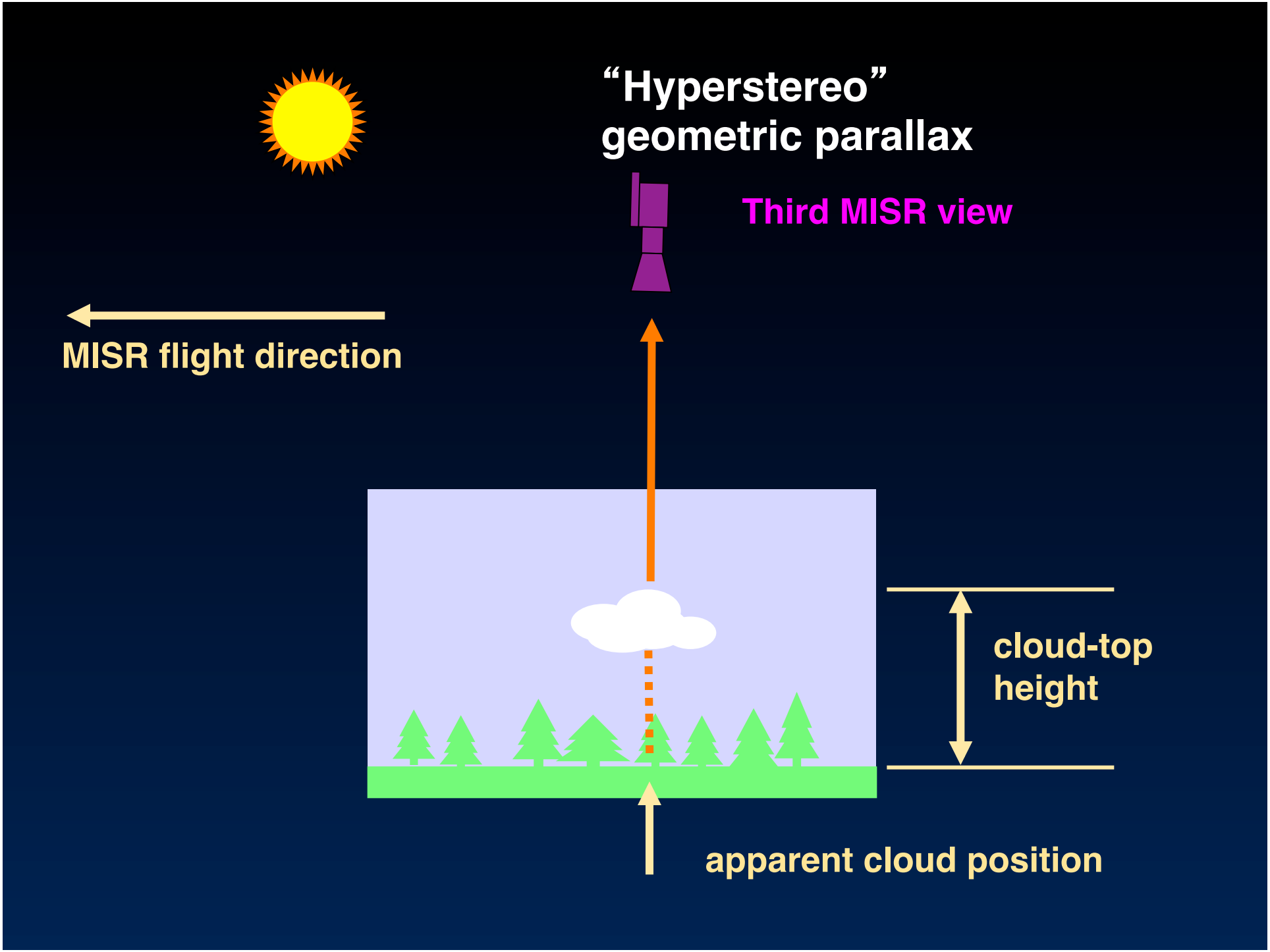
"Hyperstereo"
geometric parallax
Third MISR view
MISR flight direction
cloud-top
height
apparent cloud position

Simultaneous height and motion tracking

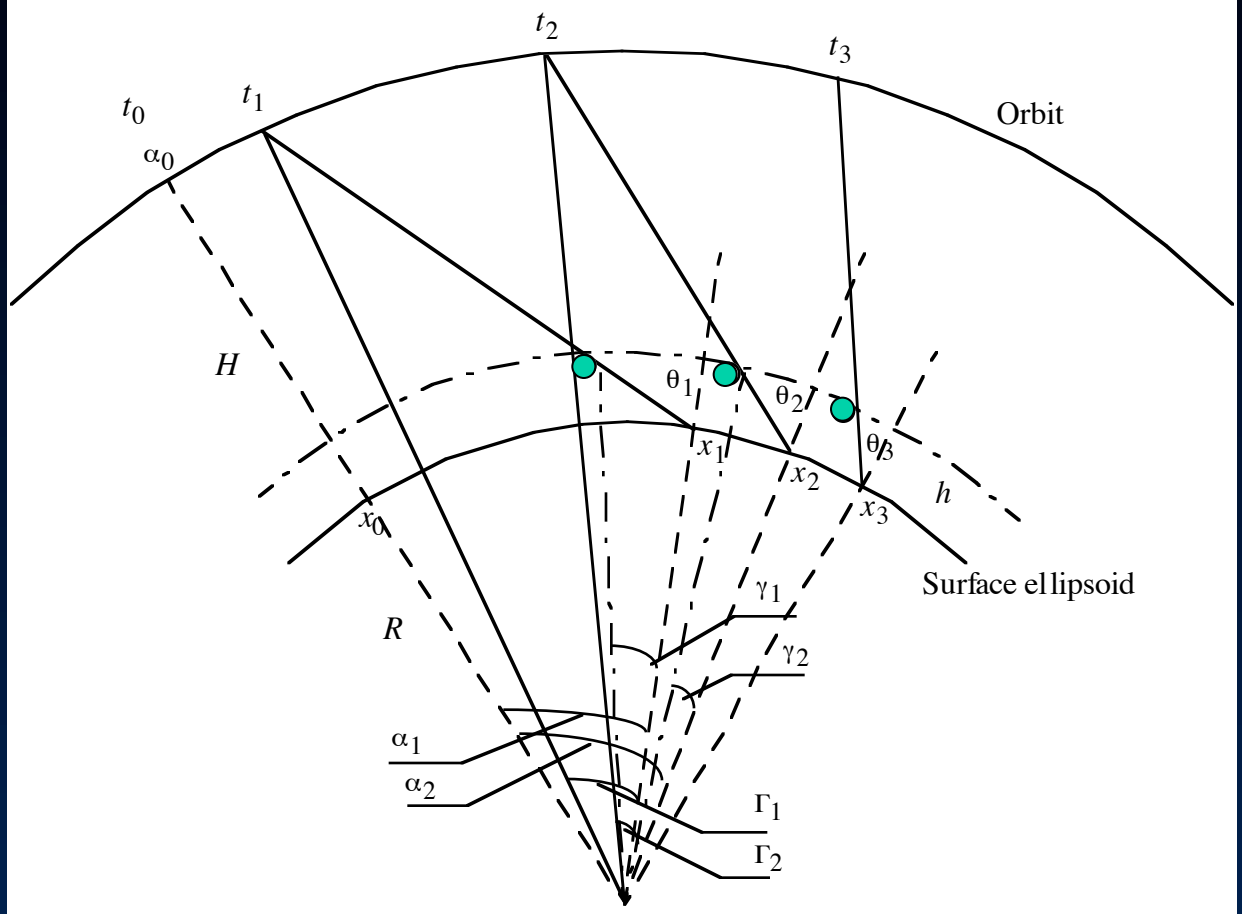

Height and horizontal motion separation requires 3 look angles

Observation from satellite altitude is required: Earth curvature overcomes equation degeneracy

Height-resolved cloud-motion winds

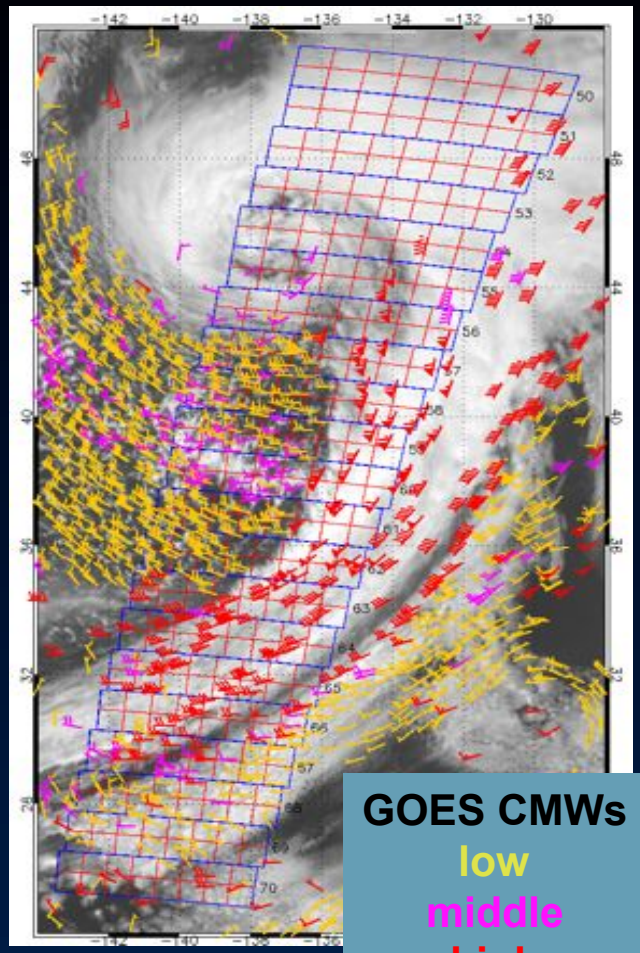

GOES CMWs
low
middle
high

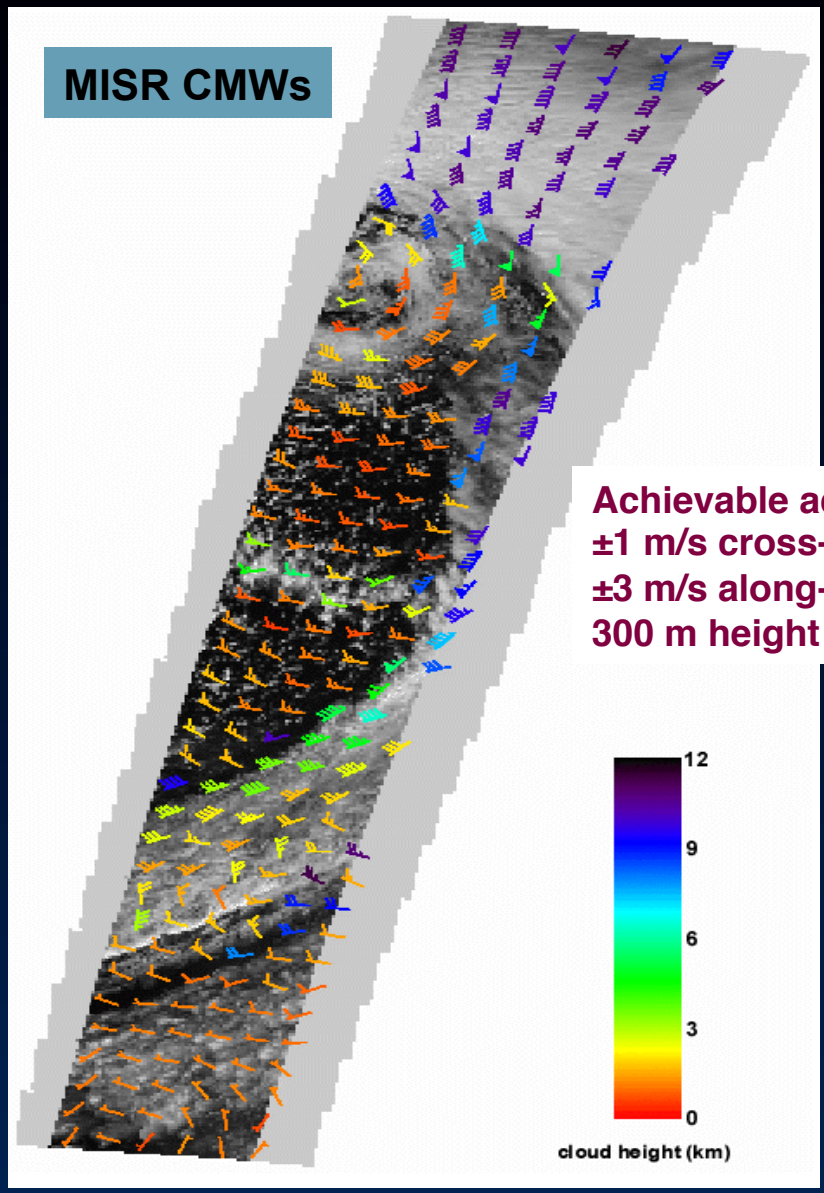

Achievable accuracies:
±1 m/s cross-track
±3 m/s along-track
300 m height resolution

A. Horvath and R. Davies (2001), TGARS
C. Moroney et al. (2002), TGARS
J. Zong et al. (2002), PE&RS

L2 TOA/Cloud Albedo Product (MIS04)

Cloud-top-projected TOA albedo and bidirectional reflectance

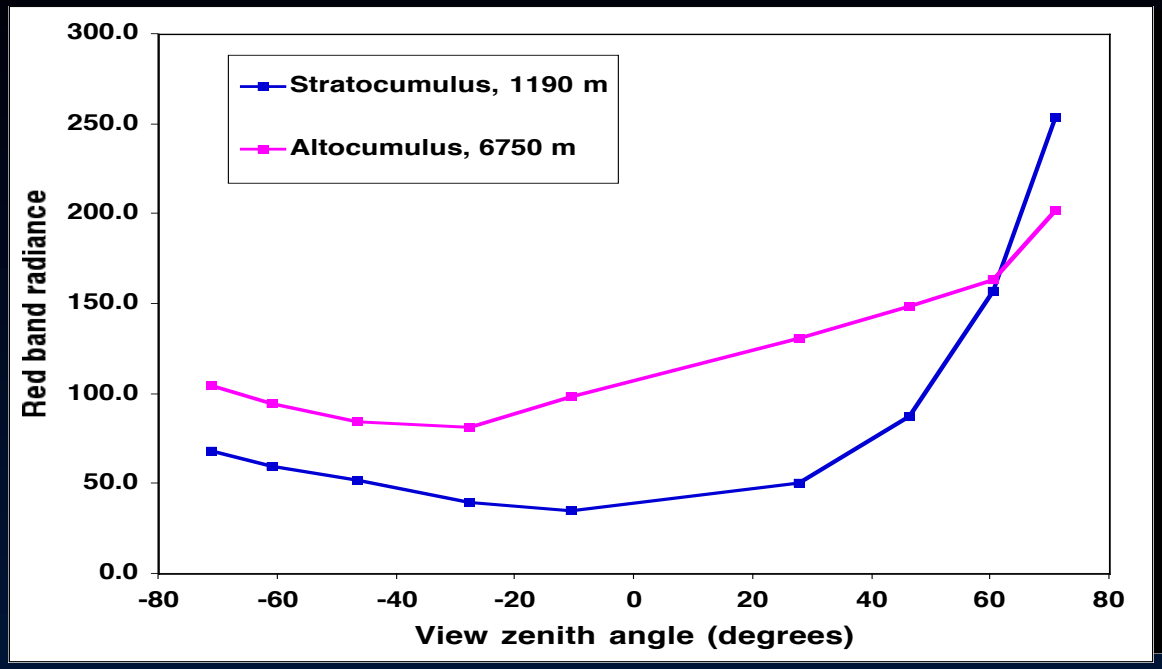

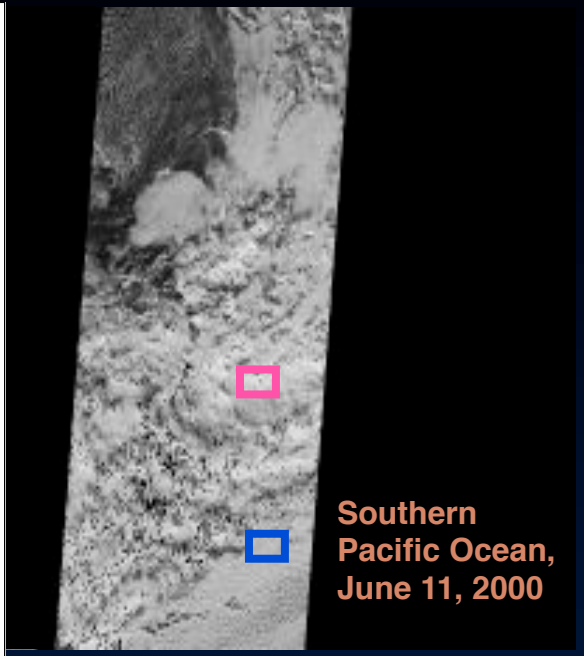

CONTENTS

- Contains “feature-referenced” top-of-atmosphere bidirectional reflectances
- Includes TOA albedos at fine (2.2. km) resolution for scene classification, and coarse (35.2 km resolution) for mesoscale radiation budget
- Regressions against CERES being used to facilitate narrow-to-broadband conversion

Multiangle tests of cloud homogeneity

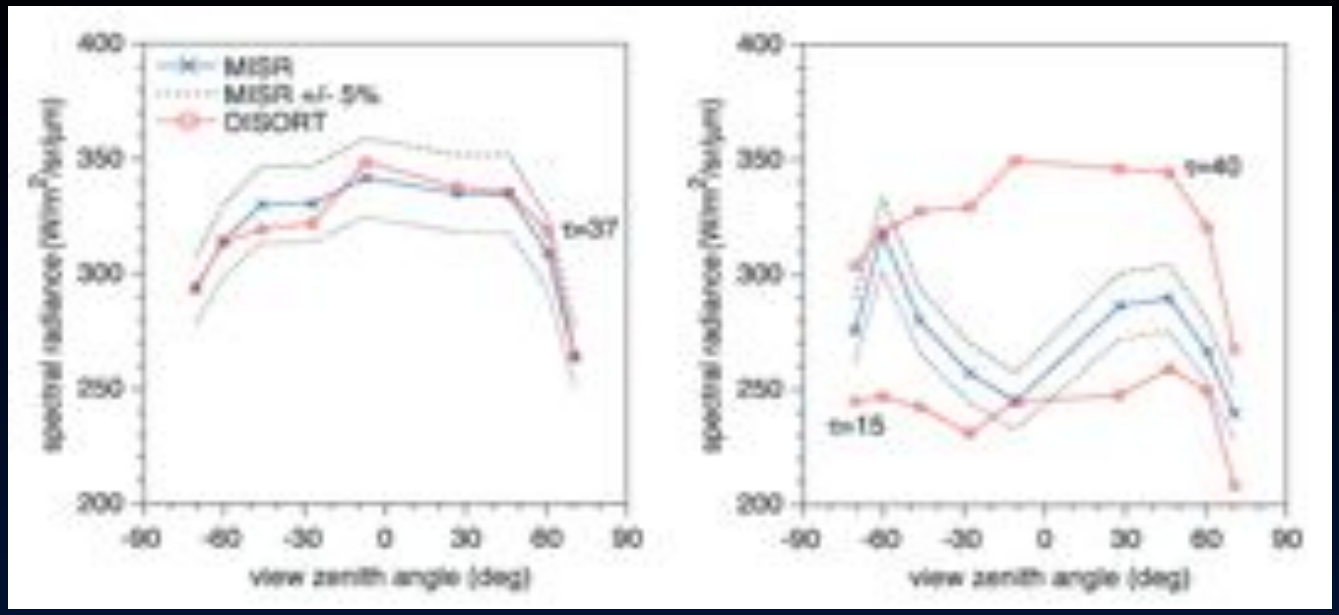

1-D theory fits MISR observations

1-D theory does not fit MISR observations

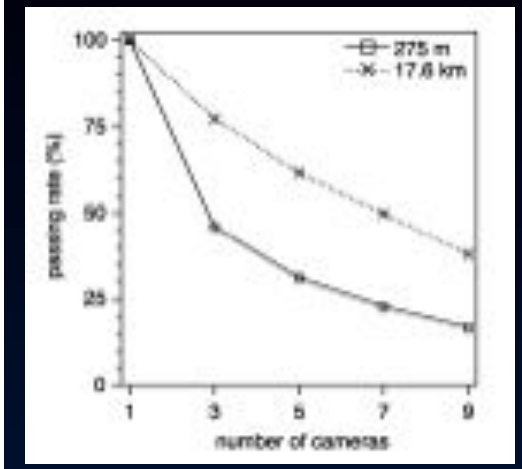

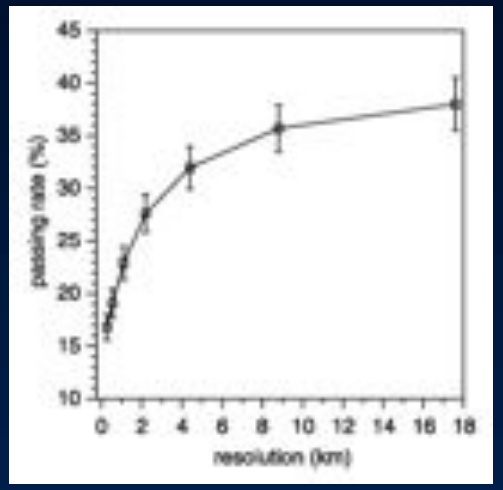

Multiangle data provides a physical consistency check on MODIS 1-D cloud retrieval assumption

Cloud morphology, not just cloud microphysics, plays a major role in determining TOA bidirectional reflectance

A. Horvath, R. Davies (2004), GRL

Example stereo and local albedo cloud products

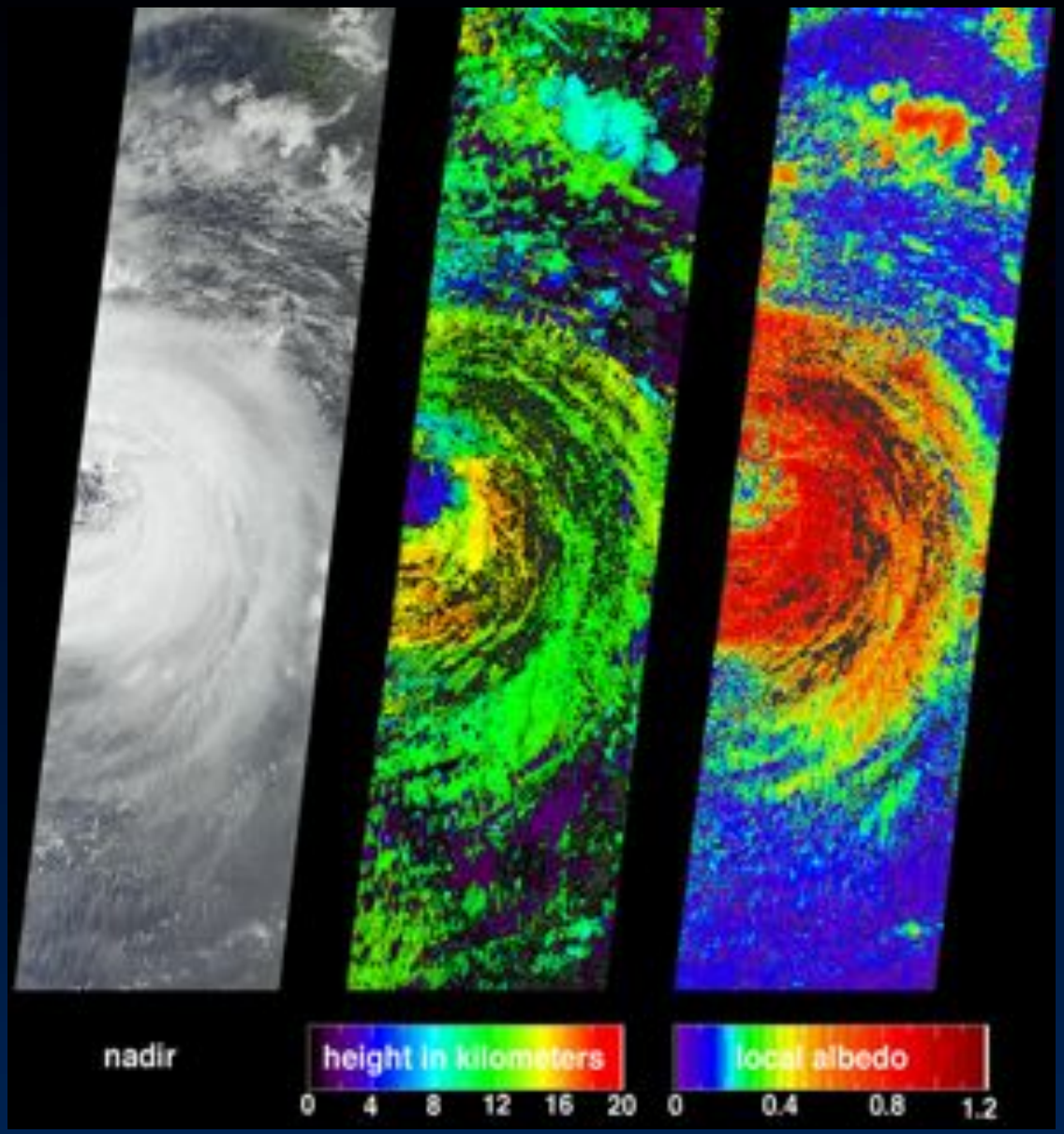

Typhoon Sinlaku
September 5, 2002

Is the Earth getting brighter?

Measurements of Earthshine on the Moon from Big Bear suggest an increase in Earth's albedo (Pallé et al., Science 2004) by about 4%

CERES Terra data show opposite trend (decrease of 2%), and about one-half of the CERES trend appears due to darkening of the optics due to UV exposure

What does MISR say?

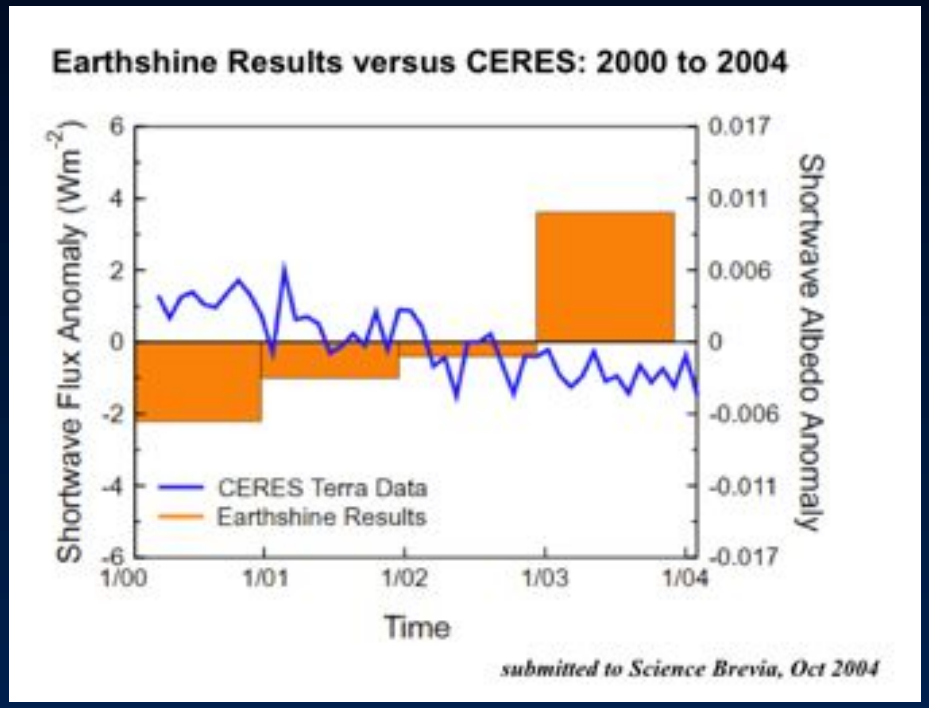

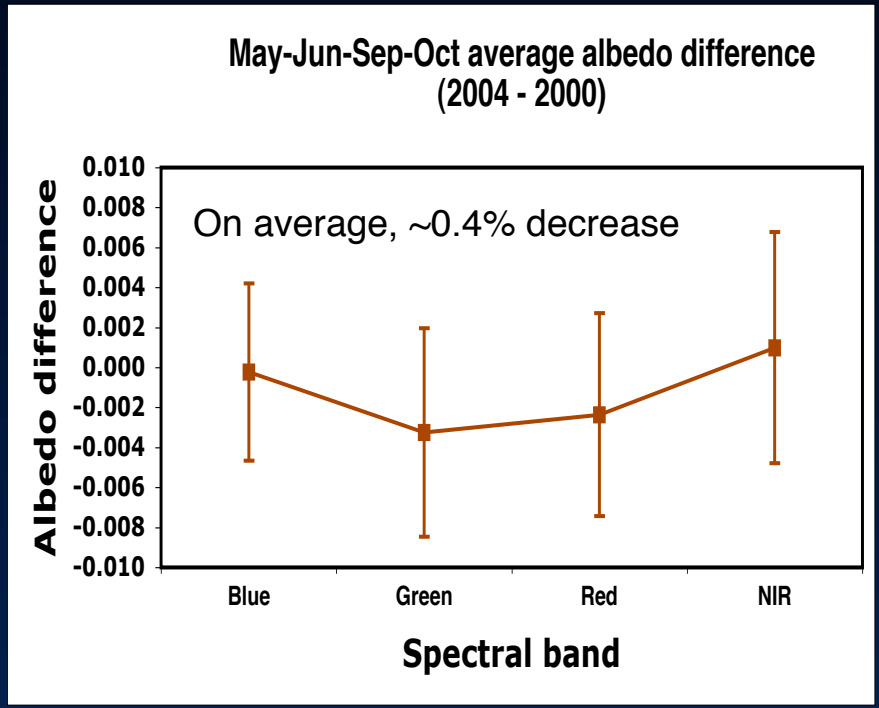

B. Wielicki et al. (2005), Science; R. Davies (JPL)

L2 TOA/Cloud Classifiers Product (MIS04)

Angular signature cloud mask and height-binned cloud fractions

ATTRIBUTES

- Angular signature readily distinguishes clouds and low-lying polar fogs from snow and ice

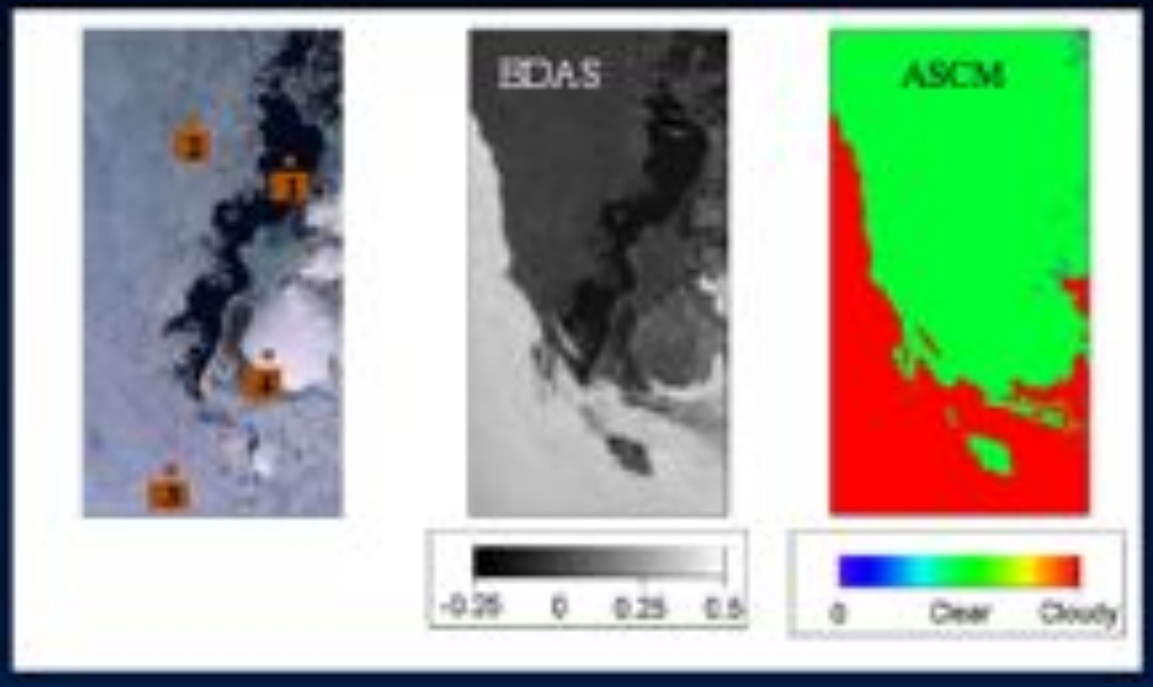

Nadir image

Band-differenced angular signature

Angular signature cloud mask

Data over the Arctic Ocean north of Russia, 3 July 2001, showing a mix of scene types:
1--open water
2--sea ice
3--cloud
4--snow-covered land (Komsomolets Island)

The cloud is difficult to see at nadir since it is at low altitude (MISR stereoscopic heights ~ 600 m), and optically thin.

Di Girolamo and Wilson (2003), TGARS

L2 Aerosol/Surface Product (MIS05)

Aerosol parameters

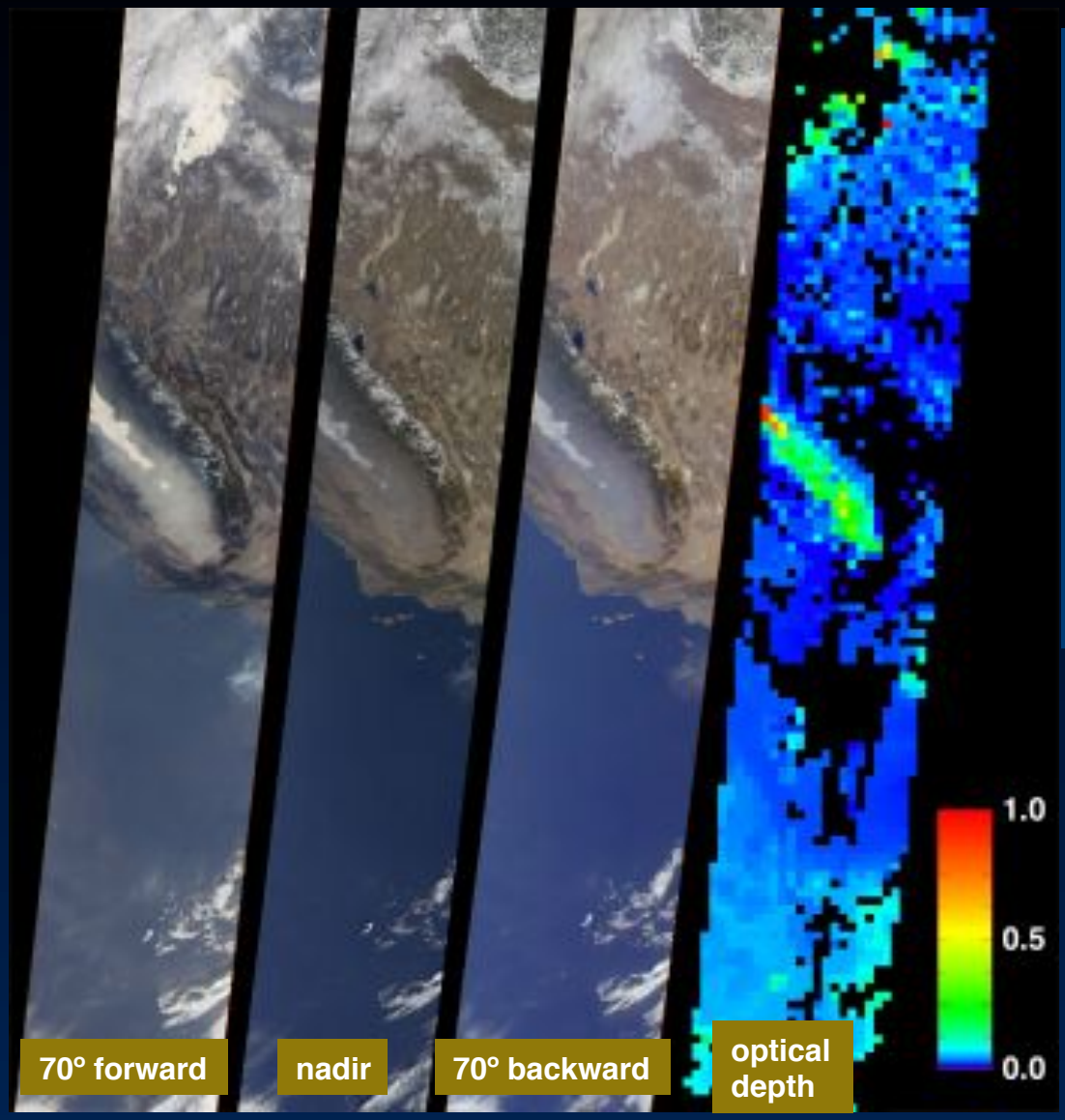

Martonchik et al. (2002), TGARS

ATTRIBUTES

- Different algorithms used over land and water
- Validation and quality assessment of aerosol optical depth performed
- Validation of aerosol particle properties under way

  --Angstrom exponent
  --Size binned fractions
  --Single-scattering albedo
  --Sphericity

Southern California and Southwestern Nevada
January 3, 2001

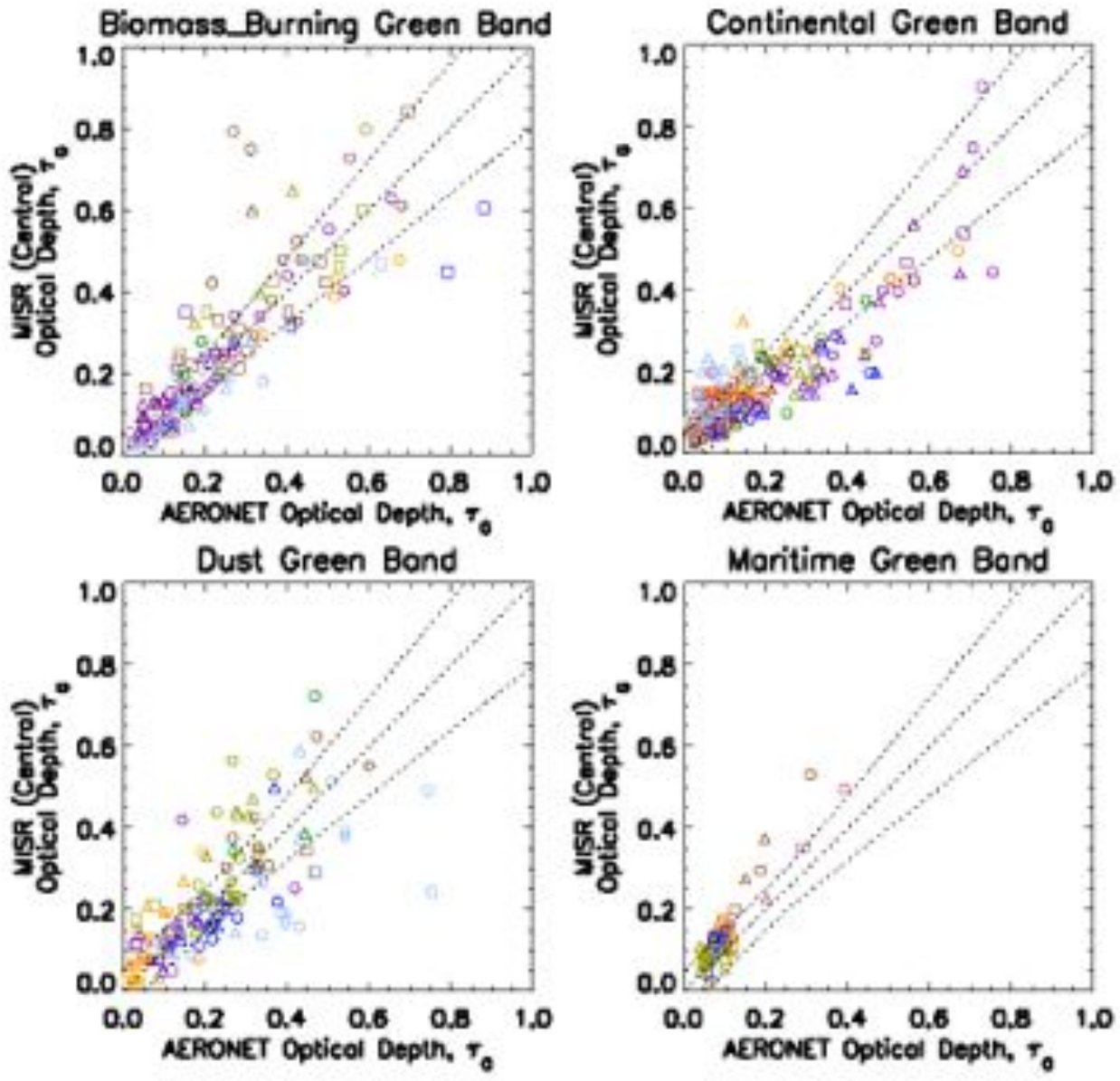

Optical depth validation

Kahn et al. (2005), JGR

A vast pool of tiny particles over India

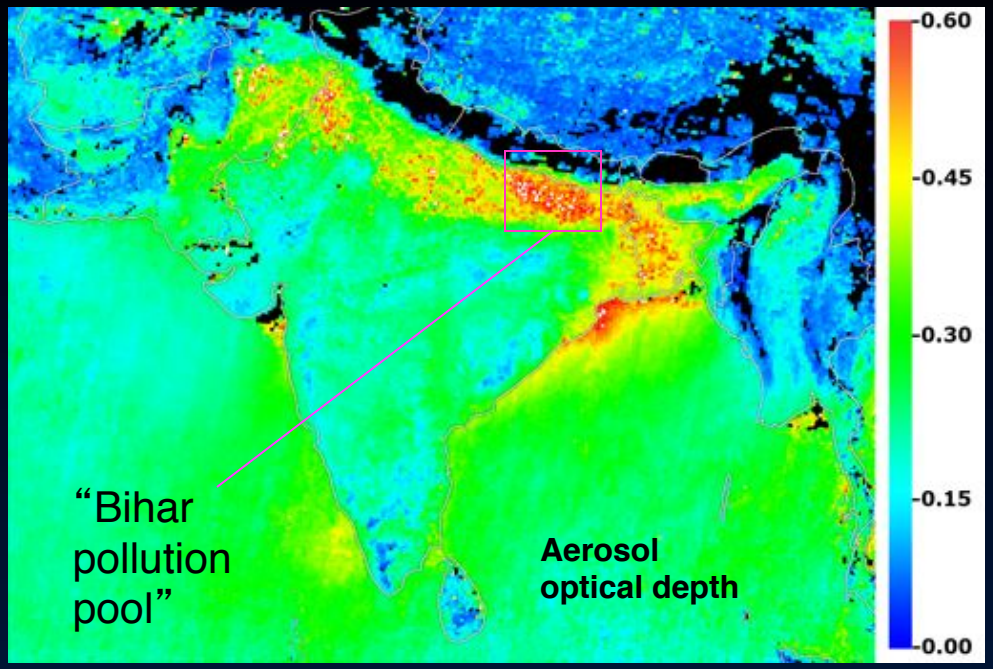

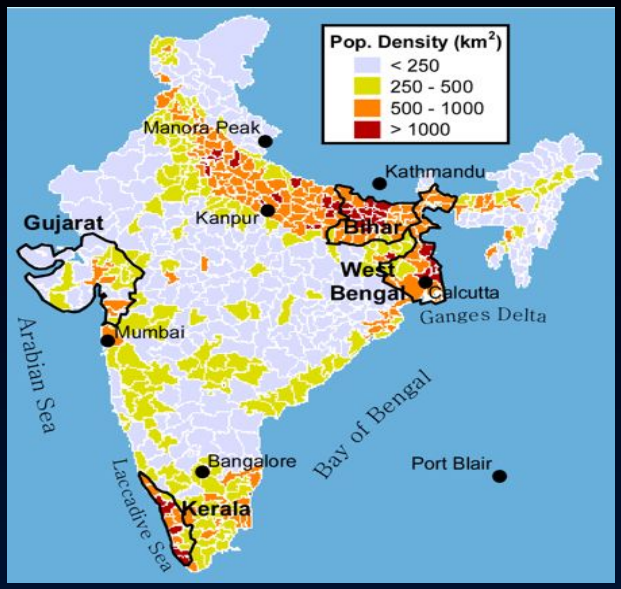

Winter aerosol climatology derived from 4 years of MISR data

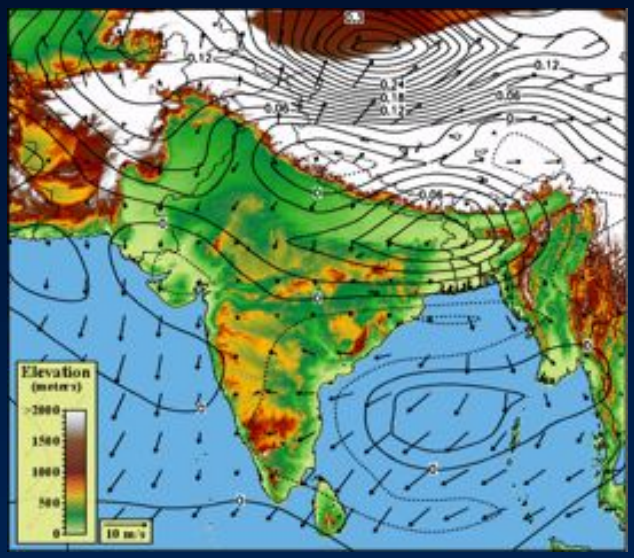

Topography and winds

L. Di Girolamo et al. (2004), GRL

MISR sensitivity to aerosol particle properties

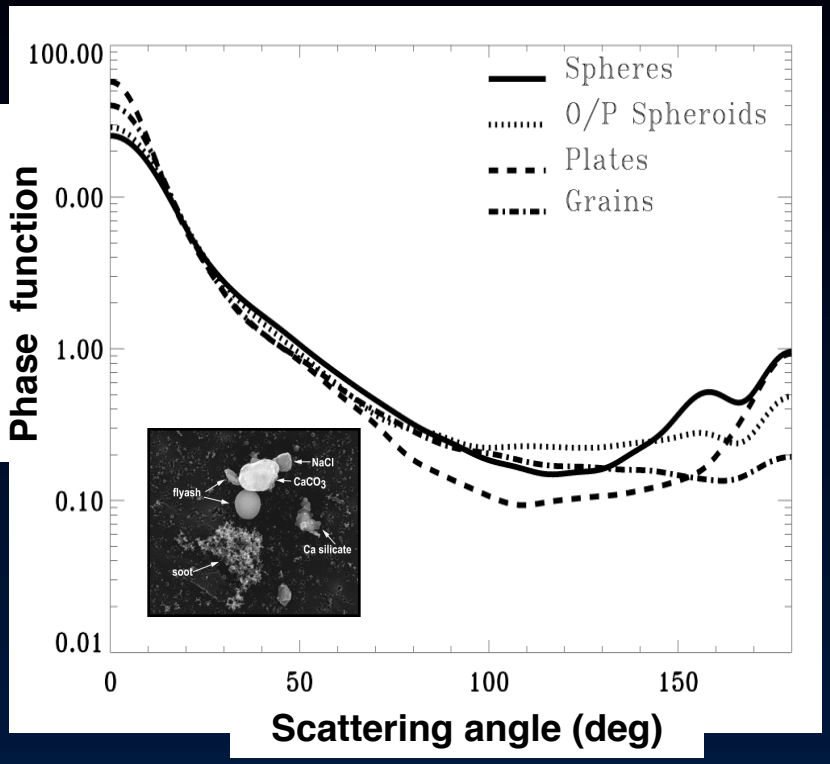

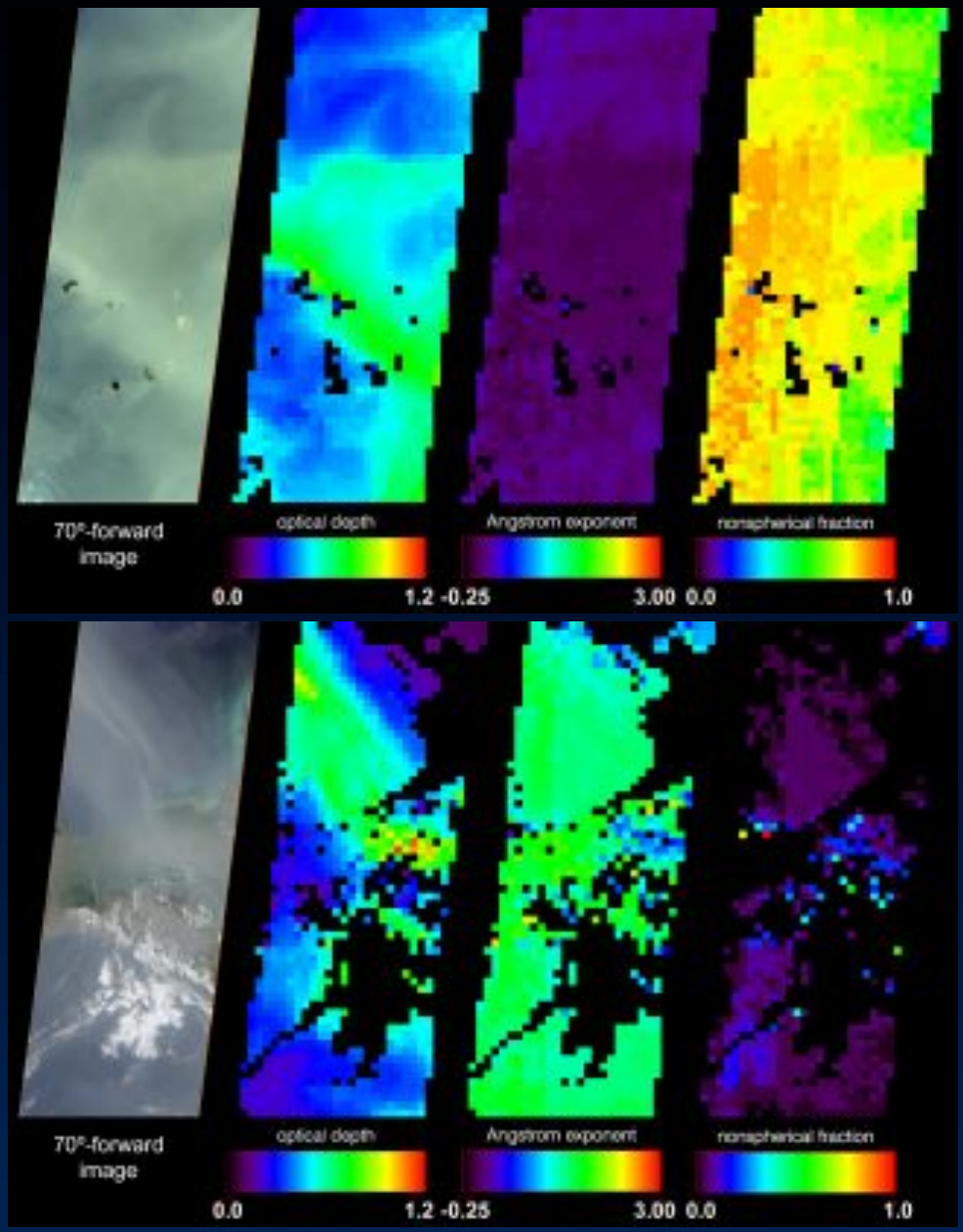

O. Kalashnikova et al. (2005), JGR

L2 Aerosol/Surface Product (MIS05)

Surface parameters

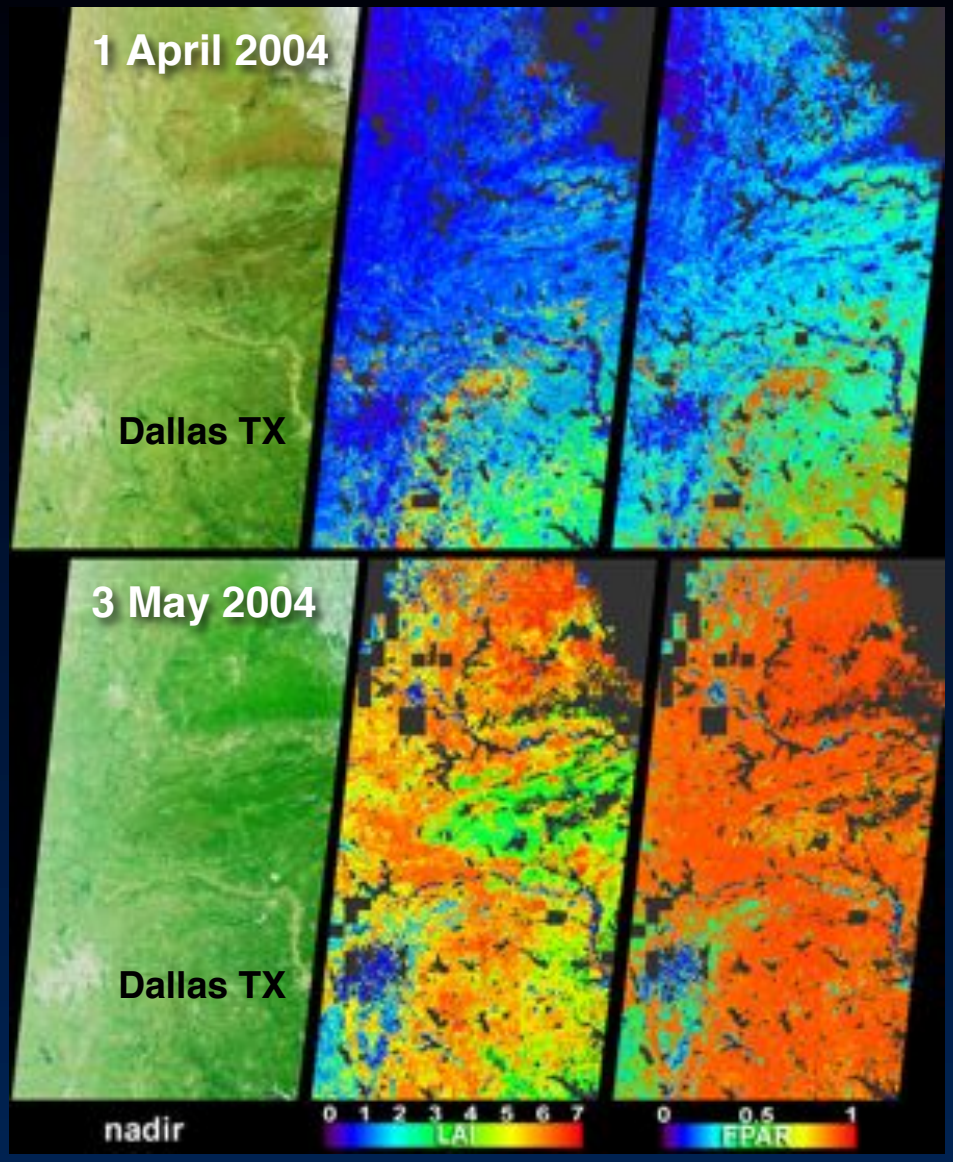

CONTENTS AND ATTRIBUTES

- Radiometric surface parameters (directional reflectances, albedos)

  Derived from single overpass-- no temporal compositing

  Atmospherically corrected

- Vegetation-related quantities (albedo-based surface NDVI, LAI, FPAR)

  LAI-FPAR retrievals are based on 3-D RT models

  Prescribed biome map is not required

Dependence of bidirectional reflectance on surface vegetation subpixel structure: parametric approach

Structurally homogeneous canopy representation composed of finite-sized scatterers

Parametric models
(e.g., Rahman-Pinty-Verstraete function)
BRF = BRF_0 * Shape term * Asymmetry term
Shape term = $[\mu\mu_0(\mu+\mu_0)]^{k-1}$

Structurally heterogeneous canopy representation composed of clumped ensembles of finite-sized scatterers

Exponent k establishes whether BRF angular signature gets darker off-nadir (bell-shaped, k > 1) or brighter off-nadir (bowl-shaped, k < 1)

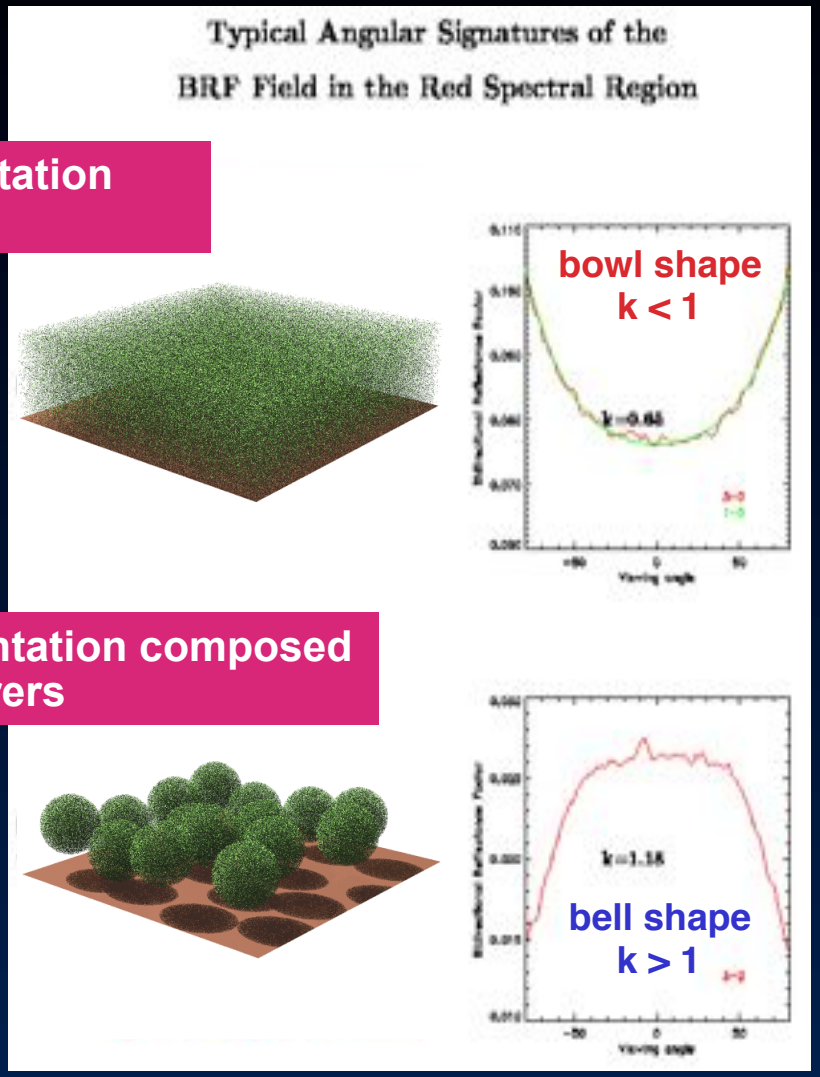

B. Pinty, N. Gobron, J-L. Widlowski, M. Verstraete

Bell and bowl-shaped BRFs

Manitoba and Saskatchewan, 17 April 2001

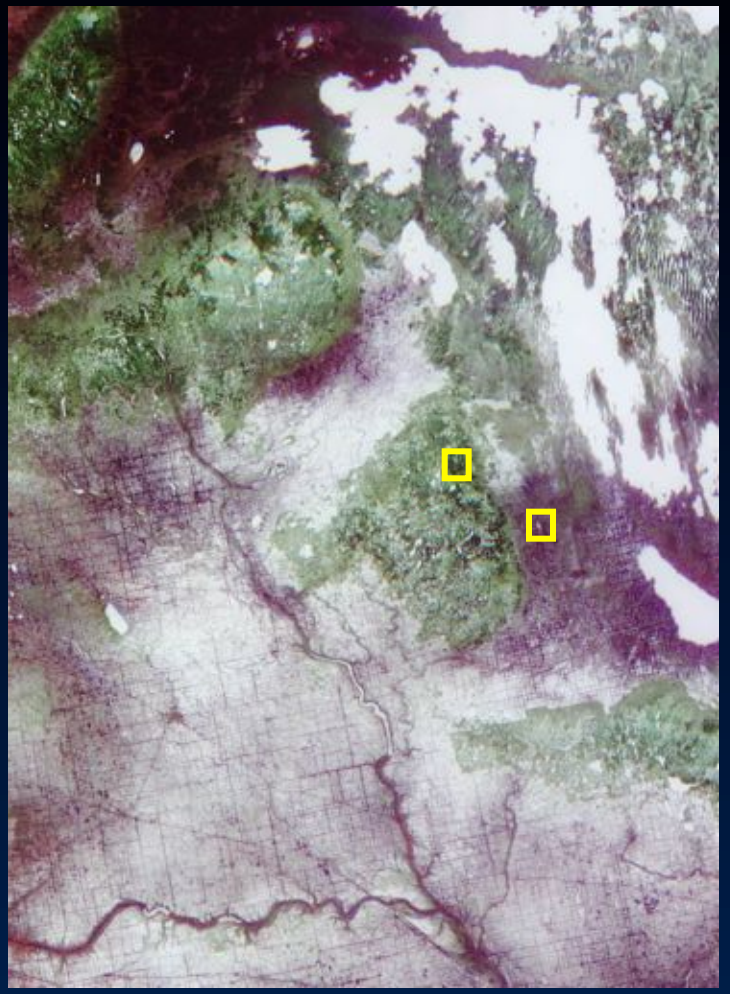

Nadir false-color composite:
RGB = near-IR, red, green

Multi-angle red band composite:
RGB = 60° backward, nadir, 60° forward

Bidirectional reflectances of surface vegetation as observed by MISR

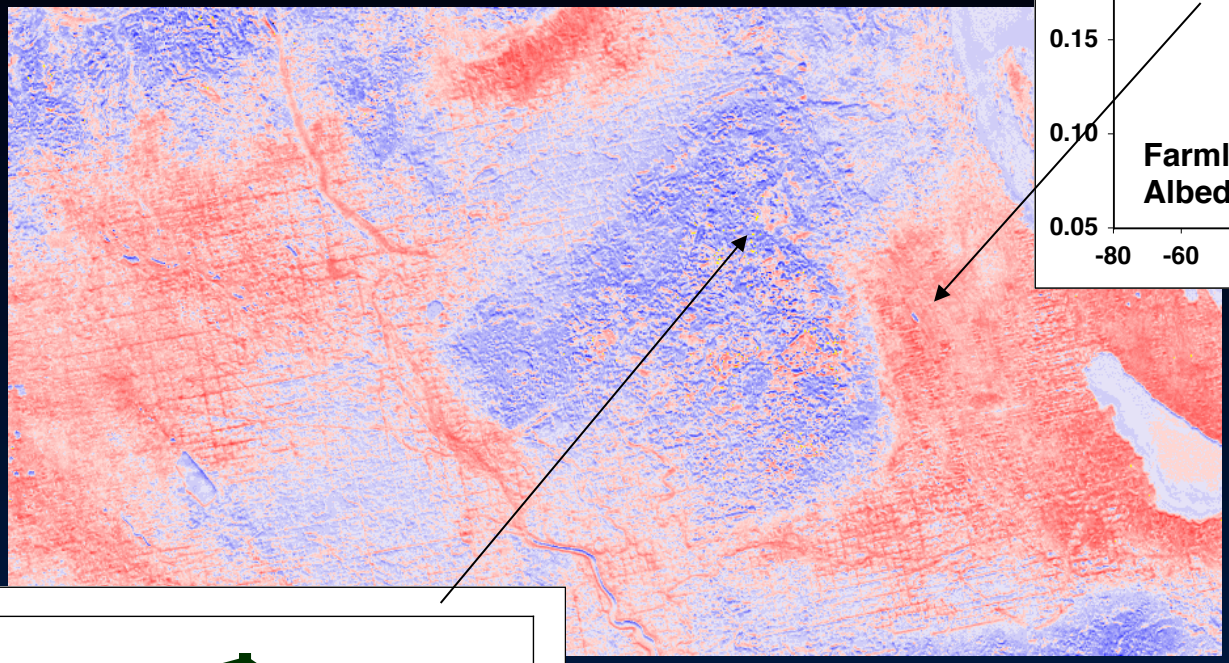

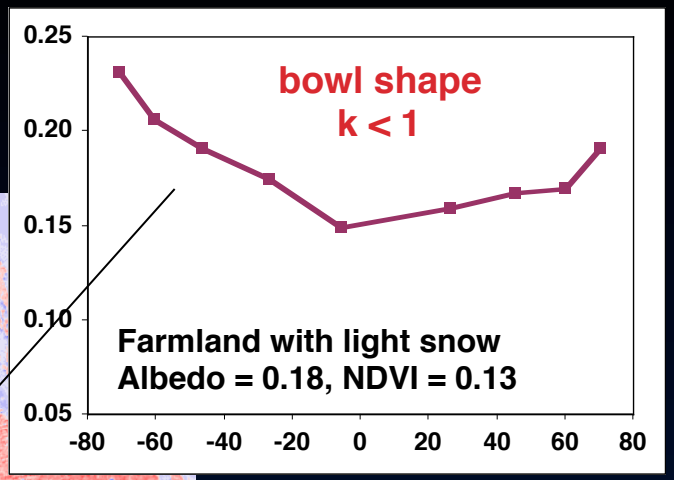

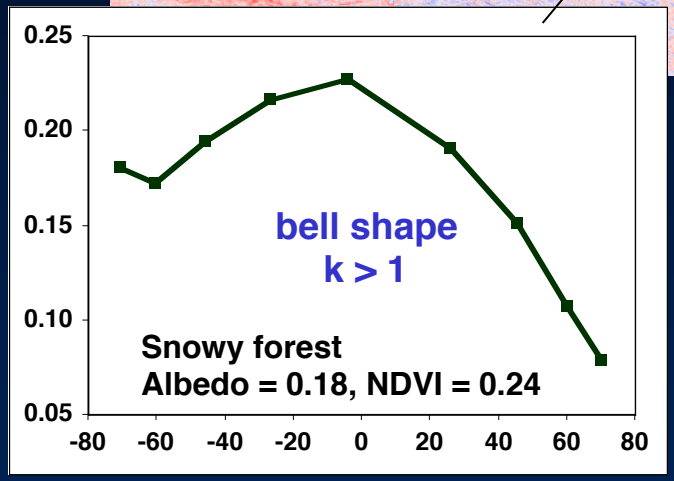

Manitoba and Saskatchewan, 17 April 2001

k-parameter

B. Pinty, N. Gobron, J-L. Widlowski, M. Verstraete

Mapping forest density over snow

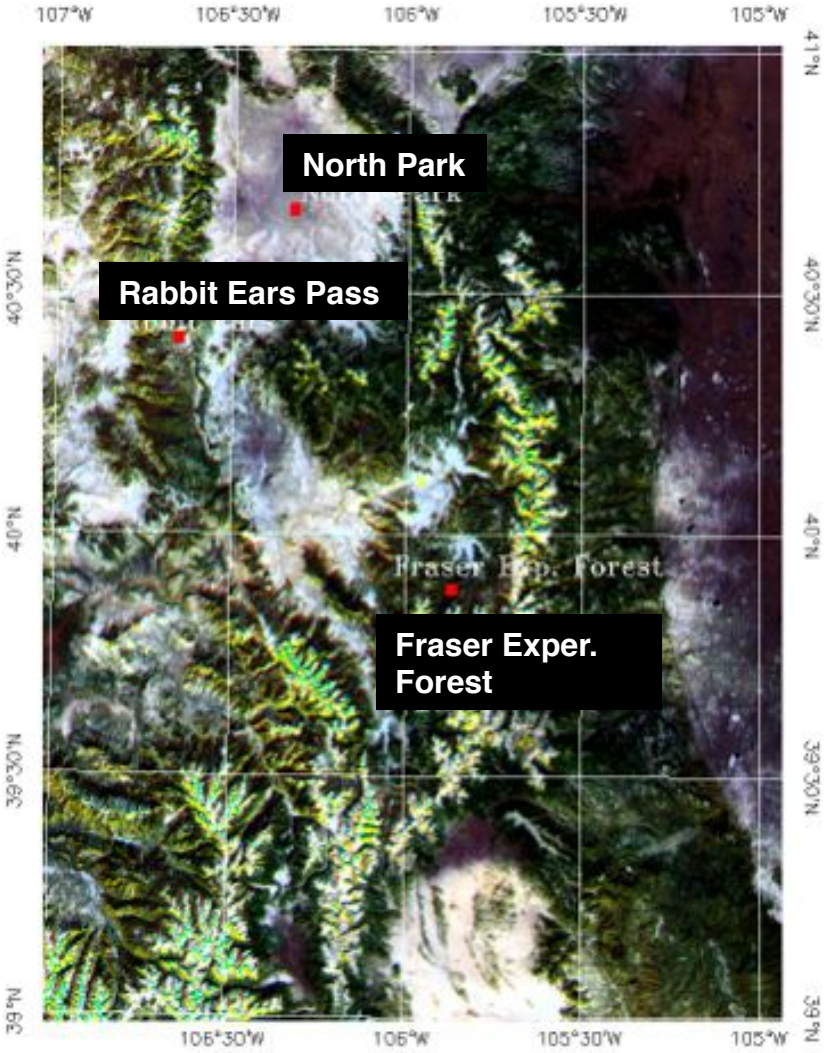

MISR multiangle composite

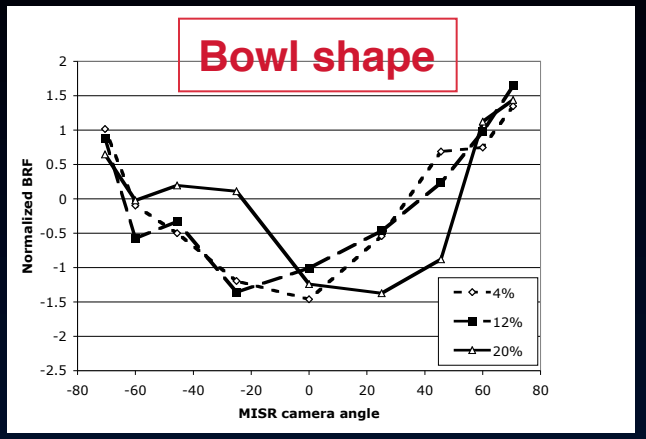

non-forested, low density

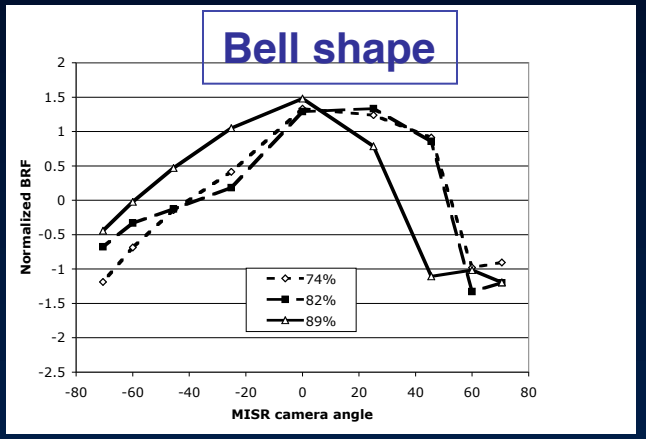

lodgepole pine, medium/high density

A. Nolin (2004), Hydrol. Proc.

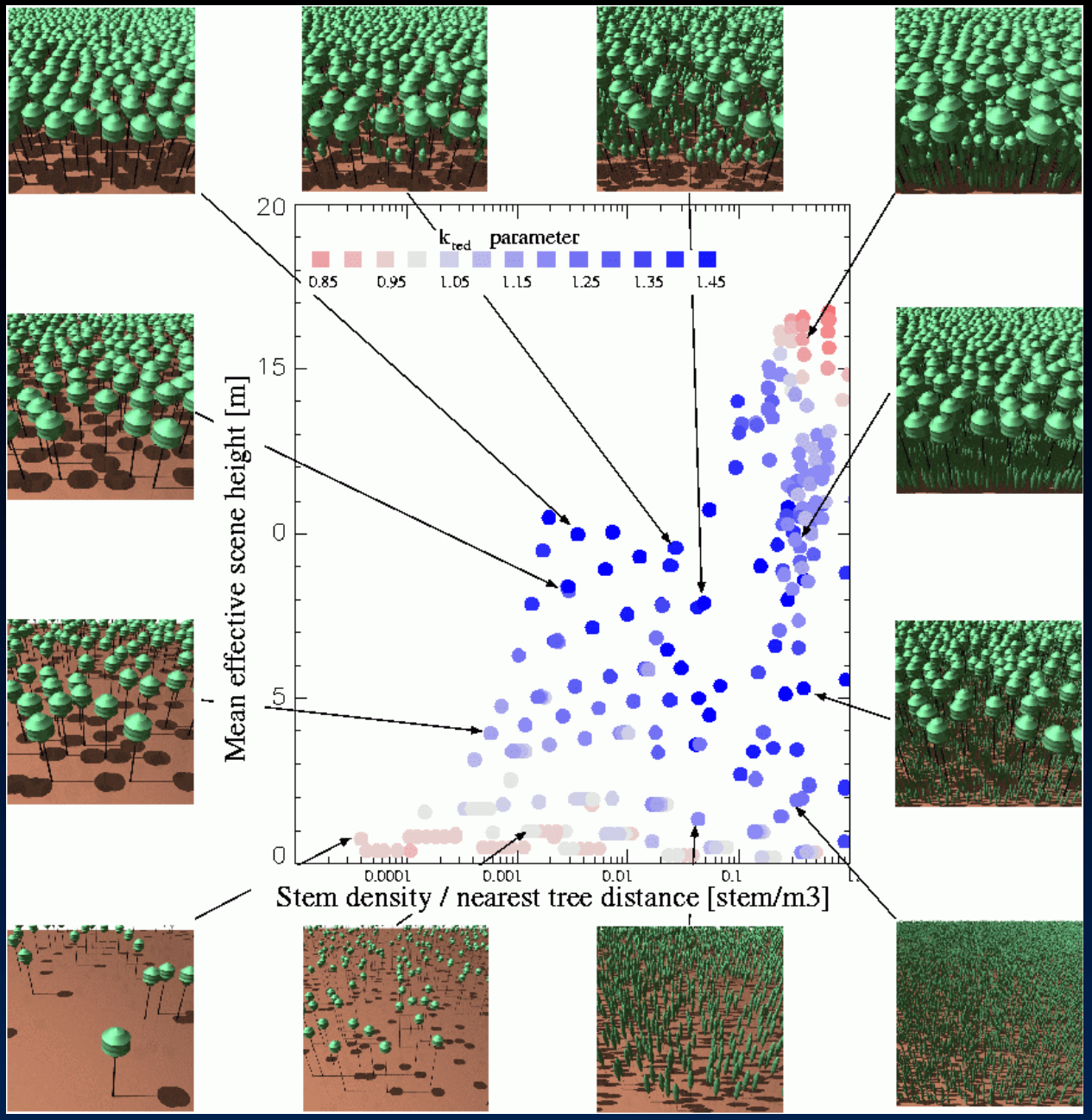

Relating bowl-shaped and bell-shaped BRFs to measures of canopy structure

Bell-shaped BRF:
Tree crowns of medium-high density against bright background

Bowl-shaped BRF:
Sparse vegetation and dense, closed canopies

J-L. Widlowski et al. (2004), Clim. Change

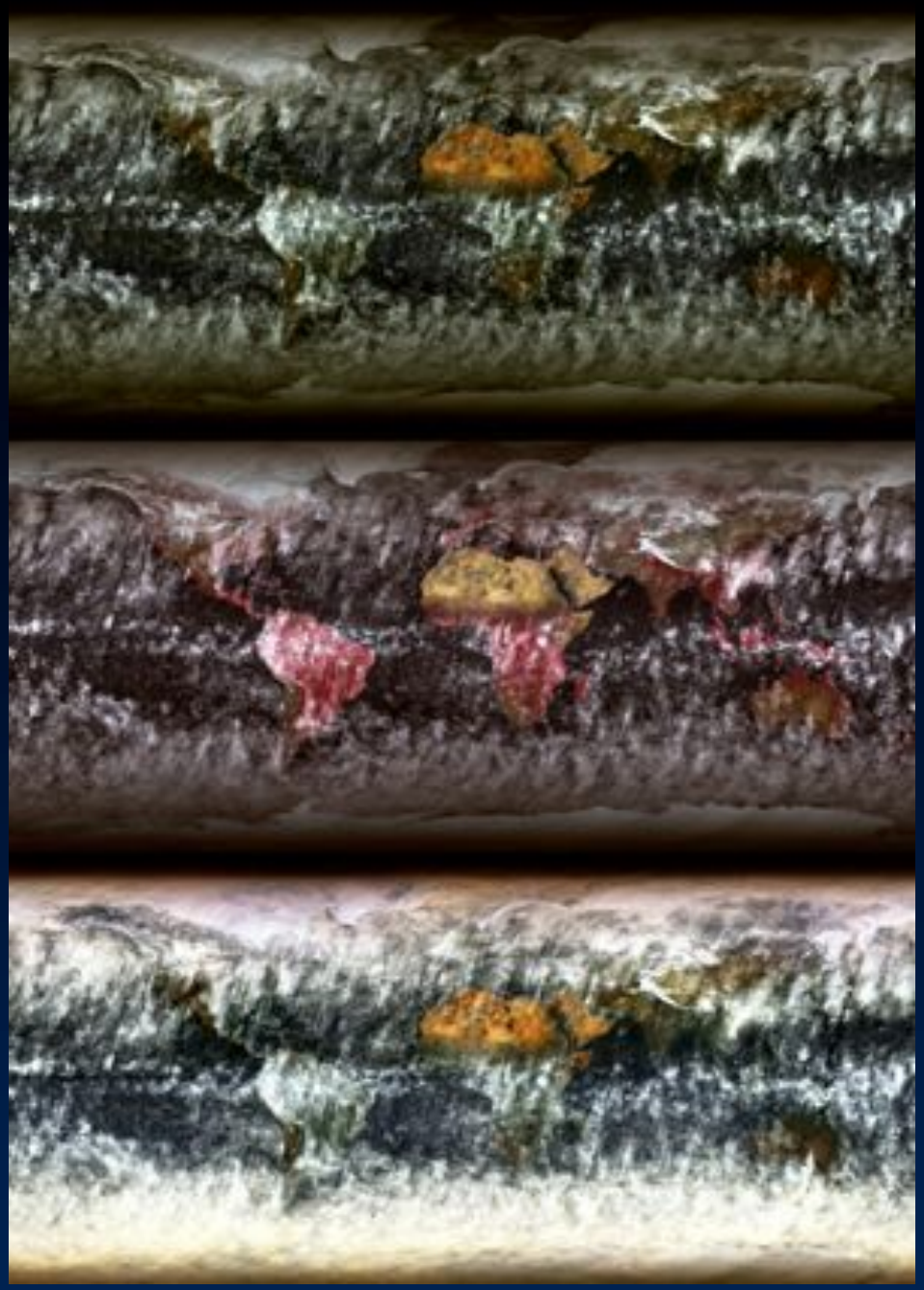

L3 Gridded Radiances (MIS06)

Means, variances, and covariances

Nadir red, green, blue

Nadir near-infrared, red, green

March 2002

70° forward: red, green, blue (N. hemisphere)
70° backward: red, green, blue (S. hemisphere)

L3 Gridded Aerosol (MIS08)

Global optical depths

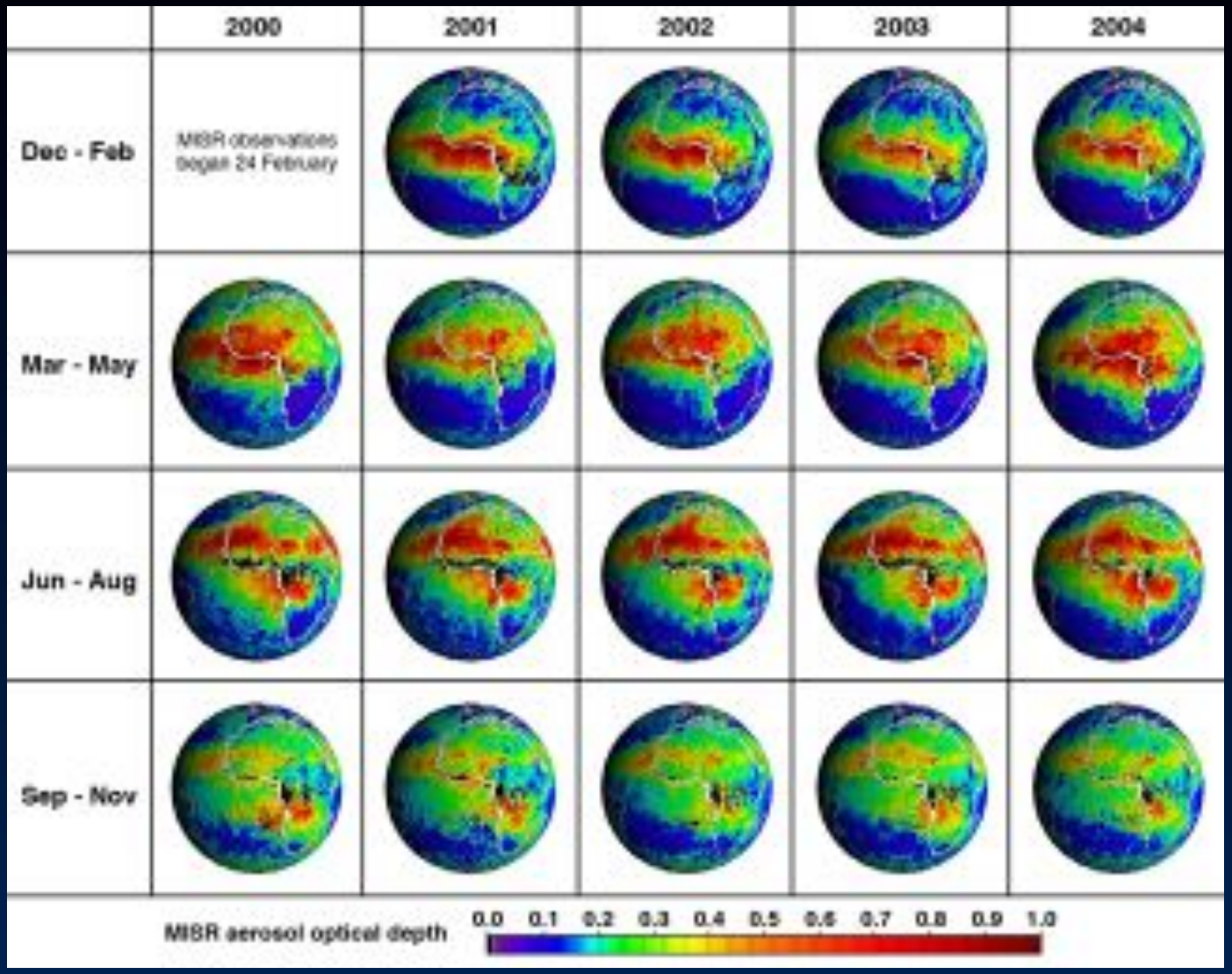

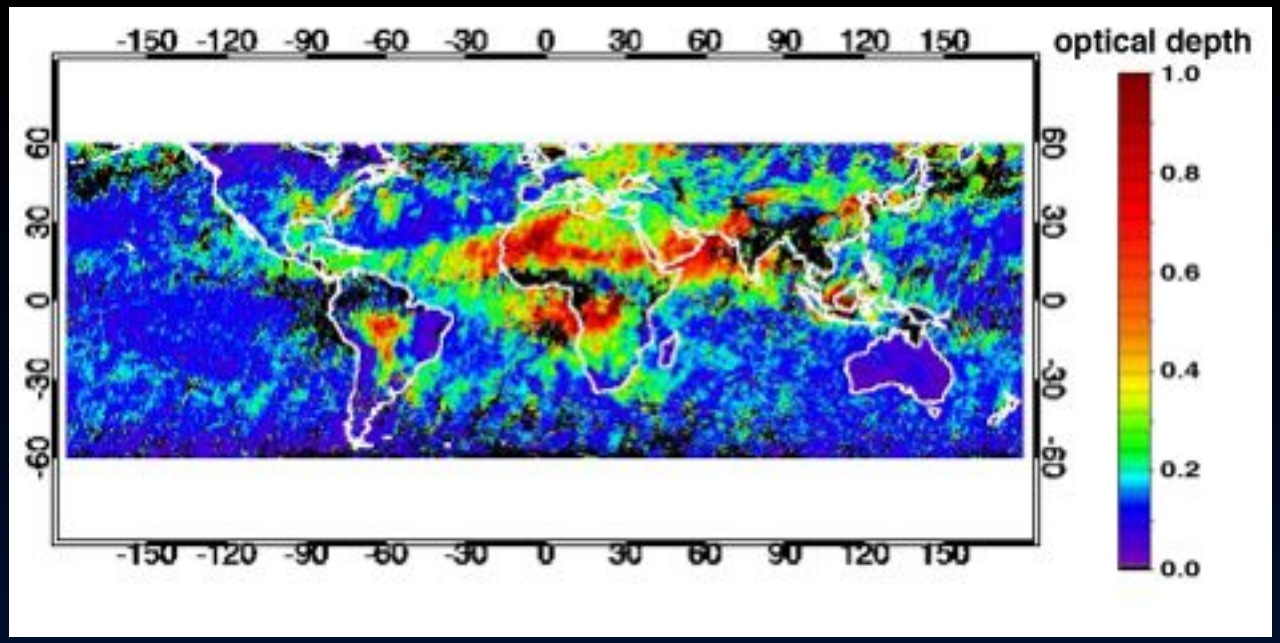

Our global village

August 2002

MISR aerosol optical depth

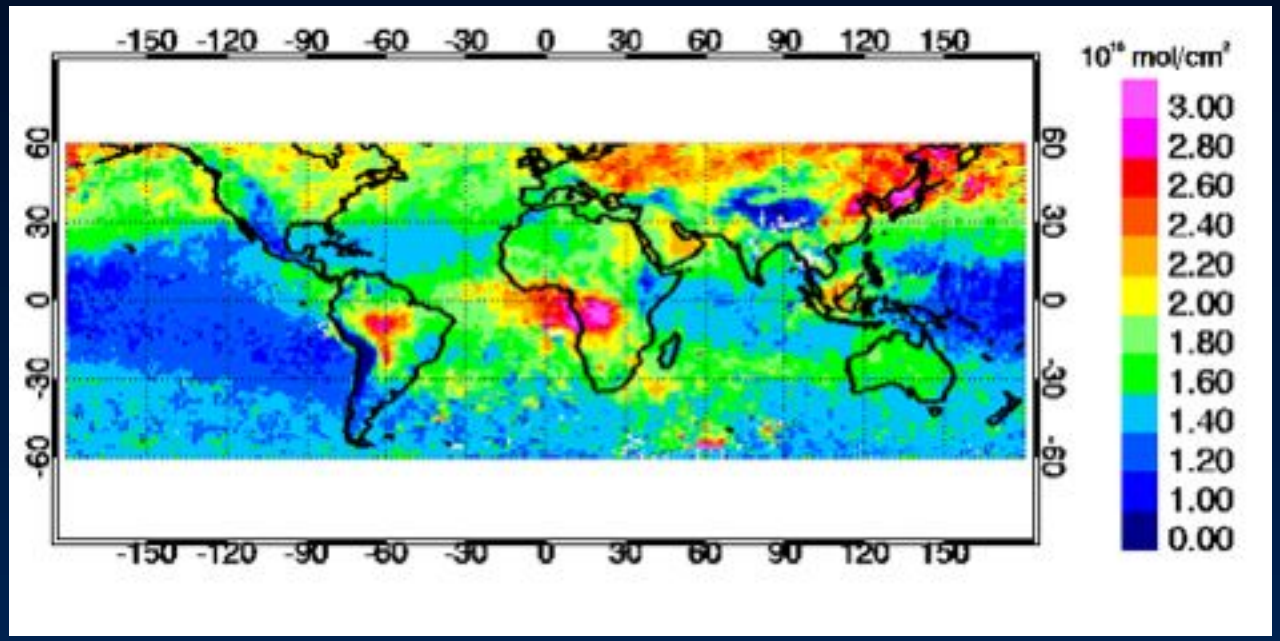

MOPITT column CO

L3 Gridded Surface (MIS09)

Radiative and biogeophysical parameters

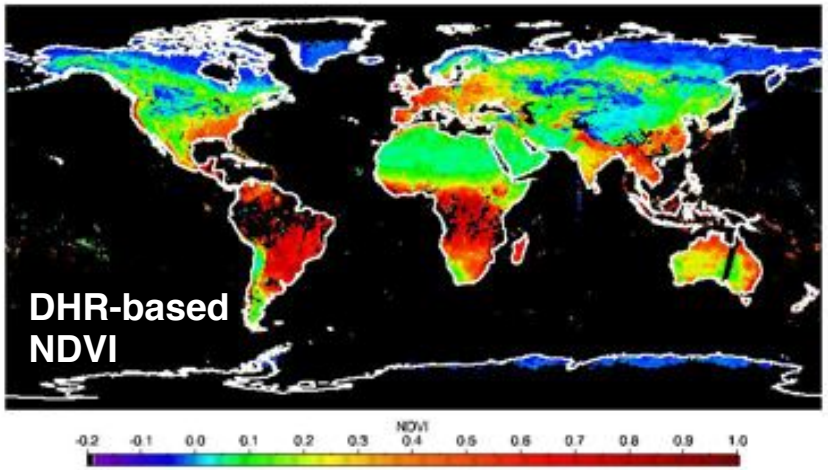

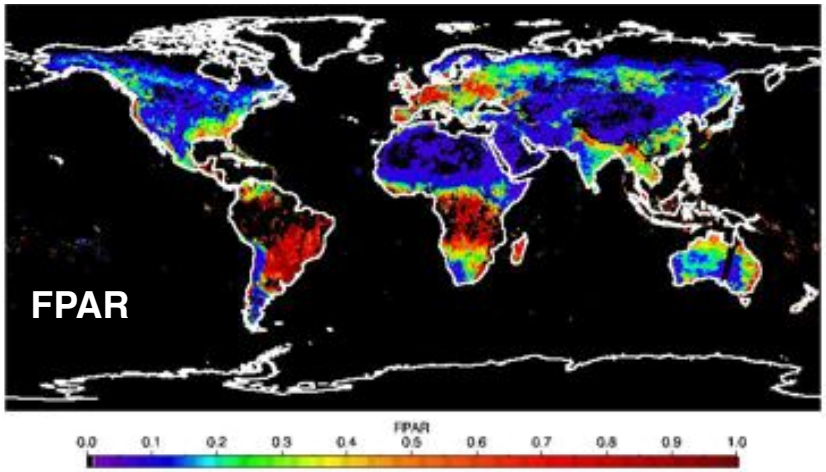

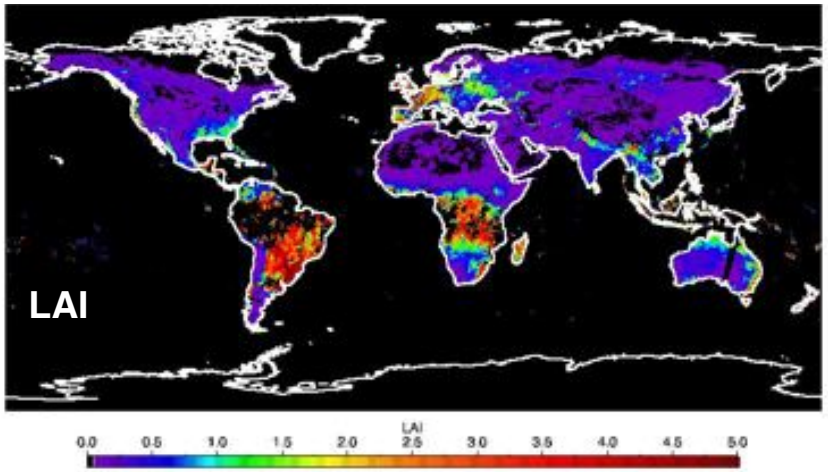

Additional products you might need

Ancillary Geographic Product

--contains latitudes, longitudes, elevations, scene classifiers for each 1.1-km pixel on the Space Oblique Mercator grid

Aerosol Climatology Product

--Aerosol Physical and Optical Properties (APOP) contains characteristics of the component particles used in the aerosol retrievals

--Mixture file contains characteristics of the particle mixtures used

Data maturity levels

Terra data products are given the following maturity classifications:

Beta: Minimally validated. Early release to enable users to gain familiarity with data formats and parameters. May contain significant errors.

Provisional: Partially validated. Improvements are continuing. Useful for exploratory studies.

Validated: Uncertainties are well defined, and suitable for systematic studies.

Mapping of data product maturity to version numbers found at:
http://eosweb.larc.nasa.gov/PRODOCS/misr/Version/version_stmt.html

AirMISR

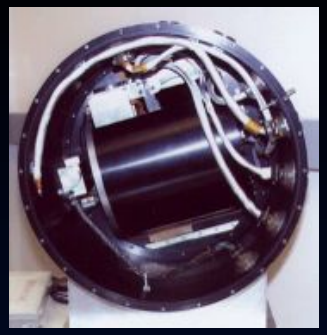

Flies in nose of NASA ER-2

Covers MISR's nine angles

Uses gimballed MISR prototype camera

27.5 m georectified spatial resolution

9 x 11 km area covered at all angles

Data available at LaRC DAAC

46° images near Howland, ME 28 August 2003

Where to get help and information

LaRC DAAC User Services
larc@eos.nasa.gov

Langley Atmospheric Sciences Data Center DAAC
http://eosweb.larc.nasa.gov

MISR home page
http://www-misr.jpl.nasa.gov

We welcome your feedback and questions!
"Ask MISR" feature on the MISR web site